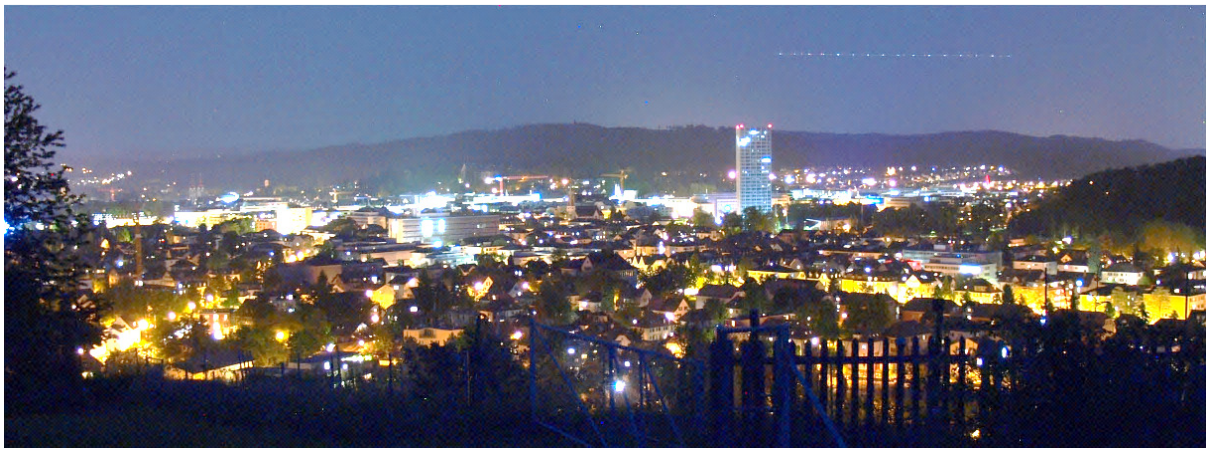


Measuring and Mapping Light Pollution at a Local Scale

DISSERTATION

Stefan M. Bruehlmann



Submitted in partial fulfilment of the requirements for the degree of
Master of Science in Geographical Information Systems (UNIGIS)

Faculty of Earth and Life Sciences

Vrije Universiteit Amsterdam

The Netherlands

November 2014



Abstract

Stefan M. Bruehlmann; Faculty of Earth and Life Sciences, Vrije Universiteit Amsterdam

Abstract of master's thesis, submitted 19 November 2014

Measuring and Mapping Light Pollution at a Local Scale

The aim of this thesis is to explore the use of Geographical Information System (GIS) technology in measuring, modelling and visualizing light pollution at a local scale. Light pollution is a worldwide phenomenon that is increasingly topical because of its detriment effects. Existing light pollution maps predominantly use and visualize remotely sensed data. This study hypothesizes that the information content of such maps is limited at a local level. A modelled approach was therefore developed to fill this lack of information. A variety of users are expected to benefit from highly detailed light pollution maps.

The research design included both, desk and field research. The most important light sources in a research area around the city of Winterthur (Switzerland) were identified. Light sources included particularly the different types of street lighting, but also the lighting of car parking or sports fields. Measurements for each light source were taken in the field by the use of a lux meter. The collected data determined the parameters for a GIS based model which allowed the production of a local light pollution map. In order to validate the modelled results, the map was compared with a DSLR night image taken from the International Space Station (ISS). A deviation map was established and analyzed.

Based on the results of this research, it could be confirmed that the use of satellite data to visualize light pollution at a local level is limited. A GIS model is however found to be a promising approach to produce detailed light pollution maps that feature a high accuracy at a regional and local level. The comparison of the modelled maps with the ISS image showed a significant consistency. Modelled maps have the advantage of being relatively cheap in their production and they facilitate the creation of scenarios. Various interest groups, municipalities and the individual citizen are supposed to find interest in light pollution data and maps at a local level.

Further research is nevertheless needed to enhance the model and to increase the significance of the presented light pollution maps.

-This page is intentionally left blank-

Table of contents

Table of contents	I
List of figures	III
List of tables.....	V
List of terms and abbreviations.....	VI
Disclaimer	VII
Acknowledgements.....	VIII
1 Introduction.....	1
1.1 Light pollution – a global concern.....	1
1.2 Detriment effects	2
1.3 Motivation of research	3
1.4 Research outline.....	5
2 Theory and Literature	7
2.1 Light pollution.....	7
2.1.1 Causes.....	9
2.2 Measuring and mapping light pollution	10
2.3 Past and current research (literature review).....	12
3 Research Methodology.....	17
3.1 Problem statement	17
3.2 Research questions.....	18
3.3 Research design	18
3.4 Research area.....	20
3.5 Data requirements	22
3.5.1 Digital maps.....	22
3.5.2 Observations in the field.....	24
3.5.3 Patterns derived from aerial/satellite imagery.....	25
3.5.4 Field measurements with 'Lux Meter'	26
3.5.5 Data from 'Sky Quality Meter'	28
3.5.6 Satellite imagery	28
3.5.7 Imagery from the International Space Station (ISS)	30
3.6 Conceptual Model.....	32
3.6.1 General.....	32
3.6.2 Data acquisition process and derived parameters	33
3.6.3 Processes and Calculation (ArcGIS).....	38
3.6.4 Mapping / Visualization.....	44
3.6.5 Preparation of ISS picture	45
3.6.6 Comparison of the 'Model output' with the 'ISS picture'	47
3.6.7 Model improvement process.....	48
4 Results and Analysis.....	49
4.1 Model output.....	49
4.2 Comparison with satellite imagery.....	54
4.3 Deviation map.....	55

5	Discussion	60
5.1	Validity of the model.....	60
5.2	Limitations.....	64
5.3	Fields of application	65
5.4	Application to other areas/regions/countries.....	67
6	Conclusion	69
6.1	Knowledge gained	69
6.2	Future direction and further research	71
6.3	Relevance of the research	72
	References	74
	Colophon	79
	Appendices.....	80
	Appendix A: Night images.....	81
	Appendix B: Study area	82
	Appendix C: Study area (land use)	83
	Appendix D: Night sky brightness scales.....	84
	Appendix E: Inventory of light sources	85
	Appendix F: Light points.....	88
	Appendix G: Albedo map	90
	Appendix H: ISS Image orthorectification	91
	Appendix I: ArcGIS model builder.....	92
	Appendix J: Luminaires and lighting situations	96
	Appendix K: EN 13 201 "Street Lighting"	97

List of figures

Figure 1: Earth at night	1
Figure 2: Light pollution in the Los Angeles (USA) area.....	2
Figure 3: Avian victims from light pollution	3
Figure 4: Night view from the top of the mountain Kronberg	4
Figure 5: Schematic visualization of research structure (simplified).....	5
Figure 6: Terms and concepts in light pollution visualized.....	7
Figure 7: Visualization of the contribution of different types of light sources to light pollution	8
Figure 8: Concepts of measuring light pollution.....	10
Figure 9: Map of the Night sky brightness over Europe	11
Figure 10: Artistic representation of the light pollution over France (Grenoble area).....	11
Figure 11: Research questions: (i.) main question and (ii.) to (v.) sub questions	18
Figure 12: Research Methodology flow chart	19
Figure 13: Research area: Location of Winterthur (Switzerland)	20
Figure 14: Research area: detailed view	20
Figure 15: Research area: View of the Old Town of Winterthur	21
Figure 16: Research area: Bird eye's view of 'Wülflingen'	21
Figure 17: Swisstopo map features; Scale 1:25'000	24
Figure 18: Swisstopo map features; Scale: 1:1000.....	24
Figure 19: Visual inspection of SWISSIMAGE.....	25
Figure 20: Visual inspection of SWISSIMAGE: (large scale view).....	25
Figure 21: Orthophotograph of Geneva (Switzerland).....	26
Figure 22: Light meter (Lux meter) used for the field measurements.....	26
Figure 23: Mobile data collection	27
Figure 24: Chart from the Mobile data collection	27
Figure 25: Sky Quality Meter – L (Narrow field of view, with Lens)	28
Figure 26: VIIRS images at different scales	30
Figure 27: Night image of the greater Zurich area by ESA.....	31
Figure 28: Night image of Winterthur by ESA.	31
Figure 29: The role of a data model in GIS	32
Figure 30: Procedure of light measurements using a LUX meter	33
Figure 31 (a-f): Measurements of light intensities.....	35
Figure 32 (a-d): Measurements of light intensities.....	35
Figure 33 (a and b): Histogram of measured light intensities and Albedo reflectance	36
Figure 34: The cosine to the third law.....	37

Figure 35: Creation of light points along polylines.....	39
Figure 36: Light modelling on sports pitches	40
Figure 37: Euclidean distance	41
Figure 38: Raster calculation of light intensities	42
Figure 39: Overlay of individual light source raster layers.....	43
Figure 40: Albedo map (detail; scale 1:80'000).....	44
Figure 41: RGB values of a single light source in function of distance.....	45
Figure 42: ISS image overlaid by the street network	46
Figure 43: Different color bands of the ISS image.....	47
Figure 44: Classification scheme for the comparison of ISS image and model output	48
Figure 45: Comparison of the reclassified values of the 'green band' image with the model output....	48
Figure 46: Model output containing more than 88'000 light points.....	49
Figure 47: True color diurnal image of the research area.....	50
Figure 48: Model output, illumination from Sports pitch is excluded	50
Figure 49: Model output, Illumination from Sports pitch is included	50
Figure 50: ISS image of the research area.....	51
Figure 51: Model output (detailed view on the city center).....	52
Figure 52: Model output at street level.	52
Figure 53: Comparison of the model output with a true color satellite image.....	53
Figure 54: Comparison of an image from the VIIRS satellite with the model output.....	54
Figure 55: Comparison of the model output with the ISS image.	55
Figure 56: Difference map.....	56
Figure 57: Negative and positive deviations are summarized and visualized in the chart.....	57
Figure 58: Detailed analysis of the 'hot spots' in the deviation map.....	58
Figure 59: Comparison of a nocturnal illumination maps from Berlin.....	60
Figure 60: Comparison of an aerial photo and the model output	61
Figure 61: Extract from the light pollution map by Cinzano et al. based on DMSP satellite data.....	62
Figure 62: Illustration of the calculated light modelling using the 'Calculux' software	65
Figure 63: Night sky brightness map.....	67
Figure 64: Digital mapped data coverage from Swisstopo (available in format 1:25000).	68

List of tables

Table 1: Swisstopo and OSM data for use in the Light pollution model	23
Table 2: Albedo reflectance rates.....	36
Table 3: Data layers and parameters for the creation of light points.....	39
Table 4: Data layers and number of created light points.....	41
Table 5: Deviation Analysis (ISS image vs. Model output)	57
Table 6: Qualitative assessment of the validity of the Light Pollution Model.....	63
Table 7: Fields of application of the model.....	66

List of terms and abbreviations

ArcGIS	Geographical Information System software by Esri Inc., Redlands (USA)
CEN	European Committee for Standardization, Brussels (Belgium)
DMSP	Defense Meteorological Satellite Program
DNB	Day/Night Band
DSLR	Digital single-lens reflex (camera)
ESA	European Space Agency, Paris (France)
EN	European Norm
EU	European Union
ETH	Swiss Federal Institute of Technology, Zurich (Switzerland)
GISCloud	Provider of mobile GIS solutions
ISS	International Space Station
LED	Light Emitting Diode
Lux (lx)	Unit of illuminance and luminous emittance
MDC	Mobile Data Collection
NASA	National Aeronautics and Space Administration, Washington (USA)
NOAA	National Oceanic and Atmospheric Administration, Washington (USA)
NSB	Night Sky Brightness
OSM	Open Street Map
PC	Personal Computer
RGB	RGB (Red, Green, Blue) color model of additive primary colors
SLL	Street Light Level
SNPP	Suomi National Polar Partnership
SQM	Sky Quality Meter
Stadtwerk	Municipal unit of Management of Light, Energy, Water, Winterthur, (Switzerland)
Swisstopo	Swiss Federal Office of Topography, Berne (Switzerland)
UAV	Unmanned aerial vehicles
ULE	Upward light emissions

Disclaimer

The results presented in this thesis are based on my own research at the Faculty of Earth and Life Sciences of the Vrije Universiteit Amsterdam.

All assistance received from other individuals and organizations has been acknowledged and full reference is made to all published and unpublished sources.

This thesis has not been submitted previously for a degree at any institution.

Signed:

Winterthur (Switzerland), 19 November 2014

A handwritten signature in blue ink, appearing to read 'Stefan Bruehlmann', with a stylized, flowing script.

Stefan M. Bruehlmann

Acknowledgements

I am using this opportunity to express my gratitude to everyone who supported me throughout the course of this M.Sc. thesis. I am thankful for their guidance, constructive criticism and useful advice during the course of my research. I am sincerely grateful to them for sharing their views and knowledge on several issues related to this thesis.

First of all, I would like to express my gratitude to my tutor Mr. Erik van der Zee. During numerous conversations and countless email exchanges he has helped me with guidance, comments, remarks and encouragement for this master thesis. He has been a tremendous tutor and is a great and inspiring GIS professional.

Also, I express my warm thanks to the responsible M.Sc. coordinator at VU Amsterdam, Mr. Niels van Manen. He has helped me with valuable support and guidance for finding this research topic and for much practical advice during this project.

Furthermore I would like to thank Melissa D. Higgins from NASA for her relentless attempt to schedule the shooting of a suitable night image of Winterthur (Switzerland) taken by the astronauts on the International Space Station.

I would also like to thank the following people who provided me with crucial knowledge and insight during my research project: Fabian Neyer from the Swiss Federal Institute of Technology Zurich (ETH) and Rolf Schatz from the Dark Sky Association of Switzerland for introducing me to the topic and providing me with useful information and documents; Markus Frei and Daniel Kyburz from the ‘Stadtwerk Winterthur’ for their data and insight regarding the local lighting situation; Christine Karch from Geofabrik Berlin for her support regarding OSM data, Tatjana Urvan from GISCloud for helping me to realize the mobile data collection, Frédéric Tapissier from avex-asso.fr who inspired me for the visualization of light pollution and Jodi Eisenhut Spitler for the careful proofreading.

A special thanks goes to my fellow student Ruud Oberndorff for his good companionship since 2011. He has been a great sparring partner and dear friend at the same time.

Finally, the author wishes to express gratitude to his wife Yoshiko and daughter Fiona for their support, understanding and patience throughout the duration my M.Sc. studies.

1 Introduction

1.1 Light pollution – a global concern

Light pollution is a relatively new phenomenon. The first electric light bulb was invented only 160 years ago. Since then light emissions have grown steadily, even exponentially in certain areas. Artificial lighting has become an integral part of our culture. It conveys a feeling of safety and wealth. Nevertheless, scientists warn of detriment effects of excessive light emissions.

In densely populated countries, naturally dark areas have become rare. The International DarkSky Association estimates that one 5th of the world population can no longer see the milky way with their naked eyes. According to light pollution maps (Cinzano, et al., 2001; NASA, 2014), large areas in Europe rank amongst the most illuminated places in the world during night time.

Astronomers of all continents have pointed to the problem for a long time. Their sight on the stars from populated places has become more and more difficult (Keeney, 2012; Posch, et al., 2012). They point out that a lot is done to protect ourselves from noise, exhaust fumes and waste, but not from excessive light. In fact, air, soil and water are important subjects of protection. The night sky is not.

Although that the night sky itself, celestial objects and starlight as such cannot be recognized by the World Heritage Convention, the organization has launched in 2007 the 'Starlight initiative' and developed the concept of so called 'starlight reserves' (UNESCO World Heritage Center, 2014).

In the late nineties, NASA started to publish pictures of the earth at night (Figure 1). This composite image of more than 400 satellite images has become an emblematic poster of the dominance of mankind on earth. Uncontestably, the image is fascinating and worrying at the same time. The light emissions towards space are originating mainly from the US, Europe and Japan. Most parts of Africa, Australia and parts of South America can still keep their darkness at night.

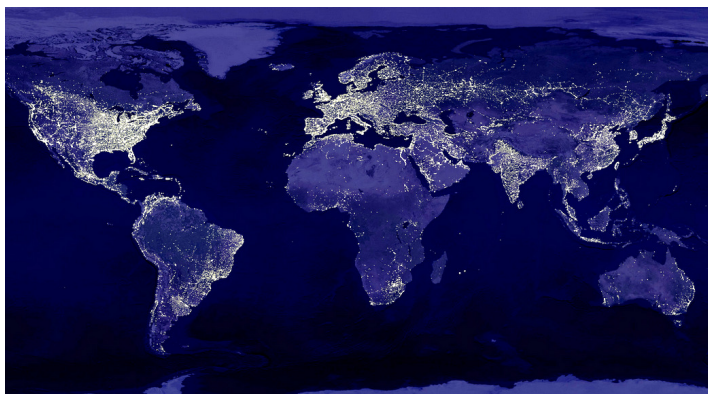


Figure 1: Earth at night. Emblematic image of the illumination of the earth at night, recorded by the Defense Meteorological Satellite Program (DMSP) Operational Linescan System (OLS).

Source: NASA (2014)

Excessive light emissions do not only have negative effects on the natural environment. They are also an enormous waste of resources. A sustainable use of light and energy pays off for the municipalities and the individual household. Although that there is no common regulation in Europe, governments increasingly recognize the need to manage light emissions. Some countries have introduced laws to limit the light pollution. Slovenia and Italy are the countries with the most restrictive regulation. Still, there are several countries with no regulation at all (Hänel, 2014).

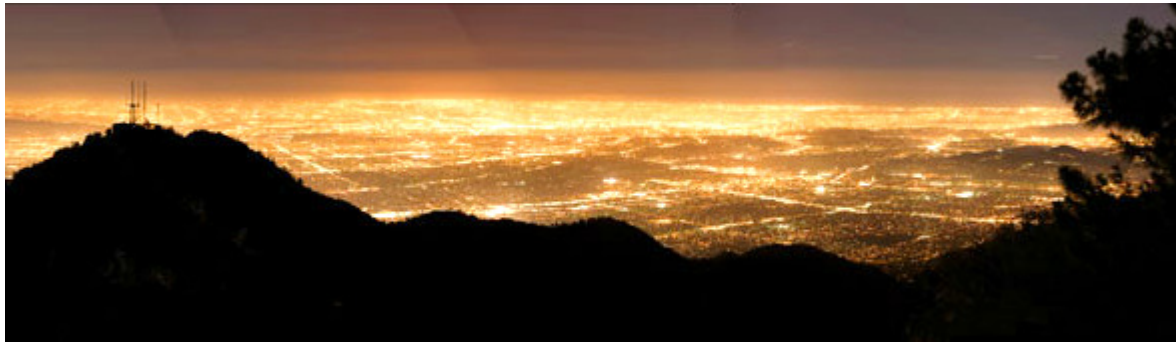


Figure 2: Light pollution in the Los Angeles (USA) area. In a 2008 view from a nearby vantage point, a mushrooming population nearing five million fills the valley, creating a sea of brightness.

Source: National Geographic (2014)

1.2 Detriment effects

The first scientists who worried about the side-effects of the electric light were the astronomers. Their work relies on the free sight on the stars. The conditions for astronomers that are observing the sky with ground based, stationary telescopes have constantly deteriorated. Faint stars are hardly recognizable from areas that are within the light domes of urbanized and industrialized areas. Experiencing a pristine night sky has become impossible in most parts of Europe. Philosophers, thinkers and artists particularly regret the loss of the night. Since the beginning of mankind, the starry sky has influenced the cultural development and has inspired all walks of life (Bogard, 2013). At present, the starry sky is about to drown in the electric light of the cities (Figure 2). One of the most impressive natural phenomenon of our earth is about to disappear.

Increasingly, researchers of different fields of study – especially medical scientists and biologists acknowledge the negative effects of excessive light. It has been proved that artificial light can become a source of irritation. Research at the University of Basel (Switzerland) has shown that artificial light at the wrong time can cause insomnia and heart rhythm disturbance and can lead to serious health hazard (<http://www.chronobiology.ch/>). Other studies suggest a statistically significant correlation between outdoor artificial light at night and breast cancer (Chepesiuk, 2009).

For many animals, darkness is a life-determining factor. Changes in the natural lighting conditions by artificial light can have ecological consequences and can possibly reduce the biodiversity (Rich & Longcore, 2006).

Nocturnal insects, for example, are attracted by artificial light. Instead of looking for food, they are exhausting their energy at streetlamps and are often dying because of overfatigue. It is estimated that in a country of the size of Germany, every night more than a billion insects are dying at artificial light sources (Eisenbeis, 2002).

Light pollution can have a significant effect on the bird migration. Every year billions of birds are migrating from Europe to Africa and back. They find their way by orienting themselves on the stars. Birds are confronted on their way with completely new lighting conditions. They are attracted by the light domes of the cities and are detracted from their optimal route. Many birds collide with high and illuminated buildings or get lost and exhausted and eventually die (Swiss Ornithological Institute, 2005).

Figure 3 illustrates the numerous avian victims caused by illuminated buildings in an urban zone in Toronto (Canada). Nocturnal mammals (bats, foxes, deer, batchers etc.), amphibian and reptilian are said to be disturbed likewise by artificial light. Negative development is also observed with plants when exposed to an unnatural night/day rhythm (Longcore & Rich, 2004).



Figure 3: Avian victims from light pollution. Collected over a three month period in Toronto (Canada) and displayed to a school class at the Royal Ontario museum. Over 1000 birds of 89 species are displayed.

Source: National Geographic (2014)

1.3 Motivation of research

The motivation for this research topic was strongly influenced by my personal interests in the observation of nature, in taking (night) photographs and in mapping. The study of light pollution in fact provides an excellent opportunity to do interdisciplinary research. Topics in light pollution cover the mentioned interests but even go beyond and include a multitude of further disciplines: optics, technology, environment, economics, society and culture, to mention a few.

The awareness of the negative effects of light pollution as described in chapter 1.2 made it easy to choose this topic. I had the belief that the intended research could be of use for the community by providing knowledge and information that is to date not easily available. The idea that the research outcome could help to position the topic of light pollution on the agenda of municipalities and into the heads of the population additionally fuelled my motivation.

The chosen M.Sc. thesis topic should involve an intensive use of GIS methods and technology. The perspective to develop a solution from scratch for the given research question with the use of GIS was tempting.

My intension was indeed to deep-dive into a desktop GIS and tests its possibilities and limits. This would allow me to develop practical expertise too. Already in an early stage of the search I perceived the link of GIS science with the light pollution topic as a natural fit.

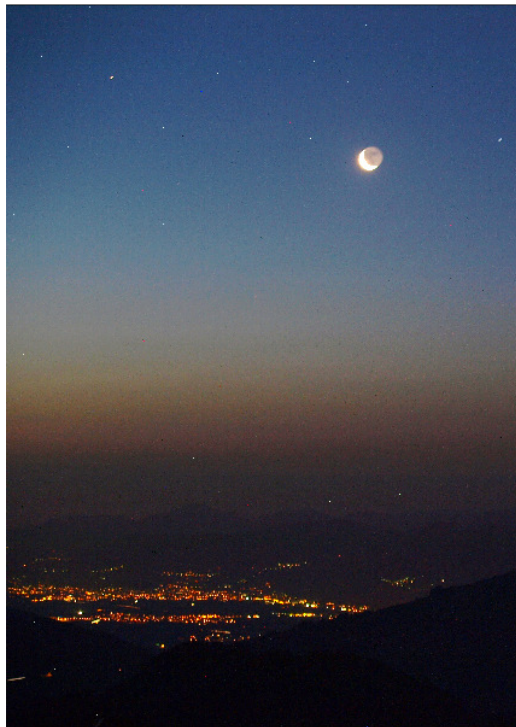


Figure 4: Night view from the top of the mountain Kronberg (1663 m above sea level) in the Canton of Appenzell (Switzerland). The photo was taken on 4 August 2013 at 3.39 am. Despite the night-time hour, a distinct illumination from the nearby city of Bregenz (Austria) is visible. The lights compromised the observation of the milky way.

Photo: Stefan M. Bruehlmann (OLYMPUS E-3; f5.4 / 20seconds, ISO 200)

A pivotal moment that eventually shaped the research question was a stay in the Swiss mountains (Appenzell region) in summer 2013. Having had the light pollution maps by Cinzano, et al. (2001) in mind, I assumed that the remote alpine regions were an oasis of darkness in the otherwise densely populated and highly illuminated country of Switzerland. Personal nocturnal photographs taken during that stay (Figure 4) actually revealed the opposite: from the top of the mountain ‘Kronberg’ (1663 m above sea level, situated in the midst of a ‘darkness island’), the lights of cities and villages were clearly present. The glare negatively affected the night sky observation. The mentioned maps that declared the area as ‘darkness island’ did not seem to match the on-site impression. The light pollution appeared to be

much more local than shown in the available maps. This insight eventually triggered the idea to produce a light pollution map at a *local scale*. It was soon understood that such a detailed map does not yet exist.

1.4 Research outline

Figure 5 illustrates schematically the content of the research in a simplified view. The detailed contents of the chapters can be seen from the table of contents (TOC). In the illustration below, the different chapters are represented with squares of different width. They represent the breadth of the topic.

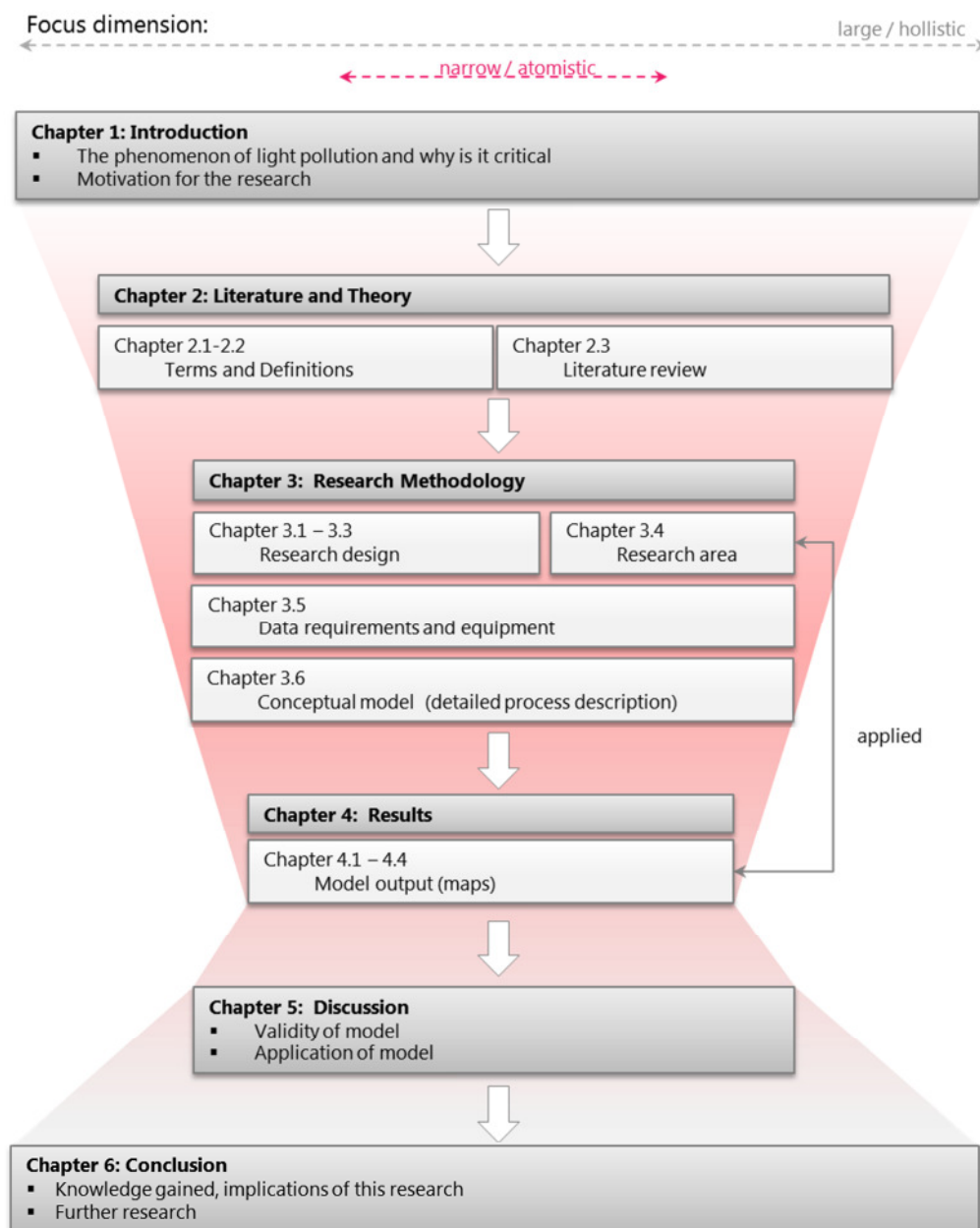


Figure 5: Schematic visualization of the research structure (simplified). The width of the squares reflect the focus dimension (from large to narrow).

The above graphic reflects the 'hourglass' approach (Web Center for Social Research Methods, 2006) which starts from a broad area of interest (light pollution) and narrows down to the a specific question. In the most narrow stage (Chapter 3 and 4), the study is engaged in direct measurements and observations and the analysis of the results. Results are generalized in the final chapter where the original questions of the introductory chapters are addressed. Hence, the sequence is as follows:

Chapter 1 introduces the topic and demonstrates the need for research in the field of light pollution. The motivation for this research is outlined consequently. Chapter 2 introduces common concepts in lighting and the key terms and measurements applied in the subsequent chapters. A literature review provides an overview of similar research done in the field of measuring and mapping light pollution. Existing studies are critically analyzed and set in context with the intention of this research.

Chapter 3 (Research Methodology) and Chapter 4 (Results) represent the main body of the research. Chapter 3 exposes and discusses the data requirements for the research. The research area in which the practical application of the conceptual model takes place is presented. The conceptual model itself is explained step by step in an extensive way.

Chapter 4 presents the result of the model (later referred to as the 'model output'). The results are followed by an in-depth analysis. The discussion in Chapter 5 is focused on the comparison of the model output with a reference case. This case consists of an aerial photograph taken from space. The validity of the model is evaluated based on this picture. Additionally, some fields of application of this study are considered. Chapter 7 finally concludes on the findings and consequences of this research and suggests a number of further research activities.

Supplementary information and images that are not considered to be mandatory for the understanding of the main text are placed in the appendix.

It has to be highlighted that this research is exclusively based on measurements and observations in the sketched out research area (Chapter 3.4) of Winterthur (Switzerland). Inferences to other geographical areas or cities are to be done with caution.

2 Theory and Literature

2.1 Light pollution

Light pollution is one of the negative side effects of outdoor lighting. Figure 6 illustrates the useful light from a public lighting and the different components and terms of light pollution. Light pollution is the consequence of misdirected and/or excessive artificial light. If light is not properly controlled, it does not go where it belongs. The result is obtrusive light (also called ‘spill’) which can be a nuisance.

Obtrusive light can keep you up at night, when it shines through your window. It can also impede the view on the night sky. When light is misdirected upwards it results in the brightening of the sky. This causes a phenomenon that is known as ‘sky glow’ (Institution of Lighting Professionals, 2012).

Sky glow is caused by either direct upward light or upward reflected light which is subsequently scattered back towards the surface of the earth. There is always a scatter because of the atmosphere which consists of air molecules. Another factor for scatter are aerosols which are particles floating in the air. They can be water droplets, dust, soot, salt crystals from the sea, ash from forest fires and volcanoes (Narisada & Schreuder, 2004).

Improperly installed light sources or light sources which are unshielded towards the sky can cause sky glow. A typical example is unshielded lamps (i.e. ‘globe lamps’). For this type of lamp most of the light goes directly to the sky (see Appendix J).

Glare is an uncomfortable brightness of a light when looked at against a darker background. Glare can cause discomfort or fatigue when experienced over extended periods. It can partly blind drivers or pedestrians and lead to dangerous situations. Finally, ‘light trespass’, is obtrusive light that goes beyond the area being lit. For example, when light of a street lamp is intruding the inside of one’s property or shining over the neighbor’s fence.

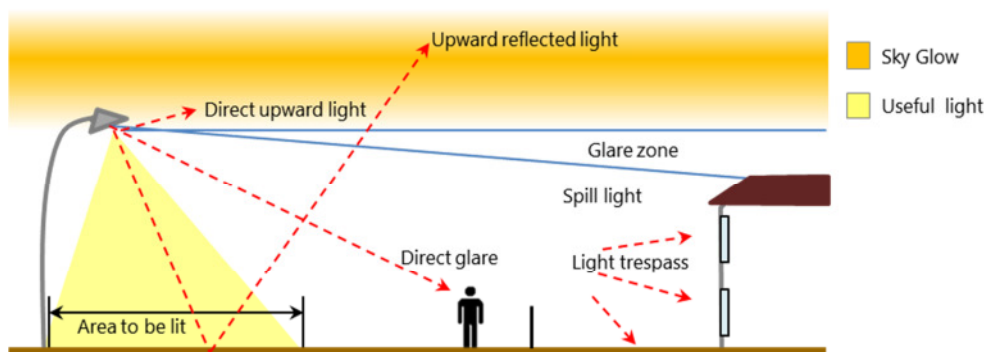


Figure 6: Terms and concepts in light pollution visualized: Light pollution is an unwanted consequence of outdoor lighting. It causes effects such as sky glow, light trespass or glare. The different phenomena are illustrated in the graphic. The focus of this study is on the upward light emissions, either directly from the light source or through reflection.

Illustration : Stefan M. Bruehlmann / adapted from Rensselaer Polytechnic Institute, (2007)

The term 'light pollution' is used in various ways and by various interest groups. What is considered as 'light pollution' depends on the focus of each of those groups: Astronomers assess light pollution in relation to the quality of the night sky (e.g. the number of stars that are visible in a particular area); city planners and municipalities bring light pollution in connection with security and aesthetic aspects and include an economic component, such as the use of electric energy and consequent costs (Deleuil, 2009). Individuals might link light pollution to the disturbance of intruding light into their living space. The most common form of light pollution perceived by all stakeholders is light scattered in the atmosphere, creating a luminous halo known as 'sky glow' (Commission Internationale de l'Eclairage (CIE), 1997).



Figure 7: Visualization of the contribution of different types of light sources to light pollution. Image A shows a rural landscape without artificial lighting. In image B three unshielded luminaires with strong light emissions towards the sky are installed. The effect of the sodium-vapor lamps (creating orange light) is visible. Almost all stars have disappeared. The situation changes considerably in case the lamps are shielded towards the sky (image C).

Source: <http://www.need-less.org.uk/images/need-less-LPsim.swf>

Figure 7 (A-C) illustrates the same rural landscape with three different illumination policies. Image A represents a situation with no artificial illumination. The sky brightness caused by artificial light is minimal. The number of visible stars is at its maximum. The opposite situation is shown in image B: Three sodium-vapor lamps of the 'globe type' (no shielding towards the sky) are installed and alter considerably the night sky. The light is not focused and wasted into all directions. Almost all stars have

disappeared. Light intrusion is assumed in the nearby building. Situation C shows a well planned alternative where the three lamps are well shielded towards the sky. They send their light only to the area to be lit. The quality of the night sky is hardly affected by the lamps and the neighborhood does not suffer from intrusive light.

This study mainly focuses on the light that is a) directly sent upward to the sky or b) light that is reflected from the ground towards the sky. The two luminous fluxes are assumed to make up the quantity of light visible by sensors on satellites and airplanes (in aerial photography). In this study, the term '*light pollution*' is therefore understood as that ***part of light that ends up in the sky and which is consequently not for functional use***. Light pollution is considered to be a waste of energy that can be avoided.

2.1.1 Causes

In its origin, light pollution is a side effect of the industrial development. It therefore occurs mainly in densely populated areas of industrialized countries (Posch, et al., 2012). The most important causes for light pollution are large cities, industrial areas, street lighting, illuminated advertising and flood-lighting. Kuechly, et al. (2012) have found 'street lights' to be the dominant source of upward directed light emissions (31.6% of all light emissions), followed by 'industrial/commercial/service areas' (15.6%) and 'public service areas' (schools, hospitals) (9.6%).

Other sources with a considerable perturbation potential include the illumination of façades, the headlights of motor vehicles and the use of so called 'sky beamers'. The latter are widely criticized and regulated by the legislators (Klaus, et al., 2005).

Finally, inappropriate lighting technology can lead to light pollution. In the planning and implementation of (public) lighting the optimal, most effective and light pollution friendly technology has to be selected: this usually consists of lamps that are fully shielded towards the sky and neighboring buildings. Further, the intensity of illumination should be adaptable and should be possible to be managed flexibly according to the time of service; meaning that the light intensity needs to be higher during times with high traffic volumes than in the early morning hours when less traffic is on the streets.

Much of the light pollution is simply caused by ignorance. The relatively low cost of electric energy literally encourages people to act in an irresponsible way. Additionally, the consequences of light pollution are – despite the increased topicality– not known to all people. Awareness campaigns could help to inform about the nuisances and negative consequences of misguided and excessive light. The reduction of light spill can lead to important savings because light is only produced and emitted where it is needed. This leads to a strong incentive for municipalities and individuals to rethink where, how and how intensively they use light in outdoor areas.

2.2 Measuring and mapping light pollution

There are various techniques, processes and devices to measure light pollution. Depending on the purpose, different methods are in use. A general distinction can be made between methods that measure the 'night sky brightness' and such that measure the 'luminous flux on the ground'. From both methods 'light pollution maps' can be produced.

Methods that intend to measure the sky brightness include a) the establishment of the magnitude of the visible stars. The faintest star of a known magnitude sets the limitation b) Star counting determines the level of sky glow by the number of visible stars of different magnitude c) Photographic surveys with digital cameras. These methods can be complemented by a more quantitative one: measurements with a Sky Quality Meter (SQM) (see chapter 3.5.5, Data from 'Sky Quality Meter'). The SQM device measures the magnitude of an arcsec^2 and puts the results on a scale from 14 (totally polluted sky) to 23 (fully unpolluted starry sky). Alternative scales to describe the night sky brightness exist. A nomogram is shown in Appendix D. If 'night sky brightness' surveys are done over large areas, the measurement method must be cheap and simple, given the intensity of labor.

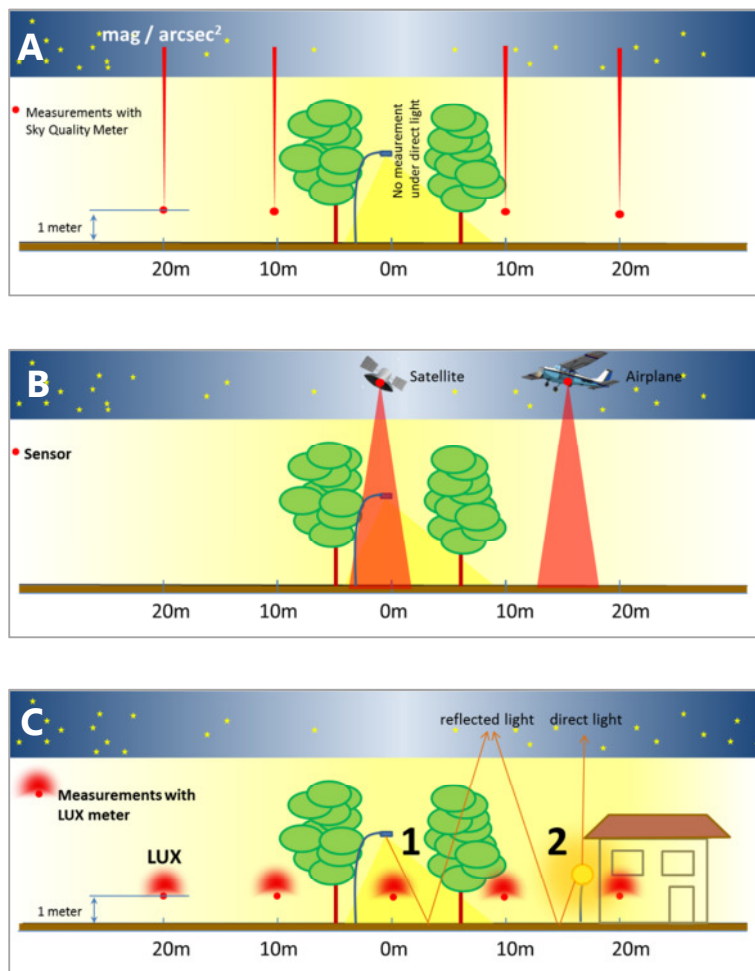


Figure 8: Concepts of measuring light pollution: Image A visualizes the concept of measuring the quality of the night sky. This can be done by a Sky Quality Meter (see chapter 3.5.5). The brightness of the sky is determined by a value in ' mag/arcsec^2 '. This type of measurement is of relevance for astronomers. Image B visualizes measurements from the sky. Satellites helicopters, airplanes, drones, etc. are usually employed. Image C describes the concept of measuring 'ambient light' from ground based light sources (e.g. lamps 1 and 2). The measurements can be done by a Light-meter (Lux meter; see chapter 3.5.4). For this study, concept C was mostly applied.

Illustrations : Stefan M. Bruehlmann

The measurement procedure with the SQM is illustrated in Figure 8 A. Measurements of this method are taken from the ground by focusing the SQM device vertically to the sky. Direct light can distort the results; therefore no measurements can be taken under street lamps.

Measurements from satellites and airplanes take the opposite approach (Figure 8 B): light magnitudes of the ground surface are measured from the sky, focusing downwards. Various flying apparatuses can be used (satellites, spaceships, helicopters, drones, etc.). This type of method is suitable for global or large region surveys. However, it is assumed that for actual lighting design data captured by satellite is insufficient in terms of resolution.

A method that measures the 'luminous flux' in-situ is illustrated in Figure 8 C: The measurements are carried out from the ground. They generally register the vertical illuminance by using a light meter (e.g. Lux meter; see details in Chapter 3.5.4). A certain portion of the measured light is reflected by the ground towards the sky where it adds to the sky glow.

In this study the light measurements were taken with a Lux meter according to method C. The device was positioned at 1m above ground and focused upwards. This way the luminous flux of the surrounding light sources could be captured and data for modelling/mapping collected. This method is also used to assess light trespass and glare. The night sky quality (sky glow) can be assessed too by light meter measurements. Narisada & Schreuder (2004) describe that the total upward flux (direct and reflected light) and the size of the area have to be taken into account for its calculation.

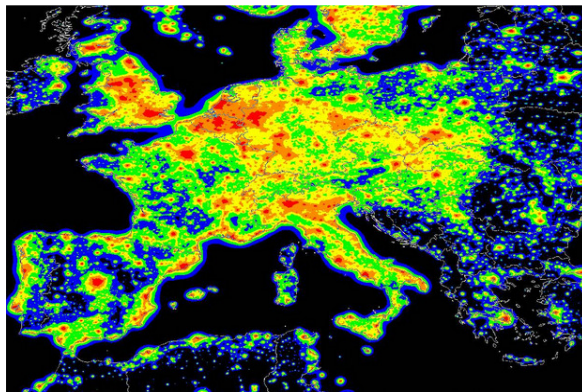


Figure 9: Map of the night sky brightness over Europe. Dark areas indicate pristine night skies whereas yellow and red areas represent the hot-spots of light pollution and low visibility of the night sky. This type of image has got a rather low resolution. The calculation and mapping is based on modelled data from satellite imagery.

Source: Cinzano, et al. (2001)

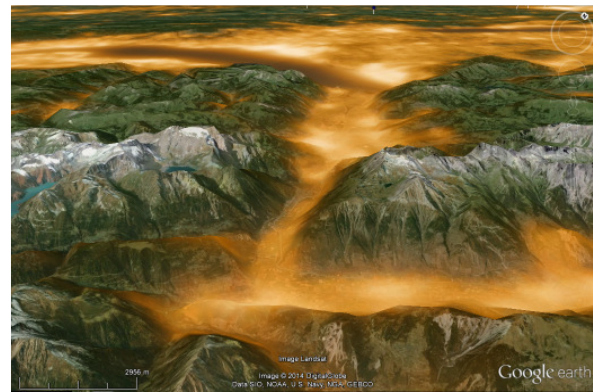


Figure 10: Artistic representation of the light pollution over France (Grenoble area). The light pollution intensities are derived from 'CORINE' land cover data. The coloration is arbitrarily used. In the image, a sodium-vapor lamp type was imitated. The light pollution layer was imported into Google Earth.

Data source: Tapissier (2014)

Cartography: Stefan M. Bruehlmann

Maps are an illustrative way to show the spatial distribution of light pollution. The two figures above show examples of very different maps in terms of technical preparation and scale. What is commonly called a

'light pollution map' can be classified into two categories: a) maps showing the 'night sky brightness' and b) maps showing light emissions on the earth's surface. Maps that visualize the 'night sky brightness' are mostly the result of a modelling process and are suitable for global or large regions visualization and monitoring. Calculations are either based upon ground based measurements, remotely sensed data or satellite imagery.

Maps showing light emissions on the earth's surface can be produced based on data gathered in-situ or acquired remotely. The most accurate maps are produced from aerial night surveys. These images usually show the visible light and give realistic impressions of the area under consideration. Satellites operating in the visible light range provide similar results, however at a much coarser resolution.

As opposed to measured data or aerial photography, light emissions on the ground can also be completely modelled. This requires detailed knowledge about the locations and intensities of the light sources. The study at hand follows a modelled approach.

An example of a fully 'modelled' map is shown in Figure 10. The shown 3D illustration is based on data from the CORINE land cover project (<http://www.eea.europa.eu/publications/COR0-landcover>). The urban land cover was used to derive the spatial distribution of the light pollution layer. The data layer was finally imported into Google Earth. The resolution of this particular approach remains however coarse and the general accuracy is low, limiting the application for detailed light planning and monitoring activities. For visualization purposes and the goal to raise awareness, the map is nevertheless illustrative and captivating.

Many ways of mapping light pollution exist. Specific forms and contents arise from different requirements. Having reliable data from measurements at hand is crucial for the quality of the maps. The different measurement methods described in the beginning of this chapter are finally determining the mapping options.

2.3 Past and current research (literature review)

A number of people have modelled and visualized light pollution in different ways. Most studies aimed to model the night sky brightness. Early fundamental research has been done by Walker (1977) who described a brightness-population relationship. Garstang (1986) created a model to calculate the night sky brightness based on various parameters, including reflectance of the ground, aerosols and population density.

An example of a recent night sky brightness map is shown in Figure 9. In this map from Cinzano, et al., dark areas imply low light pollution. Yellow or red areas represent places where light pollution is at a high

level. The latter places largely coincide with the population density over Europe. Cinzano, et al. (2001) have produced an atlas of the night sky brightness over Europe. The light pollution studies by the Italian researchers are covering most European countries. The base data of the maps was collected by the U.S. Air Force Defense Meteorological Satellite Program (DMSP). The low light images of the twenty DMSP satellites allow for a comprehensive analysis over large areas and for the comparison of different periods. Tavoosi, et al. (2009) demonstrated the application of DMSP images to document the capabilities of the combination of DMSP satellite images and GIS. The resulting light pollution maps impressively visualize the increase of light pollution in the course of a decade.

The resolution of the maps using the above mentioned DMSP data is however coarse. The night-time visible bands start with a 5 x 5 km footprint at nadir. An alternative with a considerably better resolution is the Suomi National Polar Partnership (SNPP) satellite carrying the Visible Infrared Imaging Radiometer Suite (VIIRS) instrument. Night-time imagery can be recorded by the VIIRS with a ground footprint of 742 x 742 m. Elvidge, et al. (2013) expose the advantages of the use of VIIRS data for the mapping of night-time lights. The analysis suggests the possibility of relatively detailed light pollution maps at a country or regional scale. The data of the two abovementioned satellite products are panchromatic in the visible and infrared light range of 0.5 to 0.9 μm .

Studies that use DMSP or other satellite imagery provide meaningful insight on a country level or smaller scale. For the analysis at regional or local scale, however, other data sources provide better results. Aerial night photography is an efficient, but at the same time, costly way of acquiring night time data at a large scale. Kuechly, et al. (2012) have done a comprehensive analysis of the light pollution in the city of Berlin. Aerial night photos were taken by an airplane at approx. 3000m. The resulting mosaic of more than 2600 images represents an excellent data base for the understanding of the most important light sources. Kuechly et al. additionally linked the data from the imagery to the land-use. A detailed ranking of the most light polluting sources (mainly public lighting) could be established. Aerial photography has the capability to provide light pollution information down to a street level. Frangiamone (2014) from the municipality of Geneva (Switzerland) likewise analyzed aerial night photography. The photos allowed her to detect the most polluting light sources (such as over-illuminated street corners or bus stations) and to bring the light pollution into context with other data sets such as 'crime locations' or 'road kill'.

Hale, et al. (2013) undertook a case study of urban lighting in Birmingham, a large city in the highly urbanized West Midlands metropolitan county of the United Kingdom. Aerial night photography was collected, using a regular Nikon D2X DSLR camera. GIS methods were further used to identify the point location of all lamps in the landscape. Based on the RGB values the light points could be attributed with accuracy to four broad lamp classes (low pressure sodium, high pressure sodium, metal halide and mercury vapor). Lamp type information is demonstrated as the base for detailed analysis in association with land use and building types. Hale, et al. argue that "the lack of lighting data at the city extent,

particularly at a fine spatial resolution” is the main barrier for more research, planning and governance in the field of urban lighting.

Given the cost and the organizational effort needed, aerial night photography surveys are rarely done. Only a few cities in Europe have invested into the production of such images. An alternative source for aerial images is photos taken by the astronauts from the International Space Station (ISS). The photos have the potential to provide a comparable detail. Existing ISS images can be searched for through the NASA ‘Gateway to Astronaut Photography of Earth’ (<http://eol.jsc.nasa.gov/>). The image database is however far from being complete. Only for a few cities worldwide night-time imagery exists. Even when available, the quality is often compromised by unfavorable meteorological conditions (fog, cloud cover, etc.) or biased by in-motion unsharpness.

Nevertheless, Zamorano, et al. (2011) point out the superiority of the ISS images compared to imagery acquired by satellites. As described earlier, the best satellite provides night images with a pixel footprint of 742m (Elvidge, et al., 2013). The ISS images can provide data at a significantly better resolution. Zamorano et al. analyzed a DSLR image of Madrid taken at very favorable conditions from the ISS (<http://eol.jsc.nasa.gov/scripts/sseop/photo.pl?mission=ISS026&roll=E&frame=26493>). They calculated a final plate scale of 16 meters per pixel. A Point Spread Function (PSF) needed to be taken into account to allow for the blurring effect due to the movement of the vessel (ca. 500m/sec). A resolution of approximately 80m per pixel was finally calculated by the researchers. Additional treatment processes (e.g. removal of bad pixels) to enhance the image quality were applied to come up with an image that provides useful scientific data. Zamorano et al. recommend an operational setup and detailed calibration methods to obtain more useful images taken from the ISS.

ISS imagery is indeed promising for mapping and analyzing the light pollution at a city or regional level. The coverage of ISS images is still far from being complete. For Switzerland only for the greater Zurich and Geneva area such imagery exists. The use of ISS imagery for area-wide analysis is therefore limited. Elvidge, et al. (2007) describe an optimal set up of a satellite system capable of detecting night lights with a resolution suitable to delineate primary features within human settlements. Until the introduction of a satellite providing these features, the ISS images are assumed to be a valid, but uncompleted data source.

Sky brightness measurements by the use of the Sky Quality Meter (SQM) (Unihedron, 2014) have become popular amongst both amateurs and academics. This portable device is affordable and provides accurate results of the night sky quality (Cinzano, 2005). Several studies have analyzed the capabilities of the SQM and have attempted to map the night sky brightness and the light pollution by SQM measurements.

Pun & So (2012) led a comprehensive light pollution survey in Hong Kong. With the help of more than 170 non-specialist volunteers measurements were taken in urban and rural environments in Hong Kong. The results allowed a spatial and temporal analysis of the light pollution. A consecutive survey was led by

the same researchers (Pun, et al., 2014) using fixed installed monitoring stations throughout the city which eventually established the 'Hong Kong Night Sky Brightness Network (NSN) (<http://nightsky.physics.hku.hk/index.php>). The provided maps are based on 18 distinct location from which the measurements are taken. The rather small number of monitoring points does not allow for a spatially comprehensive data coverage and consequent mapping of light pollution.

An analysis of the street level light situation was conducted by Wu & Wong (2012). Different case studies were done at regional, district and street level scales. The focus was on the measurement of the night sky brightness (NSB) and the Street Light Level (SLL). The measurements were taken with mobile light measurement devices. The study reveals useful measurement procedures and understanding about the relation between built-up urban areas and the respective light emissions. A positive co-relation between light pollution and several socio-economical factors was observed. Factors such as the height of buildings, the type of shop in commercial areas or the relation between household income and light emissions in residential areas were analyzed. The results can give clues about the set-up of a light pollution model as described in the present study.

A similar survey – although in a much larger area - was done by Biggs, et al. (2012) in Perth (Australia): the researchers used a SQM and took measurements across a 24'00km² area of the city. From the acquired data, the researchers created an illustrative map of the light pollution situation of Perth. The influence of the land use (especially commercial and industrial areas) was confirmed by the study. It is suggested that commercial and industrial areas are producing more light pollution than urban land use. Furthermore, (poorly shielded) highway lighting and lighting along established transportation routes appear to contribute substantially to light pollution. Given the random locations of the measuring points in the research area, Biggs, et al. (2012) demonstrate a process to interpolate the data using ordinary 'kriging'. The study provides a practical approach to map light pollution for an urban area and its wider surroundings. Conclusions about detailed light sources can however not been drawn from the provided light pollution map. The results rather show an overall view and visualizes the decreasing light pollution with distance from the central business district of Perth.

Birriel, et al. (2010) provide an example of a light pollution analysis at a 'neighborhood' level for the campus community of Morehead, Kentucky (USA). SQM measurements were taken in accordance with the 'Globe at Night' protocol (http://www.globeatnight.org/learn_SQM.html) and a local night sky brightness map was established. Despite the multitude of measurements in a relatively small area (4 x 6 km), the study results allow no inference to be made about the specific causes (light sources) responsible for the light pollution. Still, the produced maps are expected to support the development of more effective and efficient lighting policies in the community.

Ground based measurements are time intensive and require a considerable staffing. This type of survey is therefore particularly suitable for involving students or volunteers in collecting data. Globe at Night (2014) is an international citizen campaign to collect worldwide light pollution data and raise awareness of the issue by informing and publishing related maps. Android or iOS based applications are provided to be used by mobile devices to collect data. The data coverage appears to be still rather incomplete (16'342 measurements in 2013). Contributions are primarily made from volunteers in the US, Europe or Japan. For this thesis, the use of crowd-sourced data was dismissed due to lacking data in the relevant research area. Several similar crowd-sourcing projects are running with the goal to map and monitor the global light pollution. In future, they could possibly offer promising results provided that participation, equipment and standards evolve further.

There are only a few published studies about the modelling of light pollution based on ground based measurements of the luminous flux (Lux). Wu & Wong (2012) demonstrate the use of the Lux meter in their study of the Street Light Level (SLL) in Hong Kong. SLL is an indicator for light pollution and includes glare and light trespass. The measurements can be used to describe where the light flux is higher than given standards or regulation. Measured values were observed to vary considerably within small regions. Conclusions can be drawn related to the relation between light intensity and light source. The researchers, for example, could determine a median light flux by shop type in the Hong Kong commercial district. Such information can be useful in the set-up of a model as done in this study.

A night 'city brightness' map was produced by Nobuaki Ochi from the Yonago National College of Technology (Ochi, 2013) by taking more than 2'000 measurements in the city of Yonago (Japan). The resulting maps distinctively show a high light flux in densely populated areas (city center) and more darkness in rural areas. The results of this study can serve to raise awareness amongst citizens. To gather deeper insight, however, data would need to be brought in relation with ground based features such as the location of the main light sources, the land use or the population density. The study is part of a wider campaign to educate and inform people about the issues of light pollution.

It has to be noted that Street Light Level measurements have only a limited suitability to infer the night sky quality. If lamps at shops and in the street are properly shielded upwards, little light radiates to the sky. The abovementioned studies by Ochi and Wu&Wong mainly address light pollution at street level.

A study that particularly dealt with the capabilities of modelling light pollution within a GIS could not be identified. Abovementioned research discusses a multitude of important aspect when attempting to model and map light pollution. Various elements were considered in this study and influenced the design of the research methodology.

3 Research Methodology

3.1 Problem statement

The pollution of the natural environment is increasingly topical in the public debate. The consequences of polluted air and water are well known, addressed and mitigated since many decades. Other types of pollution such as light pollution have only recently come into the perception of authorities and the wider public. The detrimental effects are nevertheless generally acknowledged and well documented (Narisada & Schreuder, 2004). Economic factors have additionally helped to raise interest in the light pollution topic: Municipalities in charge of public lighting have understood the potential cost savings from reducing light levels.

This increased awareness lead to a rising need for light pollution related data and knowledge. Authorities, municipalities and urban developers are reportedly lacking insight about the current light pollution situation (Frei & Kyburz, 2014; Luzern, 2014). Hence, there is missing knowledge where (and how) to potentially improve the light footprint of a neighborhood or an entire city.

One of the reasons for this lack of understanding is the non-availability of relevant data and maps. Comprehensive light pollution surveys are not commonly undertaken in contrast to, for example, air pollution measurements. The process of collecting light pollution data in the field is extremely time intensive and costly. The same applies for aerial photography which could actually provide valid data but is only considered by a handful of cities worldwide (see chapter 2.3).

Existing light pollution data over extended areas does exist from satellite imagery (see Chapter 3.5.6). The data resolution of more than 700 x 700 m footprint (Elvidge, et al., 2013) of one pixel is assumed to be coarse for a detailed analysis at a neighborhood level.

The problem, therefore, consists of finding an alternative way or process to produce and map light pollution data at a local scale. A prerequisite is that the process does without the abovementioned data inputs from aerial photography or already existing light measurements. Foremost, the research requires the analysis of the spatial light distribution in an urban environment, the understanding of light propagation rules and the effects of different technologies (lamp types) in place.

The evaluation of potential data sources is of particular importance. The challenge is to find suitable mapped data sources, based on which the location and distribution of luminous sources can be derived. In the core stage of the research a process must be developed that integrates data parameters into a Geographic Information System (GIS). The calibration of the model must be an integral component of the research in order to validate the model output.

3.2 Research questions

The problem addressed by this research consists of the lack of high resolution light pollution data. The research goal is to close this gap and to come up with a GIS based process that has the capability to produce the hitherto missing data. Consequently, the research questions are as follows.

- i. **What is a suitable set-up of a GIS based model to produce an upward light emission map at a local scale and what significance can the map achieve?**
- ii. What are the spatial distribution and the parameters to set for the relevant light sources in order to achieve a realistic model output in form of an upward light emission map?
- iii. What accuracy can the model output reach compared to a reference scenario (provided by a nocturnal image taken from space)?
- iv. What are potential advantages and disadvantages from the modelled output compared to other options of light pollution maps?
- v. What fields of application for a GIS based model can be identified?

Figure 11: Research questions: (i.) is the main question and (ii.) to (v.) are the sub-questions

The research question (i.) in Figure 11 describes the general direction of the research, the sub questions (ii.) to (v.) shall address concrete issues to be answered by systematic analysis and evaluation. Further questions are inherent as part of the problem statement, but are not listed in above figure. They are dealt with inside the consecutive chapters.

3.3 Research design

The chart in Figure 12 depicts the research design with its main research steps and activities in a sequential order from top to bottom. The intended research activities are clustered into headings which are depicted in rectangular boxes. The research is structured into two main parts. The first part (desk/field research) involves preparatory research to get a general understanding of the lighting situation in the research area (the research area is described in the following chapter). The second part is entitled with ArcGIS. It includes the integration and modelling of the acquired data from the desk- and field research in a desktop GIS. The output of the modelling process in ArcGIS model builder is a map of the upward light emissions of the research area. A feedback loop from the output map to the first element of the research design is indicated by an arrow and suggests the need for iterations to improve the model.

The research starts with activities under section A: A1 includes the identification of light sources. This can be done in the field or at the desk. Field activities consist of the careful observation of the

environment with the goal to understand which man-made elements are light emitting sources. The result is a number of categories with light emitters, such as ‘car parking’, ‘shopping streets’ or ‘motorways’. Activities under A2 involve the search for digital data that serves as the basis for the consecutive modelling process. Data sources are later described in chapter 3.5 (Data requirements). At the same time, aerial night time imagery data is searched for. Images will be used as reference data.

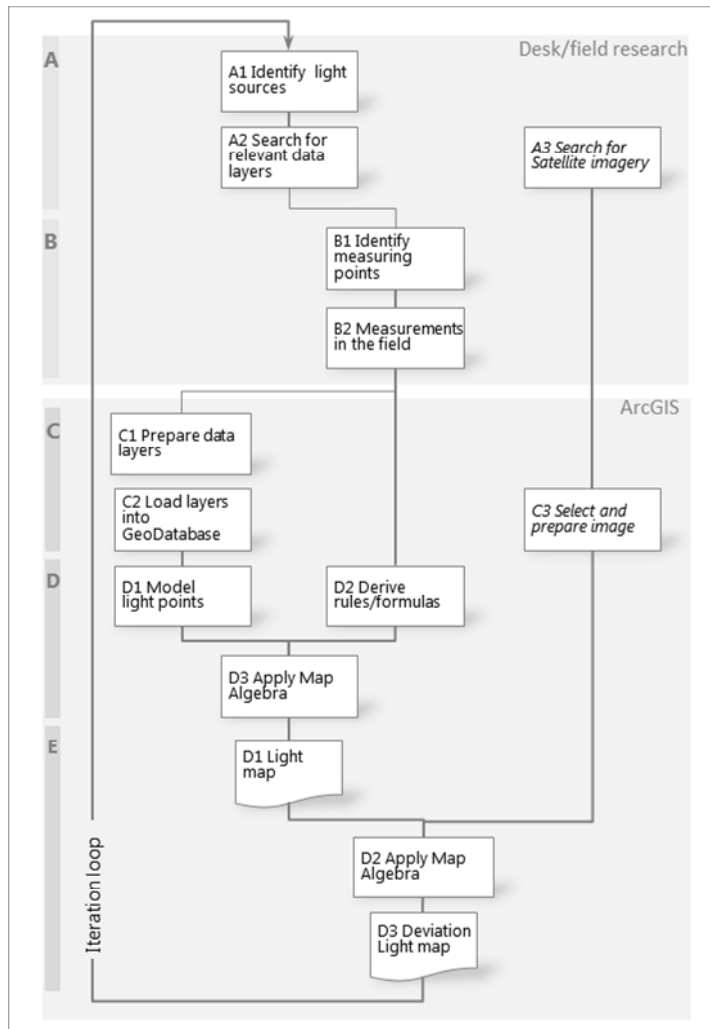


Figure 12: Research Methodology flow chart. The major steps are shown in a sequential order from top to bottom. Desk- or field research activities are shown in parts A and B. The consecutive steps in parts C to E are done within a Geographical Information System environment (ArcGIS). A loop from the output maps to the first step of the process indicates the iteration process to improve the model.

Activities in Section B (B1 and B2) include the location of suitable spots in the field to collect data. Subsequently, light measurements are taken at these spots with an appropriate device. The location of suitable places can be done either by observation in the field or by analyzing high resolution digital maps. The ‘suitability’ of a measuring spot is determined by the representativeness of the sample taken. Field measurements can only be taken at night.

Section C mainly comprises the preparation of the light feature data identified in A2 and its transformation and preparation for the integration into a geo database. C3 namely involves the georeferencing of a suitable satellite image.

Section D contains the core of the modelling process: D1 represents the creation of 'light points' according to the observations made in B1. A correct spatial distribution of these points is crucial. Further, each light must be attributed a representative light intensity and light propagation rule (D2), as measured during the field research activities in B2.

The last stage of the research involves the testing of the validity of the model output. This is done by comparing the output with a reference scenario. The evaluation of various data sources determines an appropriate reference data set. The primary goal of the comparison is the validation and calibration of the model. Another intention is to better understand the advantages and disadvantages of the modelled data compared to real (measured) light pollution data.

3.4 Research area

The research area covers a surface of 107.4 km² (extension: East-West: 11.7 km; North-South: 9.2 km). It includes the town and the suburbs of Winterthur, a city in the north-eastern part of Switzerland (Figure 13). With a population of 108'124 (Stadt Winterthur, 2014), the city ranks 6th largest in Switzerland (Swiss Federal Statistical Office, 2014). The built-up area consists of a historical center from the 15th century, surrounded by residential areas mainly constructed in the late 19th and early 20th century. At that time Winterthur particularly thrived and developed into an important industrial center (iron foundry, constructions of machinery and spinnery). Industrial areas still represent a considerable part of the city surface. With the decline of the heavy industry, the old industrial buildings are currently being transformed into offices and modern apartments.



Figure 13: Research area: Location of Winterthur (Switzerland), city of more than 100'000 inhabitants, in the north-eastern part of the country. The research area is marked in red and measures 107 km². The area covers the town of Winterthur and its suburbs and neighboring natural areas, especially woods.



Figure 14: Research area: detailed view. The area contains a rich variety of features, especially residential and industrial buildings and a network of streets at several levels. One of the most significant features is the national motorway A1 (St. Gallen - Geneva) that circumscribes the city.

Source: Base map from Swisstopo / Cartography: Stefan M. Bruehlmann

Source: Swisstopo; Cartographic modifications: Stefan M. Bruehlmann

Figure 14 shows the research area at a larger scale. It visualizes how the city is imbedded in the surrounding rural landscape, which is mainly dominated by extended woods. As for the topology, there

are seven hills around the city with an elevation of approximately 160m above the city level which is at 438m above sea level. The elevations proved to be suitable spots for nocturnal observation and photographic work. A more detailed map with further explanations on particular features, the transportation network and the land use of the study area can be found in appendix C. This detailed map provides useful contextual information for a better understanding of the research method.

The choice of this particular research area was done systematically by considering a number of prerequisites: As the goal of the research was to come up with a model that should be applicable to other areas, the research area needed to be representative. This means that it should include a maximum of different features, street levels and land uses. The area should be richly structured, comprising urban, suburban and natural elements. The street network should feature the whole variety from national motorways down to residential streets with limited traffic and low lighting. The totality of these features should be available in digital format for easy integration into a model in ArcGIS. The exact data requirements are described in chapter 3.5 .

The size of the study area was limited due to the extensive amount of data required. In the pre-study of this thesis it was anticipated that dealing with a very large area would require considerable computer processing power and could result in extended calculation times, especially because the model should produce raster data at a high resolution.



Figure 15: Research area: View of the Old Town of Winterthur (Steinberggasse). The old town area is used for commercial and residential purposes. Shops and restaurants are typically located on the ground floor and apartments on the floors above.

Photo: Stefan M. Bruehlmann, 2014



Figure 16: Research area: Bird eye's view of 'Wülflingen', a residential district of Winterthur. The picture is taken from the look-out on 'Brüelberg', 546 m above sea level. Characteristic are the hills around the city and the absence of buildings with more than 10 floors.

Photo: Stefan M. Bruehlmann 2012

A crucial, perhaps the most important point was to choose an area with which the author was familiar. Also it was considered to be an advantage that the research area could be reached easily, given the fact that multiple visits and field work at night were planned. Familiarity with the local situation would help to

navigate target-oriented in the field and to link knowledge from various sources (e.g. maps, images, existing reports, etc.) with personal experience and observations.

Finally, it would be beneficial if local authorities of the selected research area could propose help and knowledge. This could be in form of data or of expert advice. The authorities of Winterthur signaled that light pollution is a topical agenda point and that referring knowledge could be provided.

The evaluation of above points lead to the decision to apply the research to a rather limited area around the town of Winterthur. Competing areas included the Swiss towns of Basel, Schaffhausen and Zurich where the author has an equal local knowledge. The factor 'accessibility' was eventually decisive.

3.5 Data requirements

3.5.1 Digital maps

The availability of high quality digital map data was central: The model as shown in chapter 3.6 (Conceptual Model) for calculating and visualizing light pollution is mainly based on features from digital maps. The quality of the mapped data has to be impeccable. Error propagation can then be excluded. During the process of finding appropriate data, several sources have been evaluated and tested. The four criteria were evaluated in finding the right data: a) completeness, b) accuracy, c) form/usability and d) costs.

The criteria 'completeness' required that a data source did not miss any features. For example, it was important that a residential street network included 100% of the streets - even a small footpath (which usually is illuminated and therefore qualifies as a light emitting feature). 'Accuracy' was important to make sure that the digital data was recent and correctly georeferenced. The 'form and usability' as formulated under requirement c) requested that the data were available in a format that was relatively easy to handle in a desktop GIS and did not require extensive data transformation or correction. Finally, the last requirement asked for moderate cost of the data. Certain data sets come at considerable price, depending on the size of the area covered. The current study covers more than 100 km² which involves a large volume of data – therefore, potential costs for the purchase of data can rise to exorbitant levels. It has to be kept in mind that this study suggests that the research area could be extended to an even larger surface, such as the entire country of Switzerland. Considering this, costs are a crucial item in the right choice for source data.

In the research for appropriate data two possible data sources could be identified: a) Vector 25 data from Swisstopo and b) Open Streetmap (OSM) data, freely available from the internet.

Swisstopo is the Swiss Federal Office of Topography and provides datasets in a vector format at a scale of 1:25'000 (Swisstopo, 2014). The data is especially suitable for applications in geographic information systems. For the entire country of Switzerland it describes about 8.5 million objects with an accuracy of 3 to 8 meters. The data is available in ESRI shape file format.

OSM data (Open Street Map, 2014) was considered to be an alternative source to the very complete and accurate data from Swisstopo. OSM data can be downloaded and integrated into ArcGIS by using different techniques and processes. Considering the extended geographical area of this research, data downloads from OSM are however tedious and not very straight forward. Additionally, various tests have shown that OSM data would not have the same accuracy as the official data from Swisstopo. Especially it became obvious that the classification of the street network was not fully consistent and that certain important features necessary for the construction of the model were not available in the OSM data.

The priority was therefore given to the use of Swisstopo data. Only certain layers which were not available from Swisstopo were downloaded from OSM. The overview of the purchased / downloaded data is shown in the following table. The choice of the required layers was made by evaluating whether the particular layer has relevance in the modelling of the light pollution; e.g. road networks were considered to be a major contributor of light emissions and are therefore retained as data for the model. Further details are discussed in Chapter 3.6 (Conceptual model).

Table 1: Swisstopo and OSM data for use in the Light pollution model

Swisstopo		OSM (Open Street Map)	
Layer	Remarks	Layer	Remarks
1. Road network	used for model	Car Parking	used for model
2. Railway network	used for model	Sports Pitch	used for model
3. Other Traffic	not relevant		
4. Primary surfaces	used for visualization		
5. Hedges and Trees	not relevant		
6. Single Objects	not relevant		
7. Hydrological network	used for visualization		
8. Buildings	used for model		
9. Facilities	not relevant		

Swisstopo data provides nine different thematic layers, each containing multiple attributes. The table shows what data was used for the model. Certain features were only useful for visualization purposes. Swisstopo could cover almost all of the data needs except two thematic layers. Those two layers were extracted from OSM. The data used for the model includes features that are considered to be relevant for the modelling and visualization of light pollution

An example of Swisstopo data is shown in the following illustrations (Figure 17 and Figure 18): Individual buildings and streets are well distinguishable. The digital data provides features in a suitable quality and detail to model the light emitting sources of a town. For example, lights along streets can be accurately modelled given the high precision of the data.

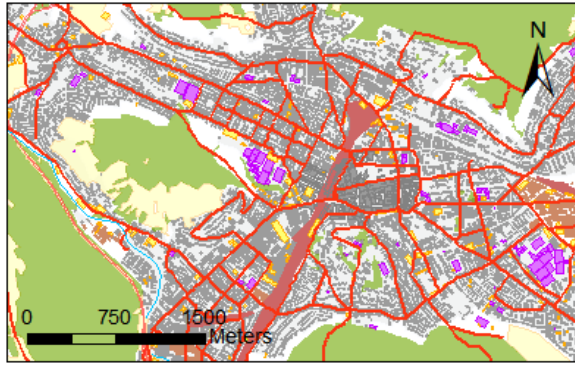


Figure 17: Swisstopo map features; Scale 1:25'000. This extract shows the main part of the city of Winterthur with houses, street network and natural areas.

Source: Swisstopo / Cartography: Stefan M. Bruehlmann



Figure 18: Swisstopo map features; Scale: 1:1000. Individual buildings are clearly identifiable. Accuracy of data is 3 to 8 meters.

Source: Swisstopo / Cartography: Stefan M. Bruehlmann

3.5.2 Observations in the field

The maps from Swisstopo provide a solid basis of all relevant natural and infrastructural features in the research area. Understanding how light sources are distributed, what kind of different light sources are in use and what are the patterns of light propagation can, however, not be derived from these maps. This knowledge has to be acquired either by maps that exactly address this topic, or by observation and measurements in the field.

For this study, no data layers about light sources in the city of Winterthur were available in a GIS format. Usually, such vector data is not publicly available and only provided to other departments of the city administration. It has to be noted that municipalities are usually not managing the totality of lights in a town. For example, the lighting of the train stations and their surrounding areas is managed by the Swiss Federal Railways. Backyard lights in residential areas are likewise out of the scope of the cities' responsibilities.

Given the lack of explicit digitized data on light sources, field observations were done. The aim was to understand particularly a) how different streets are illuminated; b) what type of lights is used and c) how light propagates. This latter point had to be understood by doing exact light measurements (see chapter 3.5.4 Field measurements with 'Lux Meter'). An additional point where data could only be collected from observation in the field was the question how light reflects from the ground: this phenomenon is also known as 'albedo reflectance' (Bariou, et al., 1985).

This question is insofar of relevance since it was assumed that all light that can be seen and measured from space is the result of the reflection of light by ground surfaces. The understanding to what extent the surfaces, i.e. streets (asphalt) reflect light is of particular interest. Albedo reflectance data is an important data element in the model.

3.5.3 Patterns derived from aerial/satellite imagery

Aerial images are an indispensable source for the understanding of the distribution of light sources in an urban environment. In the field, significant time is needed to detect, measure and understand the spatial distribution of the light sources. Therefore, satellite imagery is predestined to serve as a rich data source for desk-research based analysis of the relevant light sources.

Google Earth (Google Earth, 2014) is an ubiquitous software and can well be used for the web-based inspection of large scale images. The image quality can however be limited, depending on the location and the moment it is taken. There are providers that offer imagery at higher resolution. Superior imagery quality comes at cost, though. For this study, a composition of digital aerial photographs provided by Swisstopo (Swisstopo, 2014) could be used. The imagery was provided by the city of Winterthur and was extensively used to locate and analyze light sources and their spatial parameters. The images feature a resolution of 0.5 m. They show a very high level of detail, sufficient to locate single light sources such as individual street lamps along streets of different hierarchy. Figure 19 and Figure 20 show an example of how street lights along a motorway could be identified and how their distance could be evaluated. The understanding of how public lighting is arranged could be gained by visual inspection of this high quality imagery. It became clear that getting the same insight based on field trips was merely impossible, given the large research area and the difficulties in exactly measuring distances in the field.

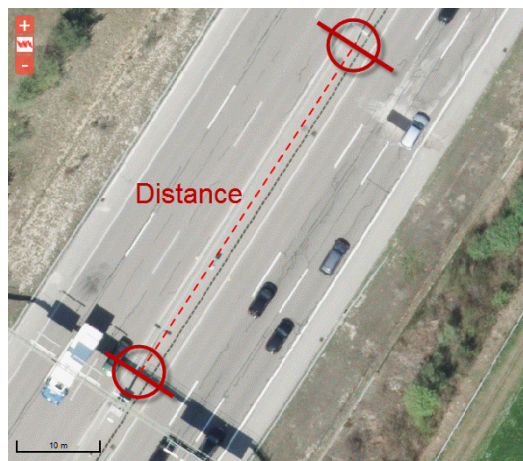


Figure 19: Visual inspection of SWISSIMAGE: Street lights in the middle of a motorway are detected by visual inspection and are marked with red circles. The distance from one street light to the other could easily be measured. This information served as vital input for the modelling process.

Source: SWISSIMAGE by Swisstopo
Cartography: Stefan M. Bruehlmann



Figure 20: Visual inspection of SWISSIMAGE: Large scale view. Small details become visible. In this picture an individual street lamp is encircled. Its shadow falls in a north-eastern direction. The high resolution of the image can be understood by looking at the car on the right-hand side of the image.

Source: SWISSIMAGE by Swisstopo
Cartography: Stefan M. Bruehlmann

Night-time aerial imagery is rarely available. One reason is its high production costs. A few studies that analyze night satellite imagery images exist and were described in Chapter 2.3. One of those studies was done in Geneva (Switzerland). Some examples images from that study could be analyzed. The inspection

of the high resolution images was providing insight about the light propagation, the visual impression of different lamp types and the reflection properties of the ground (albedo reflectance). Figure 21 shows an excerpt of an orthophoto from the study done by the city of Geneva (Frangiamone, 2014). It clearly shows the illuminated street network and the different lamp types as represented in different colors (orange, greenish, blue, etc.). Very focused light has a strong reflectance (main street lighting) whereas the white colored light lamps are hardly reflected at the ground (right-hand side of the picture.)



Figure 21: Orthophotograph of Geneva (Switzerland). Aerial images reveal a lot of information about the characteristics of the street lighting in a city. Different light temperatures imply the use of different lamp types. The propagation of light is different based on the technology too. Finally, albedo reflections depend on the type of the ground surface. Visual inspection of such sample images gives clues about the parameters of an appropriate light pollution model.

Source: City of Geneva (Switzerland)

3.5.4 Field measurements with 'Lux Meter'

Light intensities can hardly be derived from (nocturnal) orthophotographies. One of the most crucial inputs for the model are the light intensities from the different light emitting sources. For example, it had to be found out how much light is emitted by a street light in a residential street and how much by a floodlight on a sports pitch. Unless there is exact data provided by the municipality in charge of public lighting, the light intensities can only be found out by measurements in the field.

Given the absence of official data for this study, several dozens of measurements of various light sources have been taken in the field. A light meter (or Lux meter) as shown in Figure 22 has been employed for the nocturnal measurements. This device captures the environmental brightness. Specifically it measures the intensity with which the brightness appears to the human eye. A light meter uses a photo cell to capture the light. The captured light is then converted to an electrical current. This current finally allows the device to calculate the Lux value of the light which has been captured.



Figure 22: Light meter (Lux meter) used for the field measurements in this study: The device is composed of a sensor (lower part of the image) and a display of the measured light intensities (upper part of the image). The light meter captures the brightness of an environment. The unit of 'Lux' derives from the unit 'candela' which is another measurement of light intensity. (Historically, 1 candela was equal to the light intensity of one regular candle). The employed device is a handheld light meter from the Belgium producer 'Velleman', B-Gavere' (type: 'DVM1300'). (<https://www.velleman.eu/home/>) :

Photo: Velleman

During April and July 2014, twelve nocturnal field excursions were undertaken to different locations in the research area in order to measure the light intensities of preselected light sources. Totally more than 300 measurements have been recorded. After a couple of test runs and consequent improvements, the measuring procedure was stable enough to be applied identically to all selected light sources and places.

The process basically consisted of measuring light intensities of preselected light sources at different distances (see Figure 23). Measurements were read from the Lux-meter's digital display and then captured instantaneous into a handheld tablet (ASUS Fonepad ME372CG) by using the Mobile Data Collection-application from GISCloud (2014). This application allows for automatic geo-location of the measurements and comfortable export of the data into ArcGIS.

In a discussion with experts from the municipality of Winterthur (Frei & Kyburz, 2014) it could be confirmed that the applied measuring procedure conformed to the measuring procedures of the lighting unit of the municipality of Winterthur. In fact, the municipality equally uses a Lux meter to check on light intensities. Their technique is very similar to that applied in this research.

In the post-processing of the light intensity measurements, data was exported to a csv-format for establishing a light propagation chart and a regression line. From the latter, an equation shall be derived. The equation describes the light propagation by light source and is an key parameter for the light model as presented in chapter 3.6.

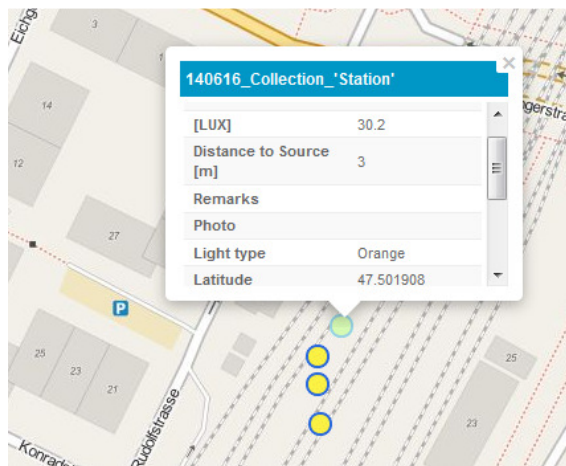


Figure 23: Mobile data collection: The map extract shows an area around the central railway station of Winterthur where light intensity measurements have been taken (yellow circles). The measurements were taken with a Lux meter and were registered on-site in the GISCloud application <http://www.giscloud.com/apps/mobile-data-collection>. The geo-referencing function allows for visualization of the measurements on a slippy map.

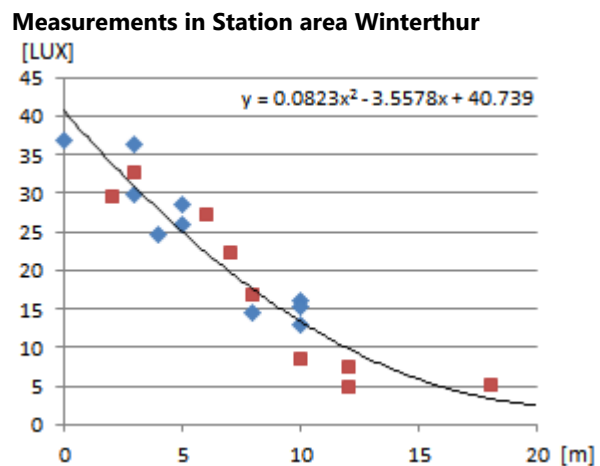


Figure 24: Chart from the Mobile data collection: data from the light intensity measurements are extracted to a csv format and further processed in order to calculate the chart above. It shows the decreasing light intensities in function of distance to the light source. An approximation line has been added. The equation of this line will be used for the calculations in the light model. Red and blue points describe different dates of measurement.

An alternative way to determine the illumination intensity of streets is the use of standardized data. The European Norm EN 13 201 gives recommendations on the use of 'Streetlight' and defines ranges of (minimum) illuminations depending on the type and use of the street. The Norm has been elaborated by

the European Committee for Standardization (CEN, 2003). It is applied in all 28 EU countries and in Switzerland. The municipality of Winterthur has to comply with these standards. The current light intensities are within the recommended ranges. The use of standard data for this study was finally not given consideration because of their broadly interpretable nature. An example of the EN 13 201 is provided in Appendix K.

3.5.5 Data from 'Sky Quality Meter'

There are various concepts of measuring the light intensities in an urban environment. As seen in the previous chapter, measurements with the Lux-meter capture the ambient light at street level. The results normally describe the direct light from street lamps. The concept of measuring the 'sky brightness' is somewhat different. It involves the measurement of a very small patch of the sky. Hence, in order to measure the 'sky brightness' the device needs to be pointed vertically upwards. For this study several 'sky brightness' measurements were taken with a so called 'Sky Quality Meter' (SQM). This handheld tool is produced by the Canadian company 'Unihedron' (Unihedron, 2014) and is offered in various versions. Its capability and accuracy has been described in a paper by Cinzano (2005), one of the most prominent researchers in the field of light pollution.

The sensor of the SQM captures the light via a lens. The measuring unit is 'mag/arcsec²' which represents the surface brightness in magnitude units related to the solar luminosity per square arc second. The 'mag/arcsec²' scale ranges between 14 (completely polluted sky) to 23 (fully pristine sky). One of the intentions of this research is to evaluate the creation of a 'night sky map' of an urban area of Switzerland. SQM measurements can provide core data for this. The exact data acquisition procedure with the two devices, Lux meter and Sky Quality Meter, is described in further detail in chapter 3.6.2.



Figure 25: Sky Quality Meter – L (Narrow field of view, with Lens). This handheld device measures the brightness of the night sky in magnitude per square arcsec. (mag/arcsec²). The SQM is produced by the Canadian company Unihedron (<http://unihedron.com/projects/sqm-l/>)

Photo: Unihedron

3.5.6 Satellite imagery

For the comparison and validation of the model output with the 'real world' situation, the research design foresees to use satellite imagery as a reference. Satellite imagery is increasingly made available to the wider public. Several providers are largely investing in technology for casting near real-time imagery from space.

In April 2014 the European Commission announced the launch of the Sentinel 1A satellite, which is the first of the six missions in the framework of the 'Copernicus' initiative (European Commission, 2014). Sentinel data products are made available as open data. For the moment, however, Sentinel1A is not providing night imagery of visible light bands. Nor do comparative commercial systems from the U.S. such as Landsat 7, Quickbird, IKONOS, Orbview3, Geoeye and Worldview 1 and 2 offer night imagery.

For more than 40 years, the only system that could collect global low light imaging data are the U.S. Air Force Defense Meteorological Satellite Program (DMSP) and the Operational Linescan System (OLS). They operate with a relatively coarse spatial resolution and a limited dynamic range. In 2011 the National Aeronautics and Space Administration (NASA) and the National Oceanic and Atmospheric Administration (NOAA) launched the Suomi National Polar Partnership (SNPP) satellite carrying the first Visible Infrared Imaging Radiometer Suite (VIIRS) instrument.

VIIRS has a number of advantages compared to the DMSP/OLS program: especially the ground pixel footprint at nadir of 742x742m (0.55 km²) compared to 5 x 5 km (25km²) for DMSP/OLS. A further advantage is the superior quantization of 14 bit compared to 6 bit and the inflight calibration of the VIIRS product. Elvidge, et al. (2013) provide a useful comparison of the two products – both able to produce Day/Night band (DNB) images.

Some VIIRS data sets are publicly available and can be downloaded from the National Oceanic and Atmospheric Administration (NOAA National Geophysical Data Center, 2014). For this research an analysis of VIIRS data was made based on a download of a cloud free composite image of Europe. Observations between April 2012 and October 2012 were used.

Tile 2 covers the continents of Europe, North Africa and parts of the Middle East. The image was downloaded in a GeoTIFF (zipped) format and then loaded into ArcGIS. Figure 26 shows the quality of the VIIRS pictures at different scales.

At a small scale, the VIIRS images provide an appropriate resolution to visualize the light emissions in Europe. Image B shows the country of Switzerland (yellow boundaries). Highly illuminated areas can be seen along the lake of Geneva (extreme west of the country) and the region of Zurich (marked with a rectangle). In the Alps (central part of the image), the upward illumination is merely absent. Image C depicts the Zurich area. The lake of Zurich is clearly visible as well as the down-town area on the north-western end of the lake. In Image D, a zoom to the city of Winterthur is shown. The cut-out is identical to the study area. Single pixels become apparent. Their footprint is 0.55km² (742x742m). The limitation of VIIRS data at this very large scale becomes obvious.

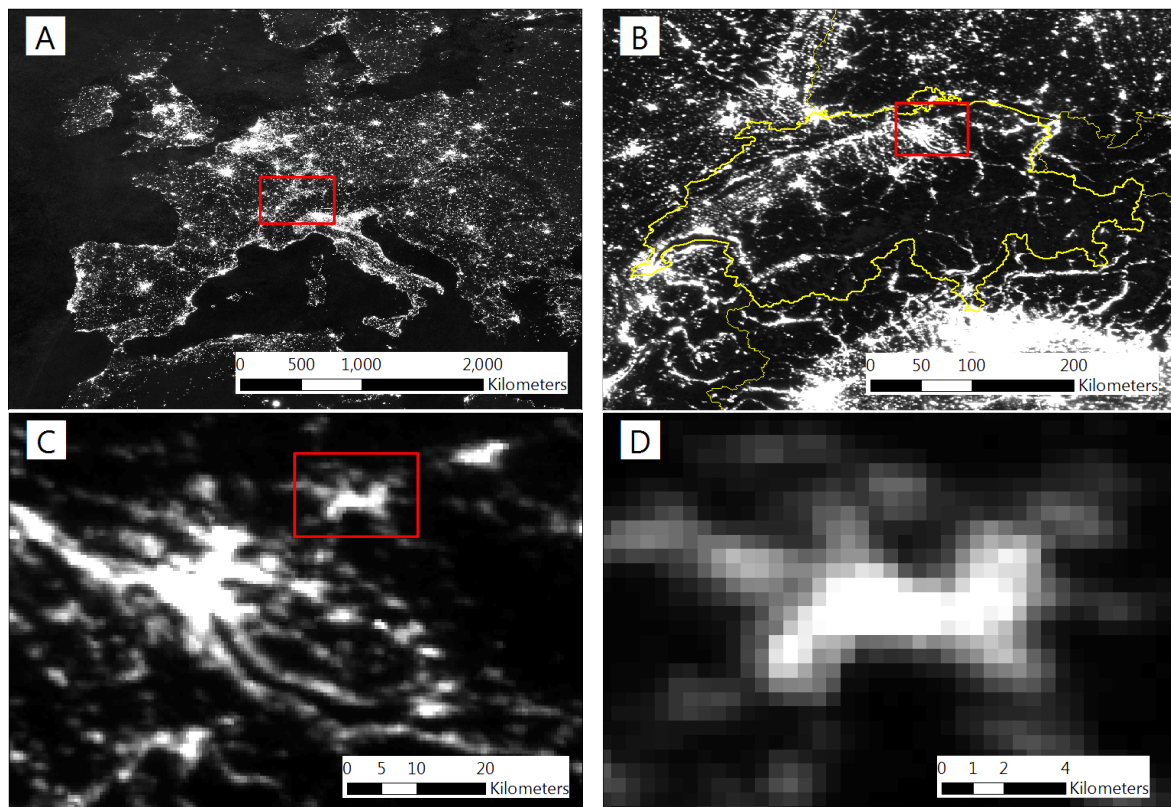


Figure 26: VIIRS images at different scales: Image A shows a view on the European continent. Image B is a zoom on the country of Switzerland. The major populated areas Geneva (on the left) and Zurich (on the top right) can be seen. Image C shows the area of Zurich. The city is visible on the middle left of the image. The lake is clearly distinguishable with its illuminated shores in the center of the image. Image D shows the city of Winterthur. The extent of image D shows the research area of this study. The resolution is at 742x742m. It is obvious that the VIIRS data has its limitations in terms of detail.

Data source: <http://ngdc.noaa.gov/eog/viirs.html> / Cartography: Stefan M. Bruehlmann

VIIRS data sets can provide valuable information for light pollution analysis at a regional or national scale. For the moment, VIIRS is probably the most valuable source for analyzing light pollution at a regional scale. Data coverage is very complete and actual. The purpose of this study is, however, to model and visualize light emissions at a *local* scale. VIIRS data is considered to have only a limited suitability for a local analysis. Therefore, other data sources have to be considered. Digital single-lens reflex (DSLR) images are an alternative. Astronauts on board of the International Space Station (ISS) are taking pictures of the earth and make them available to scientific purposes or to the wider public.

3.5.7 Imagery from the International Space Station (ISS)

The International Space Station (http://www.nasa.gov/mission_pages/station/main/) was launched in 1998. It is the largest artificial body in space. The ISS serves as a laboratory for various experiments. Astronauts on the ISS have taken several hundred thousand of images from the earth using commercially available DSLR cameras. Combined with high aperture lenses and a device to compensate for the movement of the space station (Cosine, 2013) the images are of high quality. They usually feature a pixel footprint of as little as 10m (NASA Earth Science and Remote Sensing Unit, 2014).

ISS Images can be obtained from a repository on the internet. A part of the photos was taken by night and can potentially be used for comparison with the model output of this research. To date, only a few images of Switzerland were taken at night. The most suitable image for this study is shown in Figure 27:

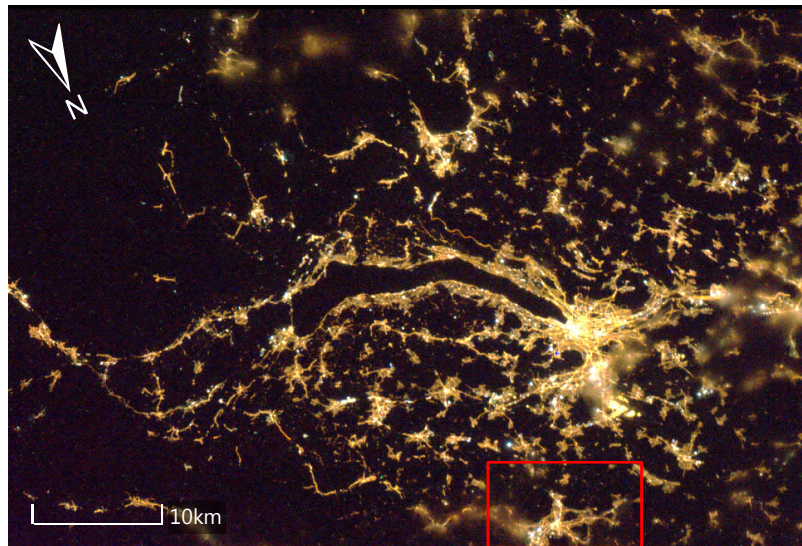


Figure 27: Night image of the greater Zurich area from ESA. The picture was taken with a DSLR camera from the ISS by ESA astronaut Paolo Nespoli on 30 January 2012. Format: JPEG (Size 564.82 kb), (ID20722)

Source:

http://www.esa.int/spaceinimages/Images/2011/01/Lake_Zurich_by_night

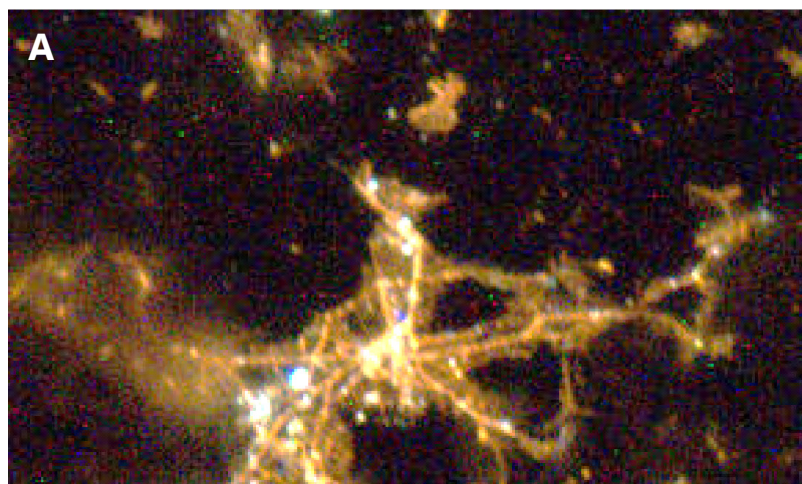


Figure 28: Night image of Winterthur. Detail of the image shown in Figure 27. (cut-out shown with a red square)

Image A: The part of the city on the left side is overcasted by clouds. Some areas of the city are not included in this image because of the limited dimension of the original picture. The highly illuminated city center and rail station area is distinguishable. The bright white points are illuminated sports fields.

Source:

http://www.esa.int/spaceinimages/Images/2011/01/Lake_Zurich_by_night



Image B: Aerial image of the same region. Populated areas as colored in red.

Source: Google Earth 2014

Cartography: Stefan M. Bruehlmann

The picture in Figure 27 was taken from the International Space Station in 2012 by the ESA astronaut Paolo Nespoli. http://www.esa.int/Our_Activities/Human_Spaceflight/Astronauts/Paolo_Nespoli. It shows the greater Zurich area at night time. The lake of Zurich is clearly visible in the center of the image, as well as the city center at the lake's western end. The city of Winterthur is located at the lower boarder of the image. The area that corresponds with the research area of this study is marked with a rectangle.

Figure 28 shows a detail of the ISS image shown in Figure 27. The view corresponds to the research area. A detailed visual inspection revealed a moderate but usable image quality at this large scale: the photo showed no major motion blur. Features such as the main roads, sports fields or the station area are distinguishable. The image features three bands (red, green and blue). The pixel size is approx. 48m x 48m. The major defect of the image is the incomplete coverage over the entire research area and the partially blurred areas because of aerosols and clouds.

In addition to using the available images from the repository, students and researchers can submit a request to have the ISS astronauts acquire new photography for their investigation (<http://eol.jsc.nasa.gov/DataRequest/>). Proposals and justification of the research will be reviewed by the Crew Earth Observations team. The author of this study has submitted a request to NASA for an image from the Winterthur area. The request was formally approved by NASA on 5 March 2014 (Higgins, 2014a). Unfortunately the image could not be realized within the timeframe of this study. The main reason was unfavorable metrological conditions (cloud cover) during most of the summer 2014.

3.6 Conceptual Model

3.6.1 General

The conceptual model forms the main part of the research methodology. The model makes use of geographical data sets and field measurements as described in Chapter 3.5. The purpose of the model is to represent the aspects of the real world in a computer system. Figure 29 depicts the role of a data model in GIS.

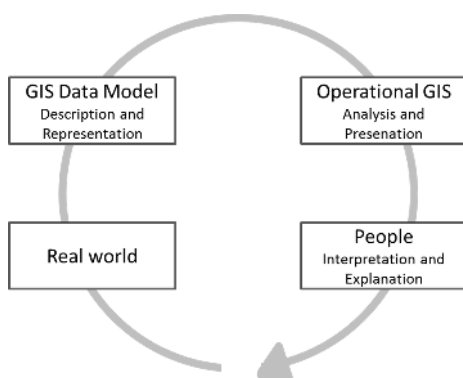


Figure 29: The role of a data model in GIS: The data model is a set of constructs to represent objects and processes of the real world in a digital environment (GIS). People interact with this system in order to do analysis and to visualize the data. This research mainly focusses on the boxes entitled 'GIS Data Model' and 'Real world' (see Chapter 3.6).

Illustration: Stefan M. Bruehlmann, adapted from Longely, et al. (2011)

The type of analyses and insight that can be gained from a model is largely dependent on the way the real world is modelled (Longely, et al., 2011). This includes decisions on what real-world elements are taken into account and included into the model. The consideration of people (GIS users) in the design of the model is of importance. Finally they make interpretations based on the model output and provide explanation. These latter aspects are touched upon in this study, too, when discussing the potential user of the modelled results.

The model proposed in this study is entirely numerical and is developed in a commercial Geographic Information System (GIS). The 'model builder' tool in ArcGIS 10.1 (ESRI, 2014) was used to logically link all elements of the model, to set the parameters and to calculate the model output. Model builder allowed for repeated adjustment of the parameters and for the repeated run of the model. This way, various output results could be produced, compared and improved. The model deals with raster datasets at a very high resolution (1 meter). Therefore, running the model requires considerable processing time. The duration is depending on the capacity of the central processing unit of the computer.

3.6.2 Data acquisition process and derived parameters

Figure 12 on page 19 illustrated the research methodology. The last step in the 'field research' section showed the measurements of the light intensities of selected light sources. This step is most crucial to feed the model and to make it work. The intention of the model is to 'rebuild' each light point in the research area as realistic as possible. Hence, reliable data from several light sources had to be taken. For this purpose, representative measurement locations were identified and measurements taken according the following procedure:

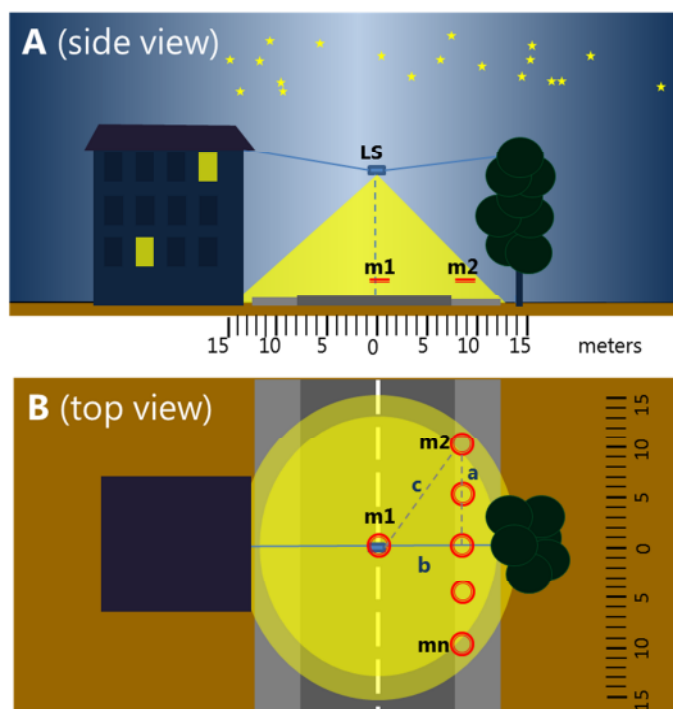
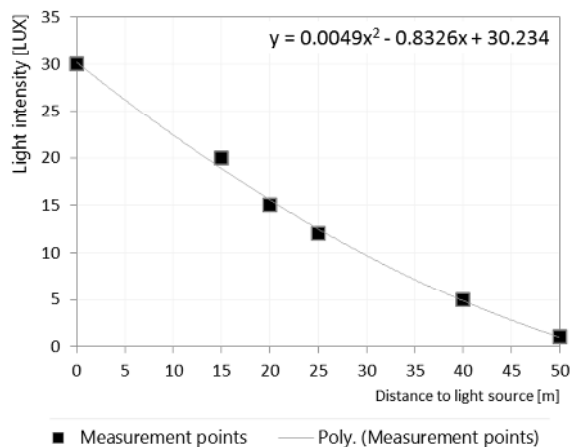


Figure 30: Procedure of light measurements using a Lux meter. The Light source (LS) is suspended over a main road and spreads a light cone. Light measurement points are indicated with a red circle (m1 – mn). Collected data was eventually plotted in a 'distance/intensity' chart and a light propagation formula was derived.

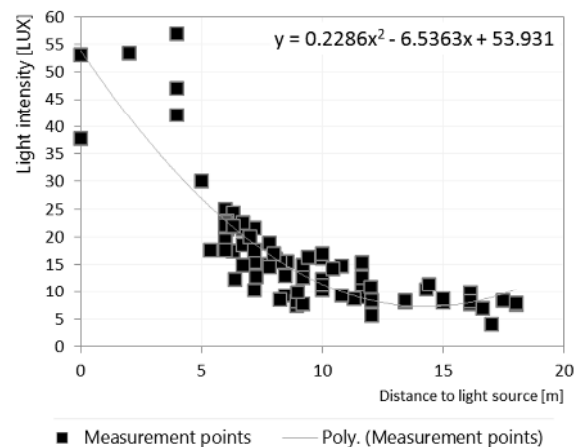
Illustration: Stefan M. Bruehlmann

The measurement procedure as shown in Figure 30 was applied identically for the light sources (lamps) of all ten feature categories (motorway, main street, residential street, etc.). It consisted of taking repeated measurements while walking along or around the respective light source. For larger streets, measurements were limited to the edge of the roads (measurement points m2 – mn only). Taking measurements at the point m1 was not possible at motorways because the street could not be entered safely. The distance ‘a’ was estimated by counting steps (two steps = 1 m). Relevant for the light model was however the distance ‘c’ (direct distance from measurement point to LS). It was calculated by applying the Pythagorean Theorem. The measured Lux value and the distances were plotted in an x/y chart (x= distance, y =Lux) and a regression line was derived. The equation of the regression line served as input parameter to model the light spread of each light point in the model. The exact measurement results and charts are shown by feature category in the following charts (Figure 31 and Figure 32).

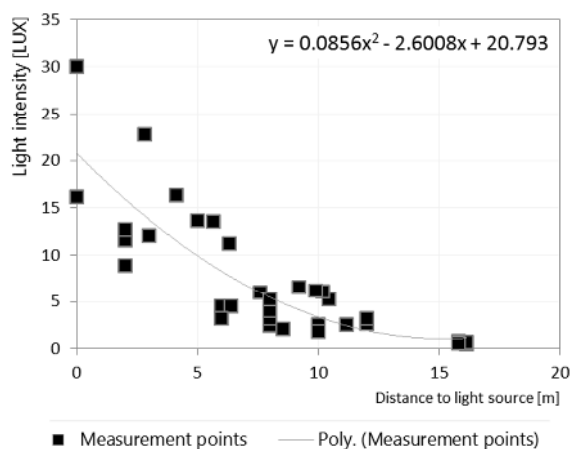
a) **Class A Roads:** Illumination in function of Distance
Source: Measurements LuxMeter; 27 June 2014



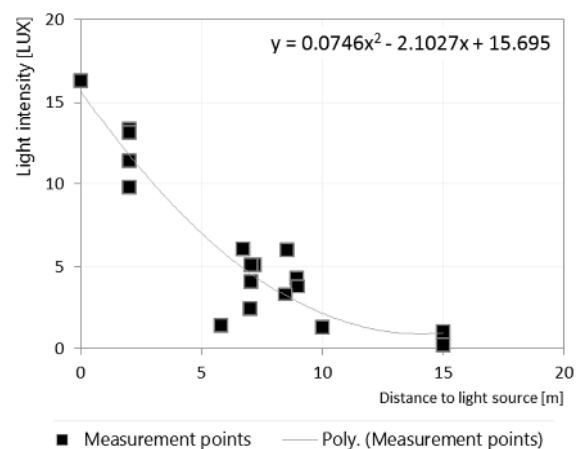
b) **Class 1 Roads:** Illumination in function of Distance
Source: Measurements LuxMeter; 18 / 27 June 2014



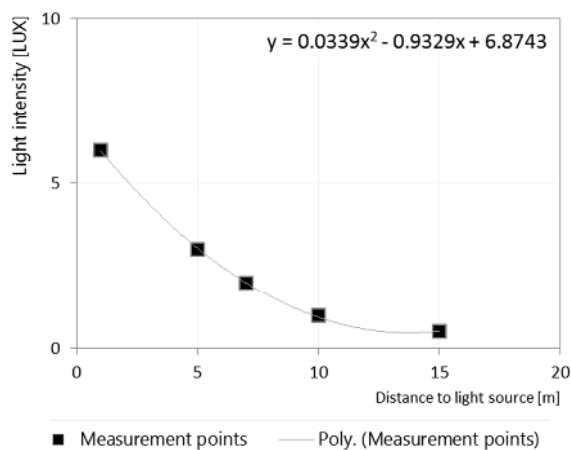
c) **Class 2 Roads:** Illumination in function of Distance
Source: Measurements LuxMeter; 27 June 2014



d) **Class Q Roads:** Illumination in function of Distance
Source: Measurements LuxMeter; 27 June 2014



e) **Buildings Residential:** Illumination in function of Distance
Source: Measurements LuxMeter; 7 July 2014



f) **Buildings Industrial:** Illumination in function of Distance
Source: Measurements LuxMeter; 7 July 2014

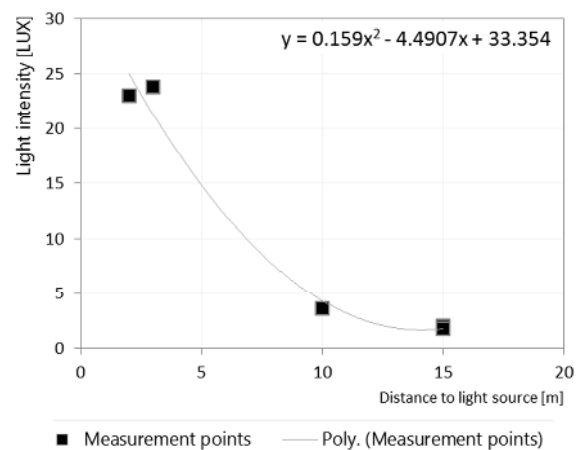
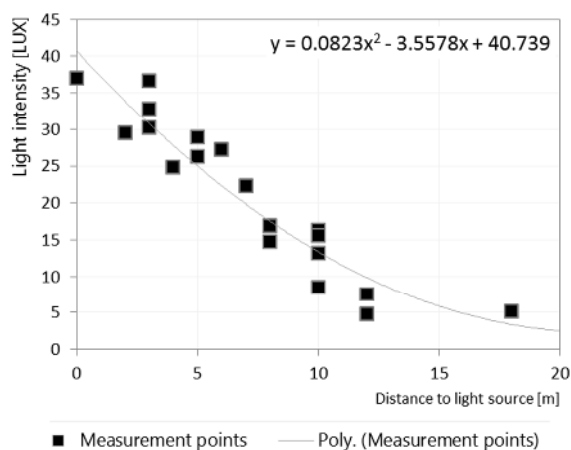
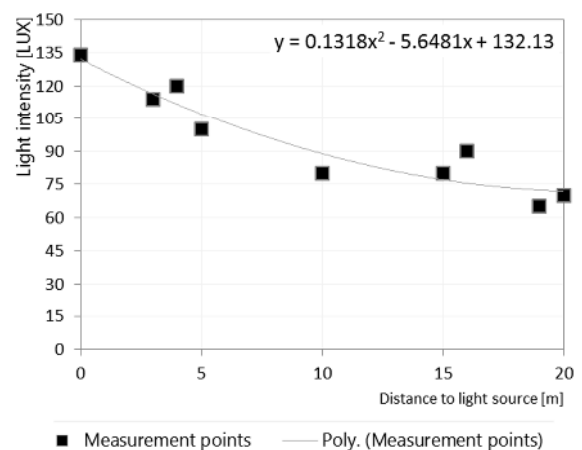


Figure 31 (a-f): Measurements of light intensities as basis for the modelling of the various light points. Measurements were taken in June and July 2014 within the research area.

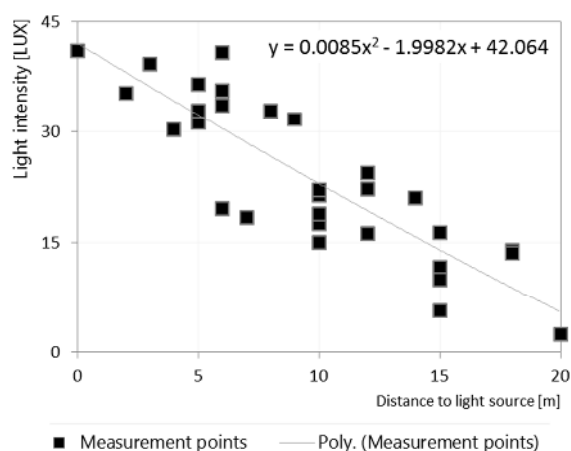
a) **Train Station Area:** Illumination in function of Distance
Source: Measurements LuxMeter; 7 July 2014



b) **Sports Pitch:** Illumination in function of Distance
Source: Measurements LuxMeter; 22 June 2014



c) **Car Parking:** Illumination in function of Distance
Source: Measurements LuxMeter; 27 June / 7 July 2014



d) **Old Town:** Illumination in function of Distance
Source: Measurements LuxMeter; 16 June 2014

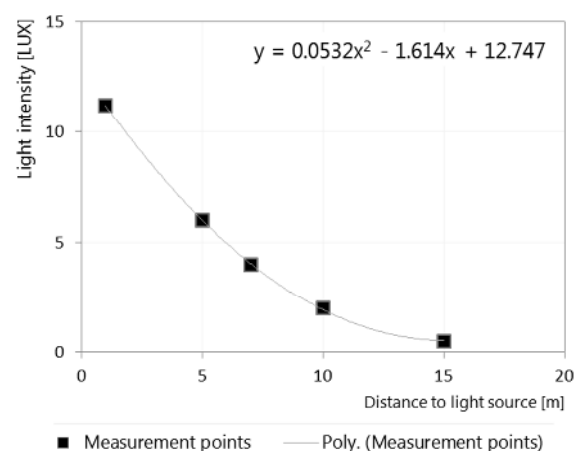


Figure 32 (a-d): Measurements of light intensities as basis for the modelling of the various light points. Measurements were taken in June and July 2014 within the research area.

Measurements in the old town were taken at 79 random locations in the shopping district of Winterthur. All measurements took place at 1m distance from the buildings and at 1 m from the ground. The measurements featured a significant variation in light intensities (Standard deviation = 12.4 Lux). This has to do with the sequence of brightly illuminated shop windows and less or non-illuminated businesses (e.g. Restaurants, habitation). For the model, the average illumination of 11.6 Lux was used for the calculation of the light spread (Figure 32 d).

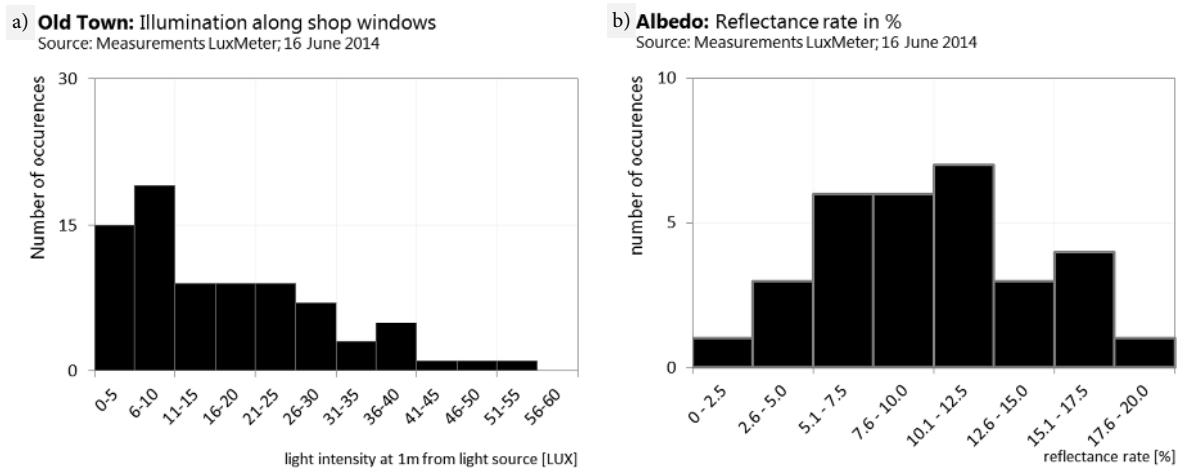


Figure 33 (a and b): Histogram of measured light intensities and Albedo reflectance: a) Histogram of measured light intensities in the old town area. There is considerable variance depending of the proximity of nearby shop windows. For the model an average of 11.6 Lux was assumed (1m from the light source) b) Histogram of the measured Albedo reflectance.

A similarly widespread pattern could be observed with the ‘Albedo’ (reflection of light on the ground) measurements (Figure 33 b). Albedo reflections were used as an input variable for the model – assuming that light emitted from light sources is reflected on the ground surface and subsequently deviated upwards into the sky.

Table 2: Albedo reflectance rates

Values used for model calculation

Model layer	Reference	Albedo	Source	Own Albedo measurement
Class A (motorway)	Asphalt	0.15	Markvart & Castaner (2003)	-
Class 1	Asphalt	0.15	Markvart & Castaner (2003)	0.120
Class 2	Asphalt	0.15	Markvart & Castaner (2003)	-
Class Q (residential)	Asphalt	0.15	Markvart & Castaner (2003)	0.118
Parking	Asphalt	0.15	Markvart & Castaner (2003)	-
Station	Bare soil	0.17	Markvart & Castaner (2003)	-
Sports Pitch	Lawns	0.20	Markvart & Castaner (2003)	-

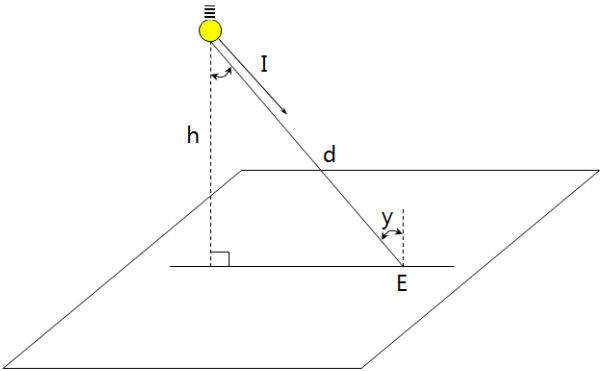
Albedo reflectance values were taken from Markvart & Castaner, 2003 while own measurements resulted in similar values. The reflectance of ‘asphalt’ largely depends on its age and condition (wet/dry). The older the asphalt, the brighter its color and the higher the reflectance (Heat Island Group, 1999).

Own albedo measurements were taken to test the ratios described by Roesch (2000), Ryer (2014), Bariou, et al. (1985) and Markvart & Castañer (2003). The albedo reflectance rates used in the model are shown in Table 2 above.

The measurement of the light intensities in the field was favored after several tests over the use of a standard light diffusion formula. The ‘Inverse Square Law’ describes the relationship between irradiance from a point source and distance (Equation 1). Lambert’s Cosine Law is described in Equation 2. It takes into account the variation of the illuminance depending on the incident angle the light is falling on the ground (Narisada & Schreuder, 2004; Ryer, 2014)

$E = \frac{I}{r^2}$	Equation 1: Inverse Square Law
---------------------	--

where *E* is the illuminance, *I* is the luminous intensity of the light source and *r* is the distance. *E* is expressed in the unit Lux.

$E = \frac{I}{h^2} \cos^3 y$	Equation 2: Lambert’s Cosine Law
	Figure 34: The cosine to the third law. <i>Illustration: Stefan M. Bruehlmann adapted from Narisada & Schreuder (2004)</i>

where *E* is the illuminance at ground, *I* is the power of light at the light source, *h* is the mounting height of the luminaires above ground and *y* is the angle with the normal. *E* is expressed in the unit Lux.

Applying either of the formulae resulted in the display of limited light cones around a light source. The light intensity decreased seemingly too quickly with distance, as compared to the impression given by field observations and the comparison with data from field measurements. The reason could mainly be found in two factors that influence the light cone: a) the technology of the lamp including the construction of the reflector. The illuminance at points on a flat and horizontal surface varies largely in function of the reflector and the optical shielding of the luminaire. Above formulae do not take into

account this factor; b) the reflection from objects in proximity of the light source. House façades, walls along illuminated streets, parked cars, billboards etc. reflect the light from the street luminaires. The effect is higher when the object has a bright color (e.g. white house façades). Above equations would need to be adapted in order to take into account this latter factor.

Since the intention was to use a simple formula for further use in ArcGIS (see chapter 3.6.3), the adaptation of the Inverse square law/cosine law was not further pursued and priority was given to a formula based on a sample of real measurements.

3.6.3 Processes and Calculation (ArcGIS)

Based on the defined light sources (Table 1, page 23) and using the knowledge gained from the desk- and field research, the light points could be modelled. This process required an understanding of the spatial distribution of the light sources. The visual inspection of 'Swissimages' provided the exact intervals (Figure 19 and Figure 20 on page 25). The calculated intervals were determining the creation of light points in ArcGIS. For this, the 'data editor' environment was used and points were set accordingly. The result is a network of light point along the specific street categories and within the polygon features.

The assumption was taken that each street category is illuminated by luminaires with an identic interval. This is an approximation but in reality the intervals do only vary by +/- 3m depending on the local conditions for placing the luminaires.

Additionally, field observations to verify the intervals had to be undertaken. The inspection of the Class A roads (Motorway) revealed that they were not illuminated throughout their entire distance. There seemed to be special rules to be applied. A correspondence with the Federal Roads Office (FEDRO, 2014) confirmed that the motorways are illuminated only where the situation requires it (e.g. on-ramp and off-ramp areas).

This insight led to the understanding that certain 'exception rules' had to be taken into account. In that case, a buffer zone around the on-ramp and off-ramp areas was created and only motorways within that buffer were considered to be illuminated. Another exception rule that was applied in the model was the non-illuminance of streets within wooded areas.

Table 3 shows the used map layers, their source and type. The most important parameter is the interval of the light source which is shown in meters. The intervals of residential/industrial building lights and shop-lights in the old town were estimated.

Table 3: Data layers and parameters for the creation of light points

Layer		Light point creation			
Layer	Source	Type	Method	Interval [m]	Evaluation
1. Class A Road	Swisstopo	Polyline	Point on polyline	50.0	measured
2. Class 1 Road	Swisstopo	Polyline	Point on polyline	30.0	measured
3. Class 2 Road	Swisstopo	Polyline	Point on polyline	30.0	measured
4. Class Q Road	Swisstopo	Polyline	Point on polyline	30.0	measured
5. Residential Buildings	Swisstopo	Polyline	Point on polyline	15.0	measured/estimated
6. Industrial Buildings	Swisstopo	Polyline	Point on polyline	15.0	measured/estimated
7. Train station area	Swisstopo	Polygon	Fishnet in polygon	30.0	measured
8. Sports pitch	OSM	Polygon	Fishnet in polygon	25.0	measured
9. Parking	OSM	Polygon	Fishnet in polygon	20.0	measured
10. Old Town	Swisstopo	Polygon	Point on polyline	15.0	measured/estimated

Ten different layers were used to model the light emissions in the research area. The column 'type' describes the type of the vector file. Light sources along polylines can be modelled with a rather simple 'interval' method. The used intervals (distance from one light point to the next) are indicated in meters. The column 'Evaluation' indicates whether the intervals are based on (field)-measurements or on estimates. Estimates had to be taken where measurements were not possible. Light sources within polygons are modelled by applying a 'fish-net' procedure.

An illustration of the light point modelling is depicted in Figure 35. The light points are created along the polylines with the given intervals.

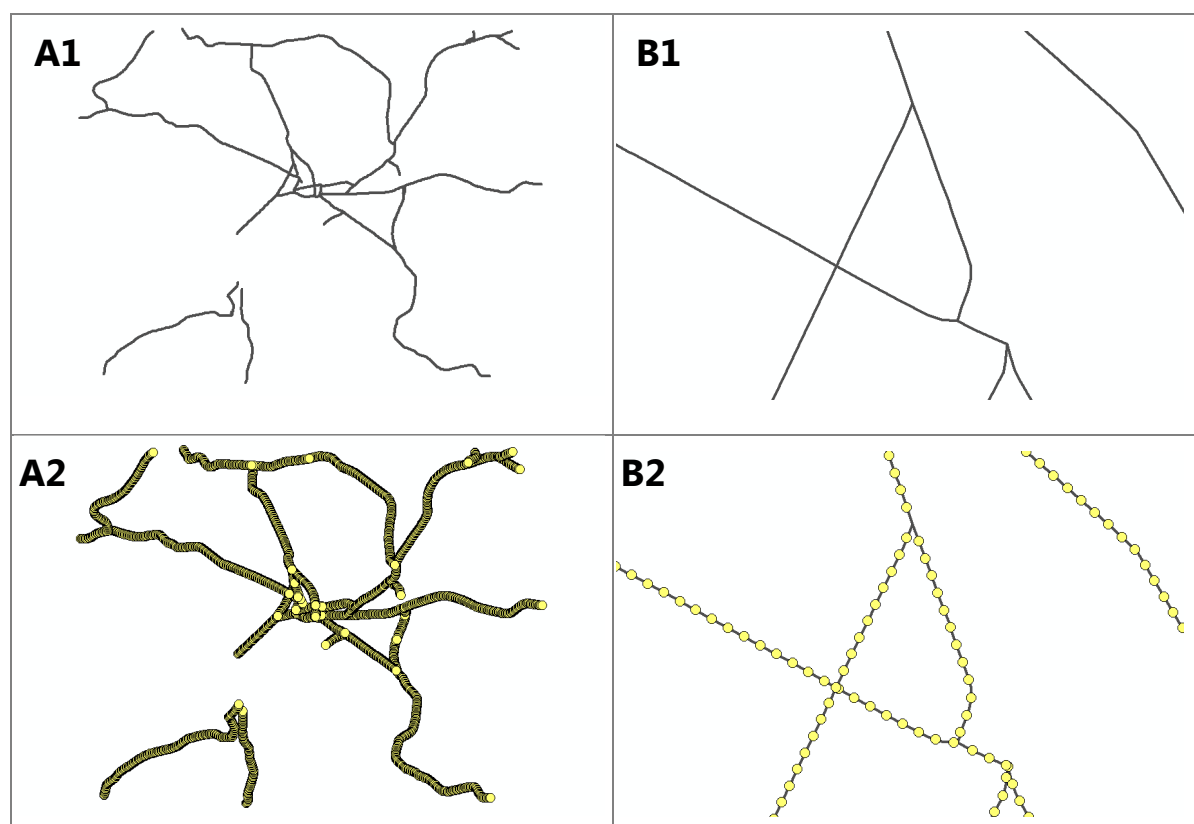


Figure 35: Creation of light points along polylines (representing luminaires along streets). Pictures A1 and B1 show the Class 1 Street network at a scale of 1:63'000 and 1:5'000 respectively. Pictures A2 and B2 represent the same view, but with modelled light points (luminaires). Light sources (yellow circles) are placed with a distance of 50m one to each other.

Image A1 show the street network (Class 1 Road) of the research area. Image B1 is a zoomed view. Images A2 and B2 illustrate this street network after the modelling of the light sources. In B2, the individual lamps (luminaires) are visible with a distance of 50 meters one to the next. The size of the light point does not reflect the true light cone. The size is chosen arbitrarily for illustration purposes. The light cone (spread of light around a luminaire) had to be modelled in a separate process which is explained later.

The modelling of light points along a polyline, based on a measured interval is a rather straight forward and logical process. During the analysis of light sources, though, several sources were detected that were not placed along a polyline. Especially parking lots and sports pitches could be classified into this category.

An alternative process was developed to model the light points within a polygon. Following, the process is referred to as the 'fish net approach' of modelling light points. The areas of the mentioned polygons should be filled with light points at a given interval. This process lead to a more equal illumination of polygon areas as opposed to lights placed *around* the polygons. Figure 36 illustrates a sports field with an overlaid fish net of luminaires.

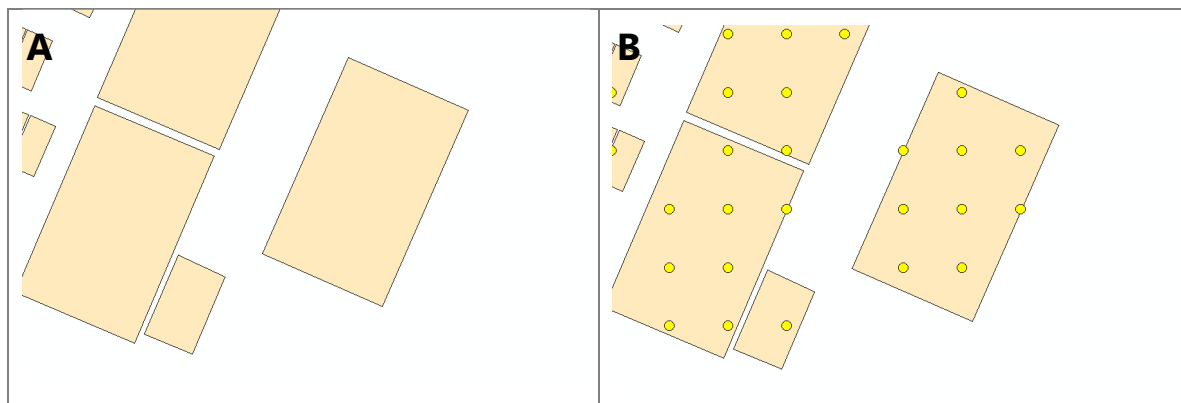


Figure 36: Light points modelling on sports pitches. Light points are created within the polygons with a given distance. (For sports pitches an interval of 50m is applied). The image shows three football fields and a tennis court.

The light points as shown in Figure 35 and Figure 36 show the modelled location of a luminaire. Its light emissions are not yet adequately represented. The sizes of the yellow points do in no way represent the real light cone of each of the luminaires. For the modelling of the light cones a multi- step process had to be applied. The process included a) the creation of an Euclidean distance around each light point; b) light measurements in the field; c) the deduction of a formula that describes the light spread and c) the application of the formula to the point feature.

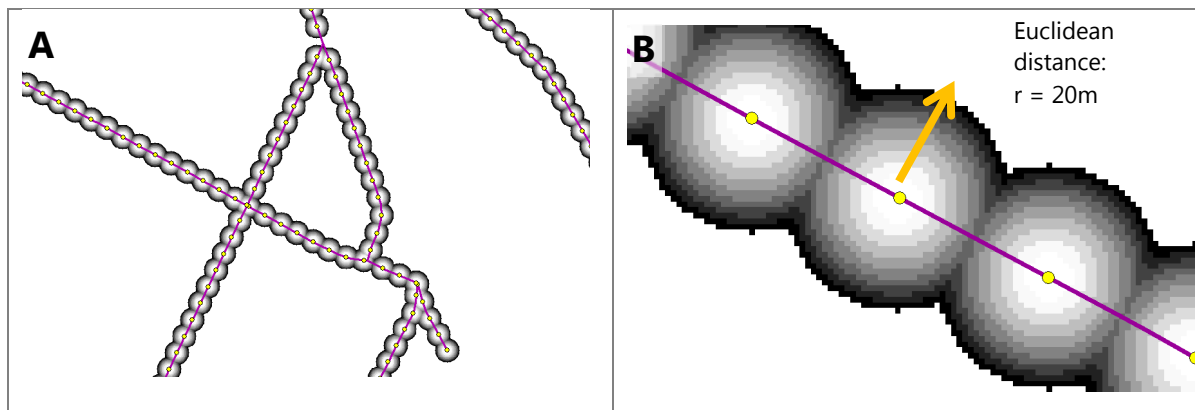


Figure 37: Euclidean distance. For each light point an 'Euclidean distance' is applied. The radii depend on the interval of the light sources. Image A shows a cut-out of a street network with light sources at every 30 meters. Image B shows a detailed view where the applied 'Euclidean distance' is visible'.

As depicted in Figure 37, an Euclidean distance function was applied to each light point (point feature) within the research area. The distance (radii) varied according to the interval of the light sources. In image B a radius of 20m was applied. For each of the 10 light source categories an individual raster file with Euclidean distances around each light point was produced. The resolution was chosen at 1m. This high resolution was necessary to allow for the consecutive calculation of the real light spread. If the raster is too coarse, the light spread cannot be visualized in a satisfactory way. The decrease of the light intensity with distance from a light source would not be 'smooth' enough.

Applying a 1m resolution increased the processing speed and the storage requirements considerably. Throughout the test area, a total of 88'609 light points were modelled and each of them surrounded by an Euclidean distance buffer.

Table 4: Data layers and number of created light points

Layer		
Layer	Number of light points	Euclidean distance [m]
1. Class A Road	418	50.0
2. Class 1 Road	2'097	20.0
3. Class 2 Road	6'051	20.0
4. Class Q Road	6'518	15.0
5. Residential Buildings	67'710	15.0
6. Industrial Buildings	2'714	15.0
7. Train station area	583	25.0
8. Sports pitch	738	25.0
9. Parking	601	20.0
10. Old Town	1'179	15.0
TOTAL	88'609	

A total of 88'609 light points were defined in the research area. The largest number can be attributed to the residential buildings. For each building light sources are modelled in an interval of 15m. The attributed light intensities are – however – very low. Street lighting (luminaires) from Class A, 1, 2 and Q roads make up for a larger impact on the image.

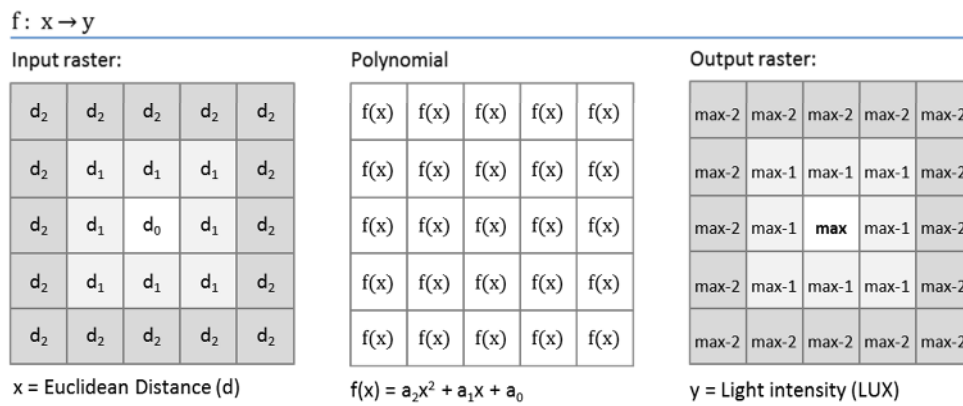


Figure 38: Raster calculation of light intensities. A formula derived from field measurements is applied to an Euclidean distance raster of each light point. The output describes the decreasing light intensities (in Lux) with distance, resulting in a cone around the light source.

From the field measurements shown in Figure 31 and Figure 32, quadratic polynomial formulae could be derived. The formulae describe the decreasing light intensity with distance from the light source. They were applied to each raster cell of the ‘Euclidean distance’ layer. Figure 38 illustrates the process: the resulting output raster layer describes the light intensities around a light point, which is depicted in the center of the grid (max). The value in the cell ‘max’ represents the Maximum light intensity. With increasing distance this value is lowering. For each of the different light source categories a different function was calculated and applied. Consequently, each light source category produces a different ‘light spread’. In order to achieve a maximal smoothness of the output raster, a resolution of 1m per raster cell was used. This process resulted in ten output raster files.

In a further step these ten layers needed to be reclassified to set the areas outside the Euclidean distance to a 0 (zero) value. For better visualization of the intermediate results these areas were colored in black. They represent locations where no light is emitted (mainly forests, agricultural areas and not illuminated gardens in residential areas).

Figure 39 depicts the process of bringing the various individual raster layers into one composite image. The process consisted of summing up the pixel value of each raster cell of all of the ten layers. It was evaluated whether a formula that retains the maximum value of each individual layer produces more realistic results over the ‘sum’ operation. The detailed analysis of the light points showed only an insignificant overlay of illuminated pixels in the individual layers $x_1 - x_{10}$. (Occurrences could be found at a few locations where two street categories are crossing). Therefore it was deemed suitable to use the ‘sum’ operation. The composite image still maintained a 1m resolution that allows further in depth analysis and serves a basis for consecutive processing/visualization.

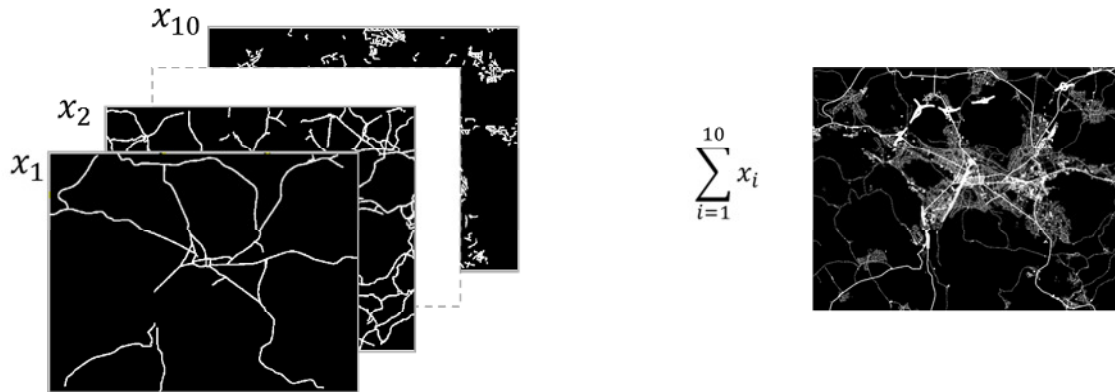


Figure 39: Overlay of individual light source raster layers. A ‘sum’ operation was used in ArcGIS raster calculator resulting in a composite raster image at a 1m resolution. The images shown are slightly edited for better contrast.

Albedo reflectance was considered to be relevant for the accuracy of the model. Personal observation lead to the assumption that the public lighting infrastructure is not sending light emissions directly into the sky. Generally, the luminaires are upward shielded. This observation was confirmed in an interview with the city’s public lighting experts (Frei & Kyburz, 2014) and in the ‘Public lighting concept 2008’ published by the city of Winterthur (Stadt Winterthur, 2008). Hence, the light which is visible from space is a result of reflectance of light sources at the ground.

In Table 2 on page 36 the measured albedo reflectance values were presented. They were included into the model and acted as ‘correction’ values to the composite output as described in the figure above. Equation 3 refers to the integration of the albedo reflectance effect.

$E_s = E_U \times \left(\frac{E_U}{E_D} \right)$	Equation 3 Upward luminance
---	---------------------------------------

where E_s is the illuminance that is directed upwards to space, E_U is the illuminance measured upwards at a height of 1m and E_D is the illuminance measured horizontally downwards at a height of 1m above ground.

An albedo reflectance map was produced in ArcGIS. The process consisted of applying the albedo reflectance rates from literature to the different land uses. The research area was categorized into four categories (asphalt; bare ground, grass, and other land use). As for the ‘asphalt’ albedo, the street network was buffered according to the measured street width (Class A road: 15m per driving direction; Class 1 Road: 15m; Class 2 Road and Class Q street: 8m). The buffered street polylines represent a typical reflectance area in an urban context. The ‘bare ground’ category was attributed to the ‘station area’, which is mainly covered with stones. The ‘grass’ category was attributed to the sports pitches. In ‘other land uses’ are mainly included the wooden land, the front/backyards of the houses, the public parks and the allotment gardens around the city.

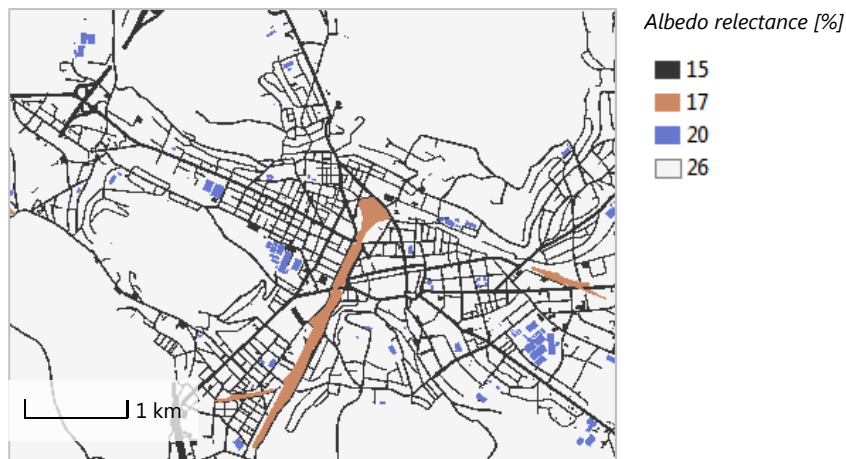


Figure 40: Albedo map (detail; scale 1:80'000). The reflectance rate depends on the ground surface. Streets were buffered according to their width and a reflectance of 15% was attributed (asphalt). The station area got a value of 17%, sports fields of 25% and all other areas (woods, gardens, etc.) a value of 26%. There is no accounting for age or wetness of the ground surfaces.

3.6.4 Mapping / Visualization

The model output consists of an achromatic raster image with a spatial resolution of 1m. In this form, the image can well be further processed – for example for the comparison with a real-world reference scenario (see chapter 3.6.6). For illustration purposes, however, the achromatic image does not provide a realistic visual impression of a nocturnal city. Hence, a method has to be developed to color the light emissions in a way that the image looks comparable to a bird's eye view during night.

For this purpose orthophotos from the city of Geneva (Frangiamone, 2014) were analyzed. The true-color images taken at night over Geneva gave valuable color information that was used in the creation of a color ramp that was applied to the model output. The public lighting of Winterthur almost exclusively consists of sodium-vapor lamps. They typically produce an orange light. Therefore, examples of similar lighting situations in Geneva could be used to derive RGB combinations and classifications that were applied to the maps in this case study.

Figure 41 A shows a typical light point of a sodium-vapor lamp in the city of Geneva. Depending on the distance from the light source, the RGB values are getting weaker, especially for the Red (R) and Green (G) color bands. An average RGB of a concentric circle was determined by using Adobe Photoshop. The RGB combinations were later applied to the model output for a realistic visualization.

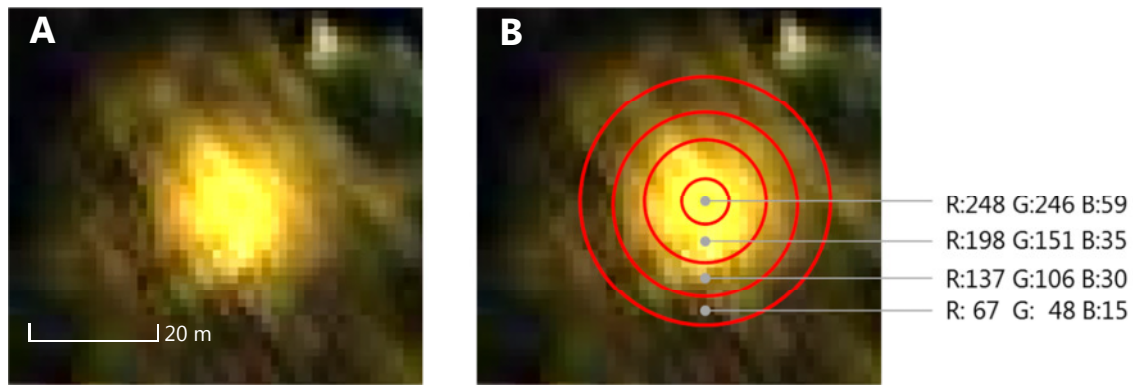


Figure 41: RGB values of a single light source in function of distance. RGB (Red, Green, Blue) values were determined according to their distance from the light source. The concentric circles describe identic distances from the light source. The RGB values are an average of the light points of the respective circle.

3.6.5 Preparation of ISS picture

An image from the International Space Station (ISS) was used as a reference for the comparison with the model output. The image had to be analyzed in detail and prepared for use in the model. In its totality (dimension: 1600x1062 pixel; format: jpg), the image provides a solid visual impression (see Figure 27, page 31). The research area, however, encompasses only approx. 3% of the full size of the picture. By zooming on the research area, individual pixels become visible. In the dark (non-illuminated) areas several artefacts (hot pixels) can be detected. The image also shows the effects from a minimal motion blur. In certain parts of the image a slight cloud cover can be seen, which acts like a blurring filter. There was a considerable terrain distortion of the image because of a camera/sensor position which was assumingly not situated directly at Nadir.

The distortion of the image was corrected using an orthorecrification process in ArcGIS. It consisted of overlaying the street network (as used in the model) with the ISS image. The streets should give the clues to 'rubber sheet' the ISS image. Given abovementioned quality flaws of the image, the orthorecrification inherently included a certain margin of error. Especially in areas where a visible cloud cover is existent, no distinct calibration points for the orthorecrification could be found. Generally, the light emissions do not everywhere coincide with the street network which makes the matching particularly difficult without detailed knowledge of the place.

Figure 42 depicts a detail of the research area where the street network is overlaid with the ISS image. The orthorecrification points are marked with red (from) and green (to) crosses. The orthorecrification process included 23 points and was preceded by a preliminary cropping, re-sizing and positioning of the ISS image.

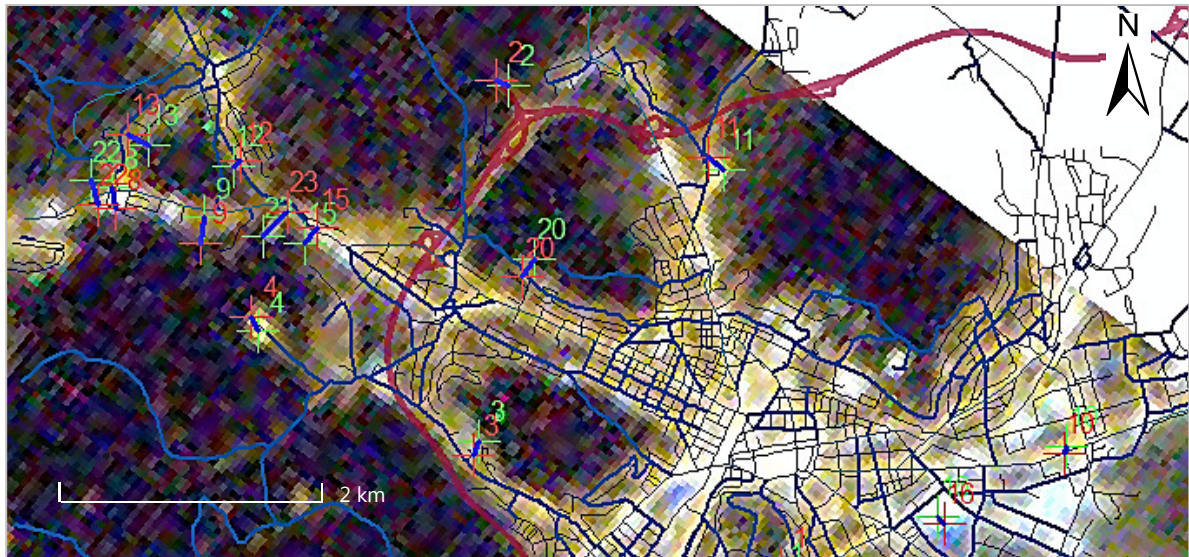


Figure 42: ISS image overlaid by the street network (used in the model). The image was orthorectified according to available visual clues, especially street crossings or extremely illuminated areas which could clearly be attributed to a known feature (e.g. sports field).

Image source: NASA; Vector data source: swisstopo

Zamorano, et al. (2011) analyzed the ISS nocturnal images as a scientific tool against light pollution. They described several processes to enhance the image quality. This included the reduction of the mentioned artefacts and ‘hot pixels’ which are mainly visible in the darker zones of the image. A program called ‘reduceme’ (<http://www.ucm.es/info/Astrof/software/reduceme/reduceme.html>) can help to correct these cosmetic defects. Given the limited occurrence and influence of hot pixels in the ISS image, the tool was not further explored or applied in this study.

On the other hand, another means to enhance the image quality, proposed by Zamorano et al. was applied in the model: It consisted of the extraction of a particular color band of the ISS image. The original image featured a ‘red’, ‘green’ and ‘blue’ image band. It was observed that the different color bands of a RAW/jpg image yield different light intensities and contrast. The ‘green’ band was considered to provide the best results. Therefore, an extract of the ‘green’ image band was done and was fed into the model. Figure 43 depicts the three color bands in a zoomed view:

The lighter areas are those where light emissions are present. The visual difference between the green and the blue color band image becomes obvious. The green band image provides the best detail and contrast. The red band features similar details as the green band, but shows significantly more ‘noise’. The blue band image shows little contrast. In particular, ground based features such as street lighting can hardly be detected. Consequently, for the comparison of the model output with the ISS image, the green light band image was used.

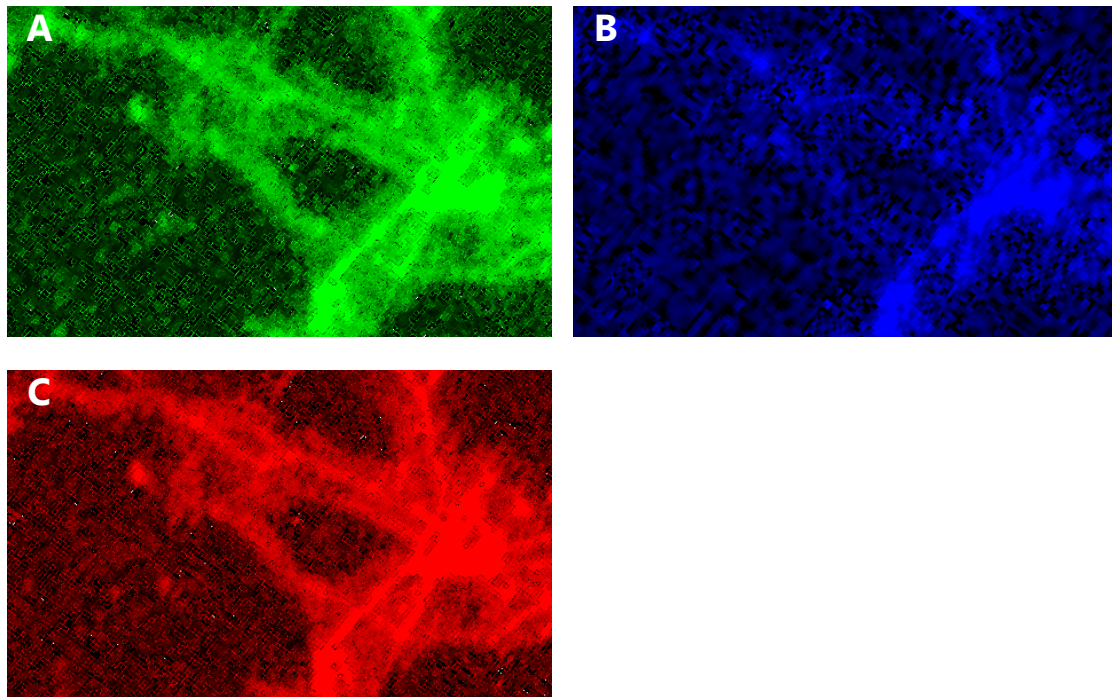


Figure 43: Different color bands of the ISS image. Image A shows an extract of the 'green color band'. The view is a detail of the research area. Ground based features such as streets are clearly discernible. Image B shows the 'blue color band' extract of the same area. Details and contrast are less distinct. Ground based features can hardly be identified. Image C shows the red band image with comparably high detail but a diffuse contrast and more 'noise' than the green band extract.

Image source: NASA / Image editing: Stefan M. Bruehlmann

3.6.6 Comparison of the 'Model output' and with the 'ISS picture'

The research design (Figure 12, page 19) foresees a comparison of the model output with a reference scenario. In this study the reference is the ISS image which was prepared as described above. The comparison should produce a 'deviation map' that shows where the light intensities of the model are different from the ISS image. The model could then be improved and adapted in a way that the difference becomes lower.

The fundamental problem of the comparison lies in the fact that the light intensities of the model are measured and displayed in a different measuring system than the ISS image. In the model, each pixel shows a Lux value whereas in the ISS image, the Lux value per pixel is unknown. The only known value is the pixel value in the RGB classification that is expressed in an integer number that ranges from 0 to 255 (digital 8-bit byte per channel). A common 'scale' had to be created to make the two data sets comparable.

Figure 44 depicts how a common classification was achieved: The total ranges of both, the RGB image (ISS satellite image) and the Model output (achromatic raster image) was split into five equal parts. The assumption was a linear increase in light intensities for both images. For the ISS image the green band was extracted and used. The five classes describe light intensities from 'high' to 'low'. Both images were re-classified into this five-class system. This was the base for a comparison of the light intensities.

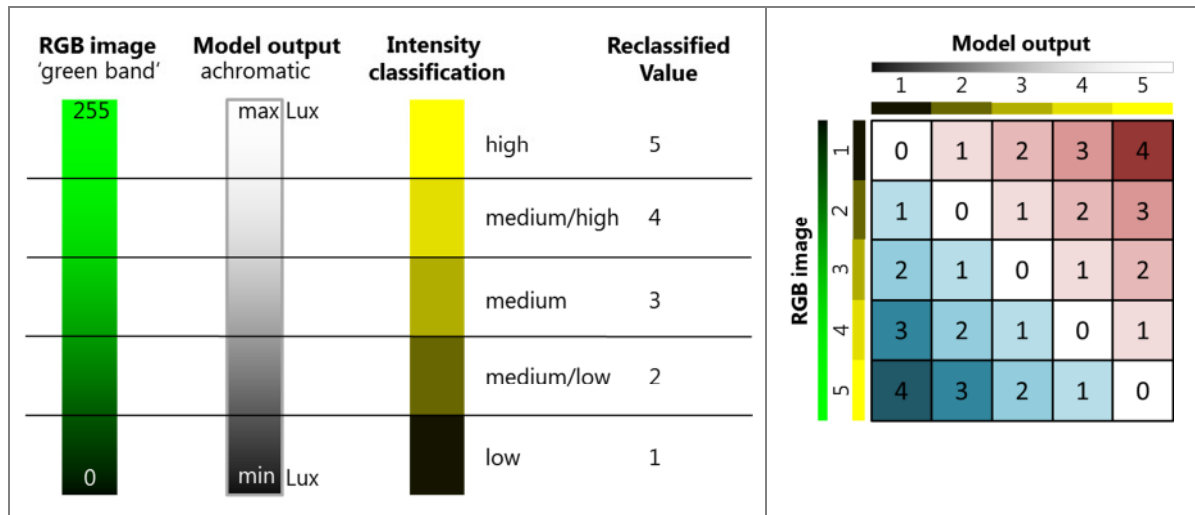


Figure 44: Classification scheme for the comparison of the ISS image and the model output. Five categories are created from 'high' to 'low' light intensities. Each category encompasses a 5th of both, the RGB range (from 0 to 255) and the model output range (values depending on the calculated light intensities in Lux). A common scale allows for the comparison of the two images.

Illustration: Stefan M. Bruehlmann

Figure 45: Comparison of the reclassified values of the 'green band' image with the model output. Red squares indicate a higher brightness of the model output; blue squares indicate that the 'ISS image' is brighter compared to the model output.

Illustration: Stefan M. Bruehlmann

The 'deviation map' was produced by applying a (subtract) raster calculation operation. The reclassified layers were compared on a cell-by-cell basis. An output layer showed the deviation of the two images according to the classification in Figure 45: Areas with the largest deviation are marked with a value '4'. Less distinct deviations are indicated with lower figures. The deviations in the reddish fields are indicating areas where the model output was brighter than the ISS image. Accordingly, the bluish fields indicate areas where the RGB image featured brighter values than the model output. The 'zero' (white) areas represent places where the two images are very similar or identical. The deviation map was color-coded with the color-scheme of Figure 45.

3.6.7 Model improvement process

The aim of the described method was to achieve the best accuracy of the model output compared to the reference image. It is natural that such a model cannot produce fully accurate results in its first run. Based on the model output the quality of the parameters and features can be judged. The output illustrates which elements or numerical figures need rework. This meant that parameters needed to be adapted, light intensities to be re-measured or additional light emission features to be integrated into the model. Therefore, the research design foresaw a loop from the final model output back to the first steps of the model. This loop points to the importance of a continuous improvement and re-run of the model if the best results – hence a low value deviation map – shall be achieved. For the purpose of this study, the model was run through multiple times. Each time small adaptations were made and the outcome documented. The method and parameters described in this chapter represent an optimal set-up for an outcome as significant as possible.

4 Results and Analysis

4.1 Model output

The model output is depicted in Figure 46: it shows a composite image of the light emitting layers plus a 'nature' layer (dark green) that illustrate the wooden areas around the city. All light points are colored according to the scheme described in chapter 3.6.4. No further alterations or enhancements were done on the image. The images clearly show a concentration of light emissions along the major roads and the train station area (center of the image). For a detailed land use map, see appendix C. Motorways are a strong light emitting source, their luminance is however only limited to areas with slip roads and motorway exits. The residential areas are moderately illuminated, mainly because of the street lighting. The image gives a general impression of a city illuminated in 'orange'. This is due to the almost exclusive use of sodium-vapor lamps. This impression will change when the city switches in future to LED lighting.

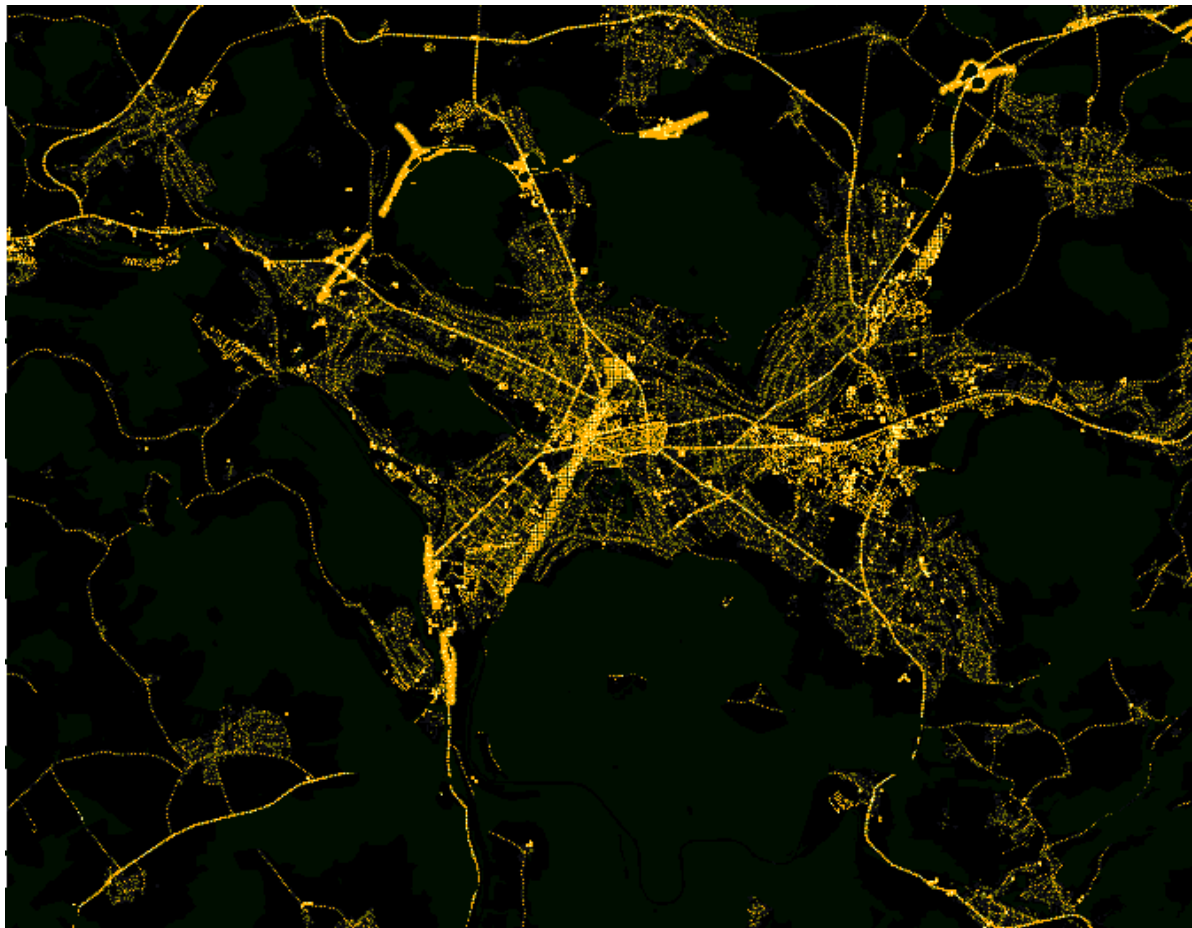


Figure 46: Model output containing more than 88'000 light points. The light points are colored according to the typical color scheme of sodium vapor lamps (as used throughout the city of Winterthur). The main light emitting features are the motorways, the main streets and the station area. The illuminations from sports pitches are switched off for a more realistic impression. For reference see the land use map in appendix C.

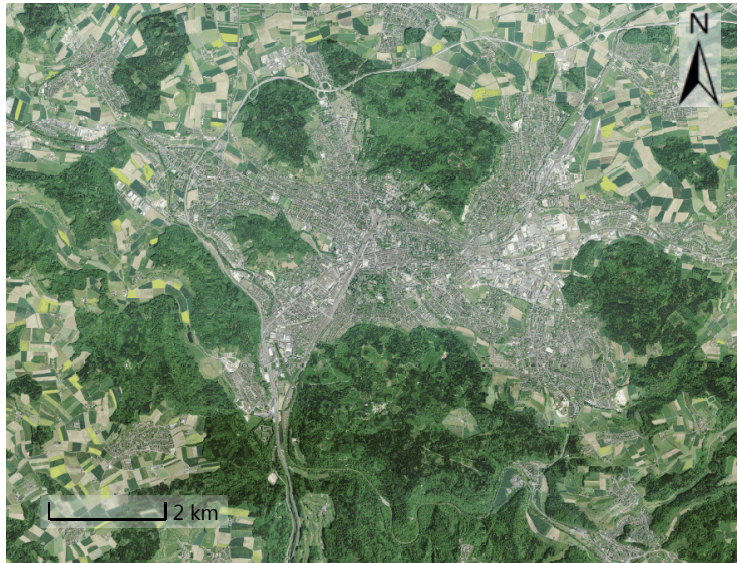


Figure 47: True color diurnal image of the research area for comparison to the model output in Figure 46.

Source: *SWISSIMAGE* by *Swisstopo*

In view of the comparison of the model output with the ISS image, the model had to show a situation as similar as possible to the ISS image. According to the municipality of Winterthur (Frei & Kyburz, 2014) the light intensity of the public lighting changes during night-time (higher illumination before midnight and decreasing illumination towards the morning). This aspect which shows a rather complex pattern was not taken into account in the model. A more critical element that has a large impact on the image is however considered: the illumination of the sports pitches.

In Figure 48 the city's light emissions are shown excluding the sports pitches. Figure 49 shows the same area with the light of all sports pitches 'on'. A considerable difference can be observed. It was deemed not realistic that all sports pitches are used and illuminated at the same time. Hence, in the analysis of the image the situation of Figure 48 was favored and used for comparison.

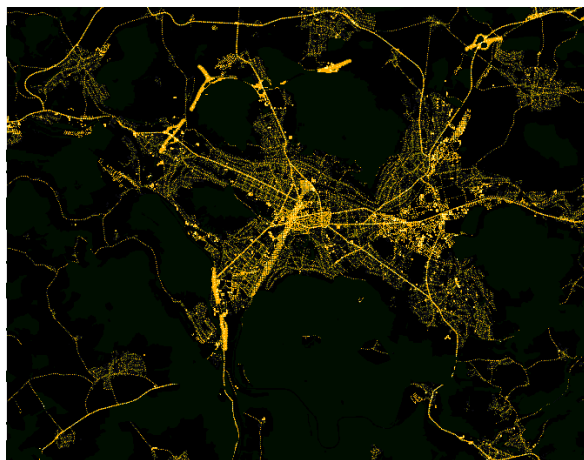


Figure 48: Model output, illumination from Sports pitch is excluded

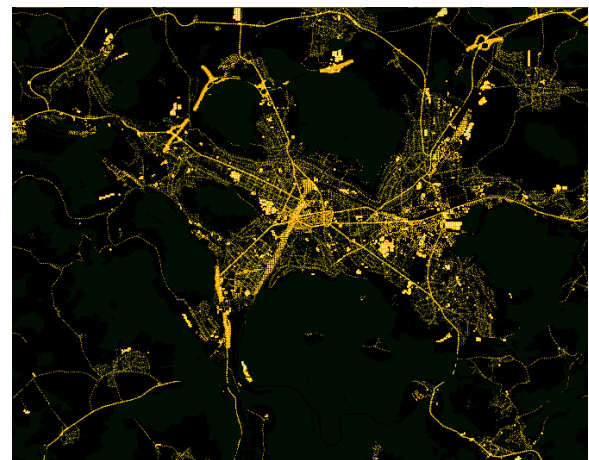


Figure 49: Model output, Illumination from Sports pitch is included

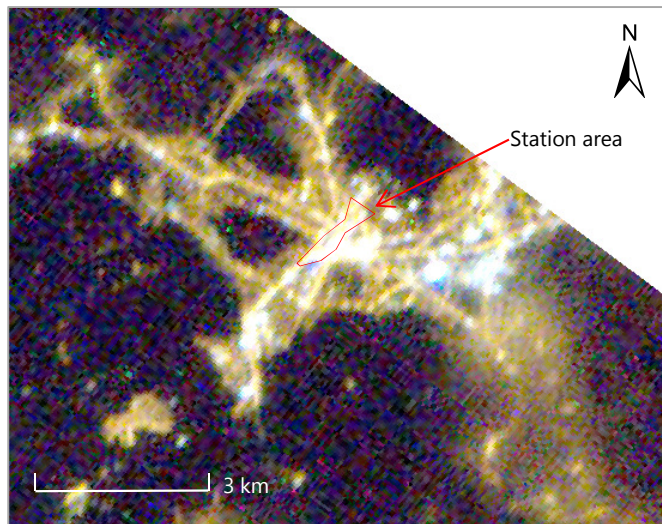


Figure 50: ISS image of the research area. (Extract from the ISS image by P. Nespoli/ESA); see Figure 27 and Figure 28 on page 31.

Source: http://www.esa.int/spaceinimages/Images/2011/01/Lake_Zurich_by_night

For comparison, Figure 50 shows the cut-out of the ISS image of the research area. Because of a certain cloud cover and assumingly other aerosols certain parts of the image appear blurred. Also, certain light sources are considered to appear larger than they are in reality due to refraction.

A detailed view on the city center on the ISS image reveals a very distinct area of illumination: The most obvious feature of the image is the rail station area that stretches from southwest to northeast and covers an area of approx. 0.35m². Joining the rail station in its western end, the old town area is strongly illuminated, due to numerous shops and relatively dense street lighting.

Around the station area, small shopping districts can also be identified as relatively strong light emitters. The course of the main radial highways can clearly be seen. They mark the skeleton structure of the city and are amongst the most distinct features. Residential areas are comparatively little illuminated, depending on the density of the houses and street network.

The natural areas such as the woods or the allotment gardens around the city do not emit any light.



Figure 51: Model output (detailed view on the city center). Distinct differences in lighting intensities can be observed from the model output at a more detailed level. (Scale: 1:10'000). The city center is largely affected by the rail station area and the old town. Woods, parks and allotment gardens are without light emissions.

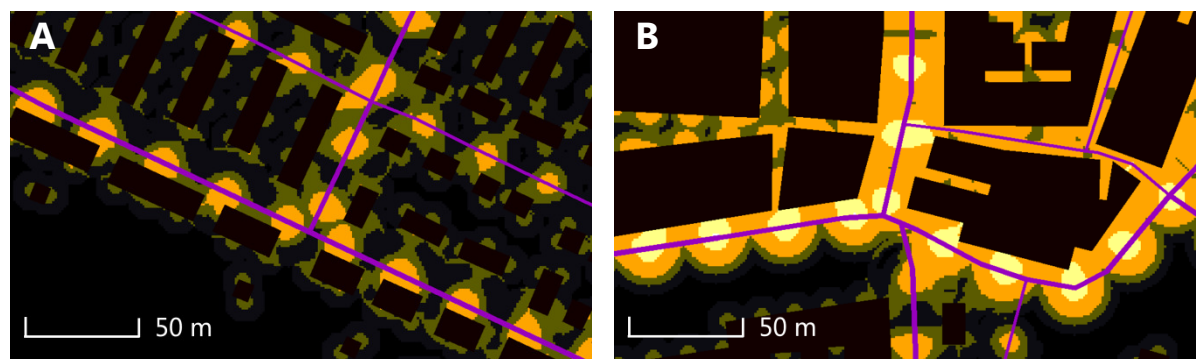


Figure 52: Model output at street level. Situation A shows a residential area with houses along a Class 2 and a Residential Street. Situation B shows an area of the old Town with strong illumination by a Class 1 Street. Streets are indicated with purple lines. The locations of the maps A and B are indicated in Figure 51 with the respective letters and squares.

The model output allows for detailed analysis because of its high resolution. Figure 52 depicts two situations at a street level detail. At this large scale the individual street lights and houses can be identified. The buildings represent an individual shape file layer that has been integrated into the final view. The light propagation is partially limited by the nearby buildings. This phenomenon can well be observed in Situation A and B (Figure 52) where individual houses and larger buildings border the streets towards one side only. The undeveloped side of the street lets the light spread further.

In Figure 53, the model output is likewise shown at a detailed scale (image A) and is compared to a true-color diurnal satellite image (image B), (Swisstopo, 2014). The main features of image A are the luminaires of the category 1 street (leading from top left to bottom right). Residential streets (lines with thinner purple color) are less illuminated. Light intensities are strongly decreasing with distance. The public park at the right-hand side of the image is showing very low light values (<5 Lux for direct measurement and < 2 LUX in terms of albedo reflectance). The light emissions from houses or other buildings are minor compared to the public lighting. In image B the real positions of the luminaires of the Class 1 streets are marked with yellow circles. The patterns of the modelled output are matching the reality check with tolerable accuracy.

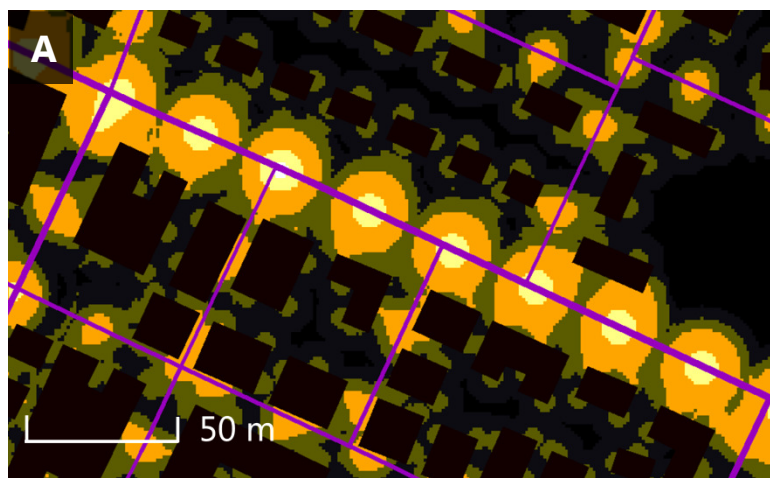
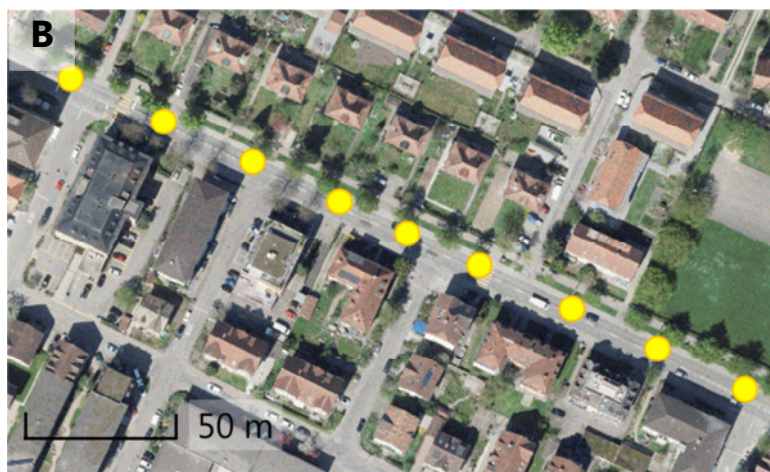


Figure 53: Comparison of the model output with a true color satellite image. Yellow circles in image B represent the true location of the luminaires of the category 1 street. The lamps of the neighboring smaller side streets are not shown.

Source: swisstopo (image B)



The details in the modelled image appear very clear and precise. This is probably not fully realistic, since there is always a portion of aerosols between the light source and the observer (sensor of the camera). This fact can clearly be understood by looking at the ISS image from NASA: Large parts of the image are covered by fog or clouds and produce a certain 'glow' or 'blurry effect' on the image. For a fully realistic impression a certain 'aerosol' factor shall be applied. This issue is further discussed in the section 5.2.

4.2 Comparison with satellite imagery

As described in chapter 3.5.6 (Satellite imagery), the VIIRS satellite currently provides the best nocturnal images with worldwide coverage. The resolution of the images is at approx. 700m /pixel. Despite this rather large ground footprint, the VIIRS images can give valuable indications when analyzing large areas.

The research area measures 107.4 km². A visual comparison of the model output with the VIIRS image was attempted. In Figure 54, a comparison between the VIIRS satellite image and the model output is shown. In the VIIRS image (A) a high concentration of illuminance is visible in the center of the image. This area can be attributed to the old town and the rail station area. The illumination of the outskirts is recognizable. The peripheral areas appear less bright und rather blurred. This could be because of the presence of a predominant cloud cover at the moment the image was taken. The exact meteorological conditions and the exact cloud cover could not be traced back. Such information would be important for an in-depth comparison. The resolution is coarse and for a detailed analysis of e.g. a particular neighborhood, the satellite image does not provide sufficient detail.

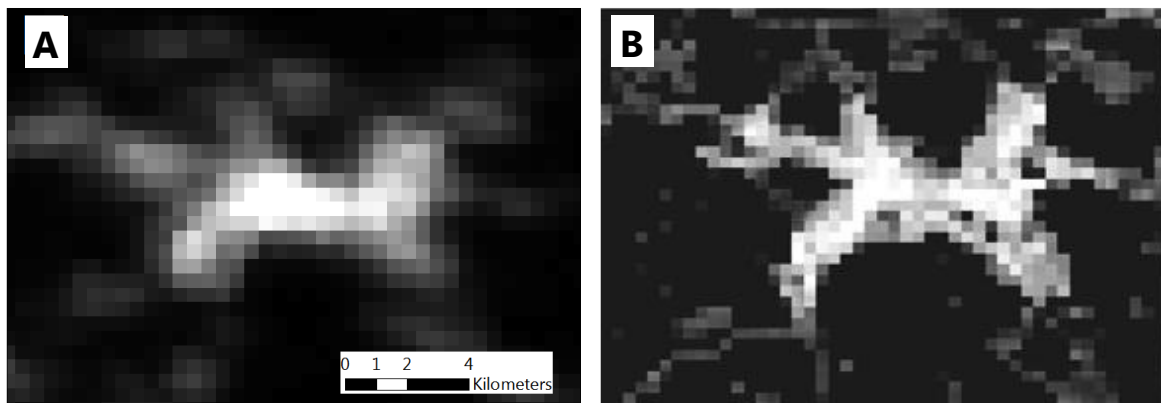


Figure 54: Comparison of an image from the VIIRS satellite with the model output. The image A (VIIRS) shows a smoother distribution of the light. This could be because of unfavorable meteorological conditions (cloud cover). Image B shows the model output which is resampled to a comparable pixel size. A general congruency can be observed

Data source (image A): <http://ngdc.noaa.gov/eog/viirs.html> / Cartography (image B): Stefan M. Bruehlmann

Image B shows the model output in a chromatic version. The image was resampled to a resolution comparable to the VIIRS image. Image B has not been matched to the projection system of the VIIRS image. Therefore there are distortions that impede a one to one spatial comparison. Additionally, some image editing work was applied (brightness, contrast, and gamma) to image B. This should allow for better visual inspection and comparison of the image. The resulting image compares roughly with the satellite image. There is a general similarity of the illuminance and the shape of the illuminated areas. The satellite image (A) gives a more balanced impression. The most illuminated areas can be identified in both images. There is an approximate overlap of the light islands. The VIIRS image roughly confirms the model but does evidently not provide a conclusive answer on the quality of the model output at a local scale.

The lacking background information about the details of the image and the generally too coarse raster resolution are the main flaws of the VIIRS image. A quantitative comparison between the VIIRS image and the model output was therefore subsequently not envisaged.

Nevertheless, there are a number of inherent advantages of the VIIRS images compared to other data such as ‘ad hoc’ imagery taken from the ISS. This topic is touched upon in the discussion in section 5.

4.3 Deviation map

Pictures taken from the ISS provide a nocturnal image source with a distinctively higher resolution than the satellite images from VIIRS. An ISS image from the Zurich area was described in chapter 3.5.7. This image was used as the ‘reference situation’ for the validation of the model output. The subtraction of the pixel values of the two images should provide a ‘deviation’ map that indicates the areas where the main light intensity differences occur. Figure 55 depicts the two images with an identical reclassification (from 1 = lowest illumination to 5 = highest illumination). Image A shows the output from the model. Image B is the orthorectified ISS image of the same area. From the visual impression, Image B has more extended category 5, 4 and 3 areas. In the outskirts of the city there are similarly a lot of category 2 areas. Areas with no or very little reflection are colored in black.

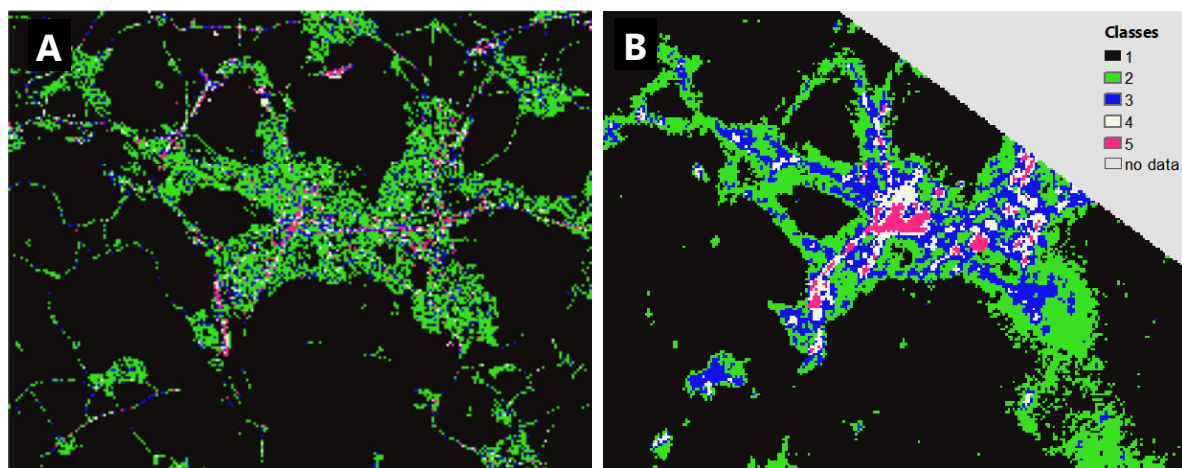


Figure 55: Comparison of the model output with the ISS image. Image A is a resampled and reclassified version of the model output. Image B is a resampled and reclassified image raster of the ISS jpg. The illumination classes are from 1 to 5, with 5 representing the highest illumination. The ISS image shows a generally higher light intensity.

Data source (image B): <http://ngdc.noaa.gov/eog/viirs.html>

The deviation map (Figure 56) visualizes the main differences in illumination for the research area. The top right corner of the map provides no data because the ISS image did not cover this area. The blue pixels indicate areas where the ISS image has a brighter illumination. This can be mainly observed in the central areas of the city and at selected spots in the periphery. Some spots feature a deviation of the value of 4 which means that either of the two maps showed a maximal light reflectance whereas the other map

was dark at this particular place. Some of these situations are marked in the deviation map with the letters A to D. Situations A and B are analyzed and explained further in Figure 58.

The red pixels describe areas where the model output is brighter than the ISS image. Such areas can mainly be located along the motorway and the street network in the north western part of the image. One street in the south-western part of the image also appears distinctively red. Areas where the ISS image is brighter than the model output are marked with the points A1, A2, and B1. These spots are of particular interest for further analysis.

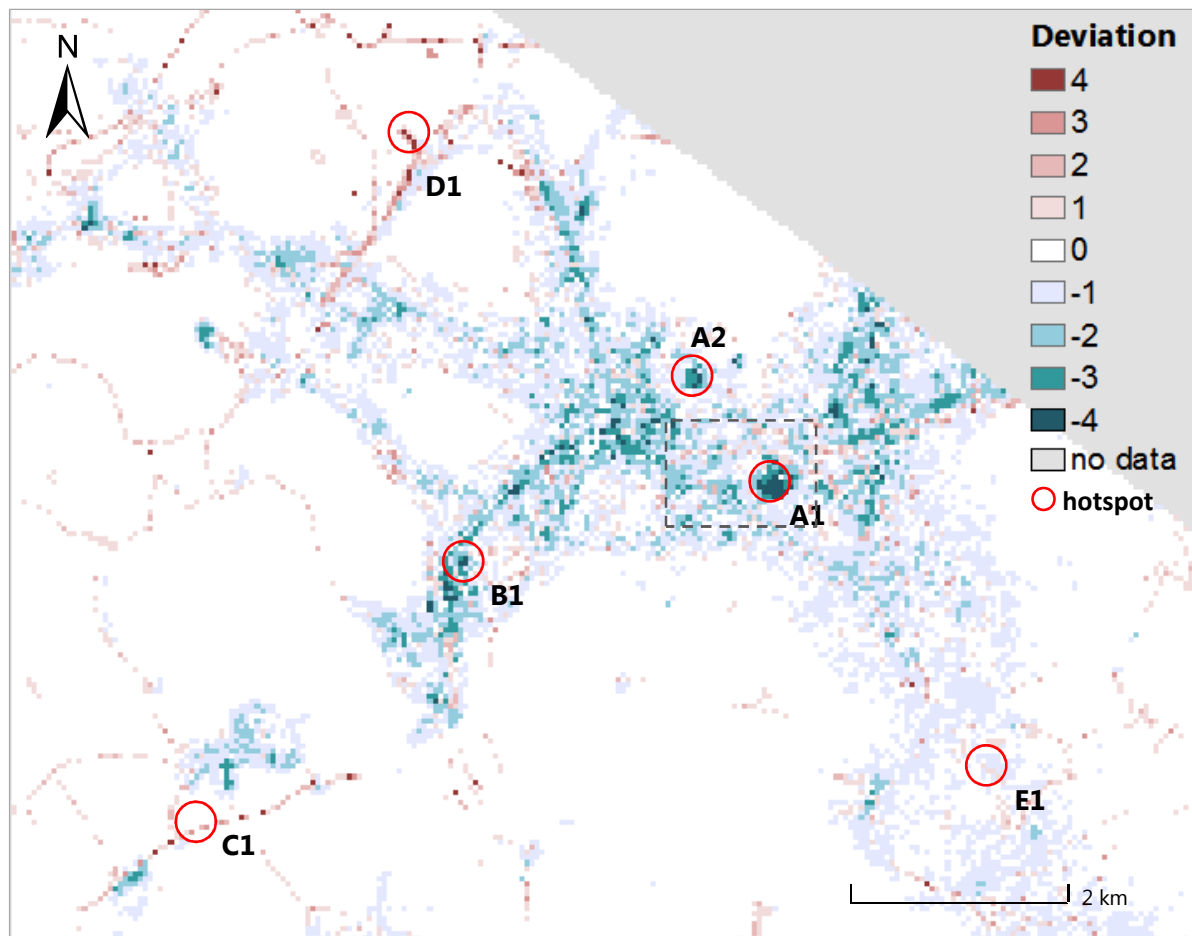


Figure 56: Difference map. The number of deviating categories is shown in the scale. Bluish deviations indicate that the ISS image is brighter than the model output. Reddish areas indicated a higher illuminance of the model output compared to the ISS image. White areas feature no difference. The main differences can be observed in the city center (ISS image is brighter) and along the motorways (model output is brighter). Large areas in the south-eastern part of the city are identically illuminated. The letters A to D indicate 'hot spots' with high deviations which are explained further in the text.

Despite above deviations, the statistics in Table 5 (below) show an overall satisfying result of 75.7% of pixels that do not show any deviation (Deviation Class 0). If the classes 0 and +/-1 are added, as much as 93.1% of the surface features no or very little deviation in illumination. The areas that account for the highest two deviation classes (+/-4 and +/-3) account for 1.8% of the total research area. Thus, these deviations can be understood as punctual and are not suspected to influence the overall evidence fundamentally.

Table 5: Deviation Analysis (ISS image vs. Model output)

Observed	Statistics		Description
Deviation	Pixel count	Percentage [%], of total pixels	
-4	80	0.2	Very high (ISS image is brighter)
-3	391	1.1	high
-2	1'417	4.0	moderate
-1	4'996	14.0	small
0	27'012	75.7	none
1	1'240	3.5	small
2	388	1.1	moderate
3	145	0.4	high
4	4	0.0	Very high (model output is brighter)
Total	35'710	100.0	-

75.6% of the pixels feature an identical or almost identical illumination value (Lux) in the two images. At the extremity of the scale (deviation class +/-3 or +/-4), only a minimal number of pixels could be observed.

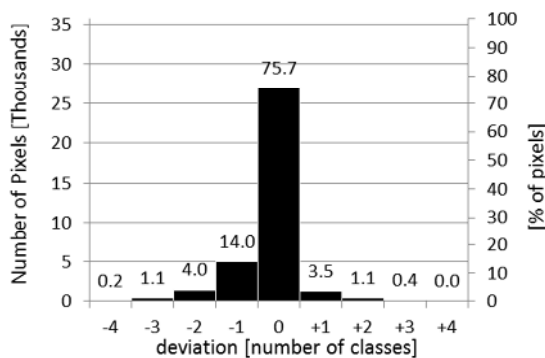
Deviation Analysis: Number of pixel and respective magnitude of deviation

Figure 57: Negative and positive deviations are summarized and visualized in the chart. Areas with no deviation or a deviation of either -1 or +1 account for 93.1% (75.6% + 17.5%) of the total surface. Larger deviations are minor. The deviations of magnitude 4 are negligible for the overall image.

By analyzing the main deviations (following referred to as 'hot-spots'), (A to D in Figure 56), five main categories (reasons) for the deviation could be identified:

- 1) Temporal aspects
- 2) Rule based aspects
- 3) Exceptional characteristics of a feature
- 4) Orthorectification issues
- 5) Prevailing conditions (e.g. cloud cover, season)

Deviations due to 1) Temporal aspects of light sources can be explained by the fact that light sources can be either in activity or switched off during night-time. Sports fields are usually illuminated only for a comparably small portion of the evenings/night. The model output was assuming a situation without any light emission from sports fields. The assumption was confirmed by the observation that the illumination usually stops at 10 or 11pm. During the largest part of the night there is no light pollution coming from these features. Hence the 'default' situation is a non-activity of these light sources.

The ISS image is assumed to be taken in the early evening hours. (The exact time when the image was taken could not be traced back). One of the largest outdoor sports facility in the city is brightly illuminated (see Figure 58/ image A1/a). In the image A1/b the pitches are visualized in purple color. In the model, no light was calculated for these areas. Image A1/c provides a zoom view on the area. It becomes obvious that the illumination or non-illumination of a feature such as the sports pitches make a large difference. Because of their high brightness (134 Lux measured at ground level) the reflectance towards the sky can temporarily be considerable.

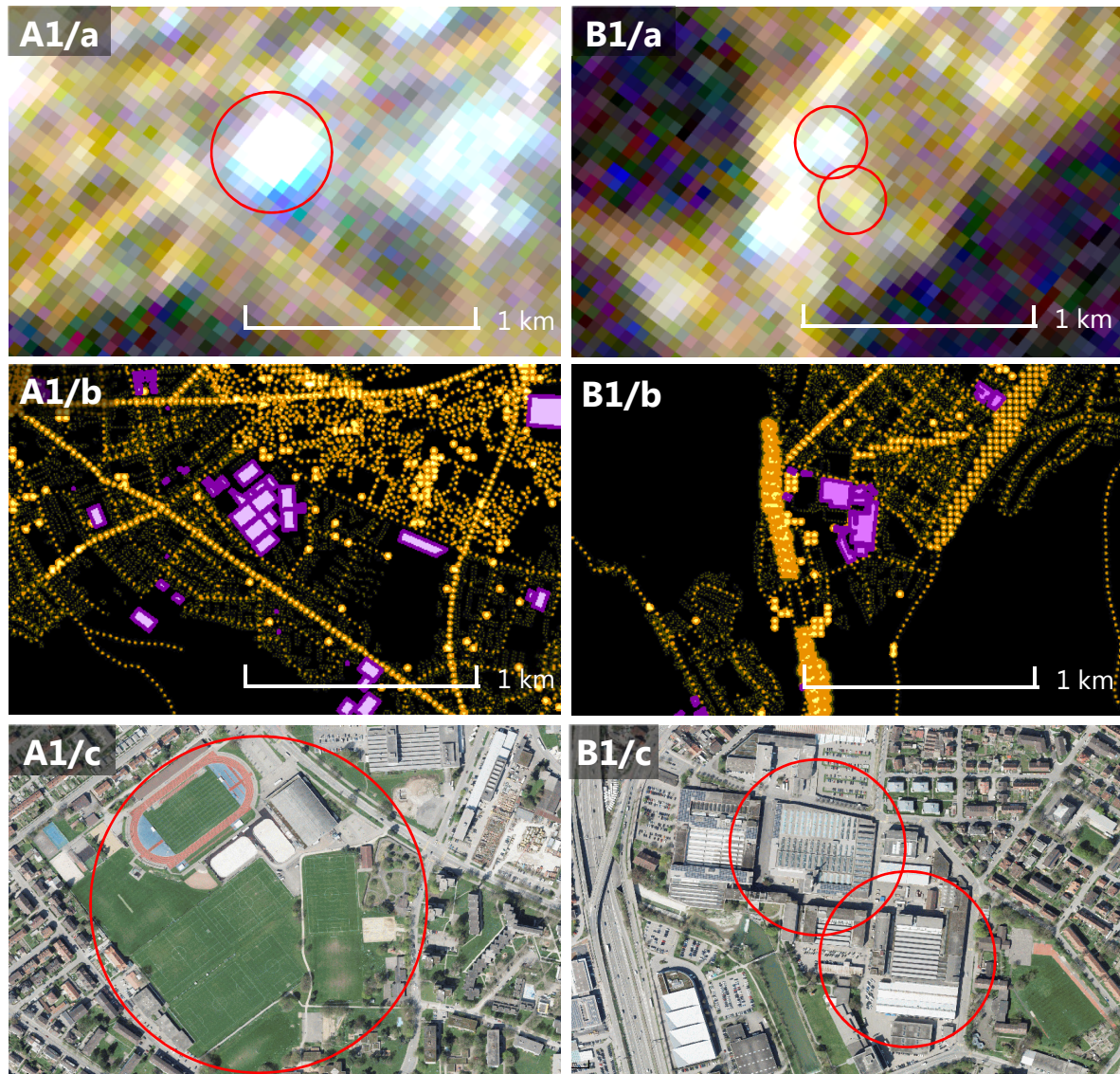


Figure 58: Detailed analysis of the 'hot spots' in the deviation map. Images A1 a-c show an area with multiple sports pitches. Because the illumination from sports pitches was excluded in the model, there is a high deviation at this spot (see Figure 56, point A1). Images B1 a-c show an industrial area. Although industrial buildings were modelled with a certain light emission, the two buildings indicated with red circles were underestimated in the model because they appear to have an important upward light emission because of not anticipated roof-lights (see Figure 56, point B1).

Data source (images a): ESA/NASA

Cartography (images b): Stefan M. Bruehlmann

Data source (images c): Swisstopo

2) Rule based aspects describe the fact that certain features (e.g. streets) have particular illumination rules applied according to their spatial situation. It could be observed that streets are not illuminated in wooded areas. The model took into account this rule. However, further rules apply. The situation C1 (Figure 56) shows a large deviation of light for a particular street in a rural environment. The street is outside the city in a comparably less populated area. The rule appears to be that this particular street is not illuminated. The deviation between the modelled output and the real situation stems from the fact that such exceptional rules were not included in the basic design of the model. This is an area of further research.

3) Exceptional characteristics of a feature: Deviations can result when features have exceptionally different characteristics compared to the modelled assumption. Figure 58 shows such an exception. Images B1/a to B1/c show an area with industrial buildings which produce strong light sent towards the sky. Extended illuminated areas can be observed in the ISS image (a). The model however did only account for the illumination *around* industrial buildings and not for roof-top illumination. The analysis of the orthophoto however showed that these particular buildings have roof-lights that produce a strong light pollution. Images B1/a-c prove that a large influence can stem from buildings that emit light through the roof.

4) Orthorectification issues: One of the key conditions for a proper comparison of the model output with the ISS image is the exact orthorectification of the latter. The available ISS image included a large area from which only a very small cut-out was used as the 'reference scenario'. Additionally, the area used for the comparison was apparently altered by a certain cloud cover, particularly in the lower left part of the image (Figure 28, page 31). The orthorectification was difficult because of missing details in the map. In the carried out process, the orthorectification could only be done in an approximate way because of the rather low resolution of the ISS image and because of the blurring of large zones due to cloud cover and aerosols.

A correct orthorectification is nevertheless crucial for a correct comparison. The large deviations at the location D1 (Figure 56) can partly be attributed to a slight offset of the two maps due to an inaccurate orthorectification of the ISS image. A better orthorectification could not be achieved because of missing distinct features that were recognizable in the respective area.

5) Local, prevailing conditions (at the moment when the image was taken): Due to the absence of detailed metadata about the ISS image, the interpretation of the data remains vague. In the provided image there appears to be a significant influence from clouds and/or aerosols. Meteorological information could be useful to flow into the comparison process. Such information was unavailable from the metadata. Therefore it is assumed that some deviation in the map in Figure 56 has to be attributed to the prevailing conditions.

5 Discussion

5.1 Validity of the model

The initial question of this study was whether a GIS based model can be used to calculate and visualize light pollution at a local scale and how this model has to be set up. As observed in various other studies (Frangiamone, 2014; Kuechly, et al., 2012; Zamorano, et al., 2011) reliable light pollution information at local scale could only be produced by the use of either orthophotographic surveys or DSLR images taken from the International Space Station. Satellite imagery was a priori deemed to provide a resolution too coarse for a significant analysis at local scale.

In this research a detailed map of light pollution was produced and presented, based on a GIS process. The process included the modelling of light sources derived from ground based features, particularly the street network and the public lighting. The produced results (light pollution maps) are available at a 1m resolution which allows for detailed analysis. The comparison of the results with a ‘real life’ reference scenario (ISS DSLR image) proved a high accordance of the light emissions. Zamorano, et al. (2011) describe the ISS images to be useful as a scientific tool for the understanding of light pollution. The validation of the model output by an ISS image is therefore considered to be a meaningful approach. Despite some deviations in light intensities (Figure 56) the model was able to produce results that also hold for detailed analysis.

The study of Kuechly, et al. (2012) presents detailed nocturnal maps of the Berlin metropolitan area. The map shown in Figure 59 A extends for an area of approx. 300 km². The image was taken by an airplane at 3000m above sea level. This type of map can be produced only with enormous time effort and cost. The image shows a mosaic that consists of 2647 single images each at a resolution of 1m.

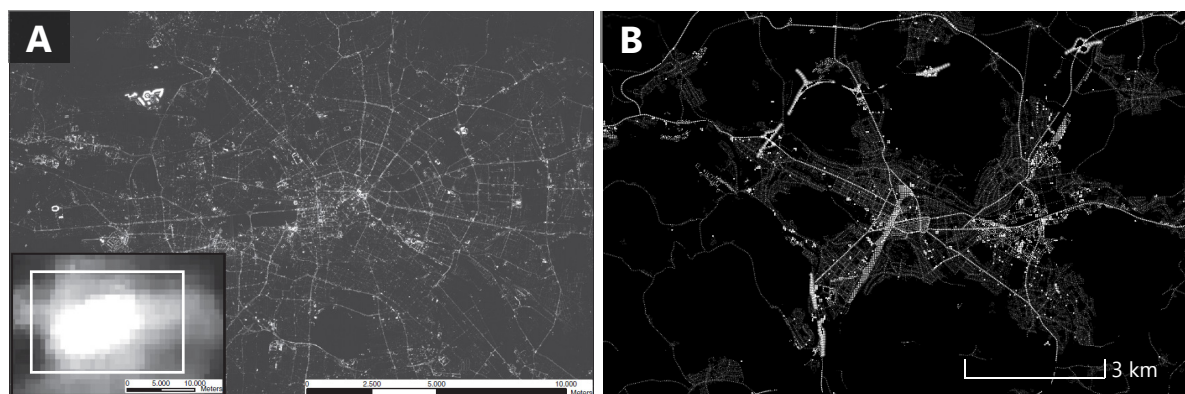


Figure 59: Comparison of a nocturnal illumination map from Berlin (A) with the model results. The image from Berlin is a mosaic from 2647 individual images taken by an aircraft (Cessna T207A) at approximately 3000m above sea level. Image B is the monochromatic output from the light pollution model for the research area (Winterthur). The two images give an impression of the similarity of output for two completely different approaches of measuring and visualizing light pollution.

Data source (image A): Kuechly, et al. (2012)

The street networks represent the main illumination features, other areas are less intensively illuminated or fully dark (however showed in a certain shade of grey). Distinct features such as the civil airport extrude clearly out of the image. For the comparison of the Berlin raster image with the model output of this study, the modelled image was produced in an achromatic version (Figure 59 B). It becomes apparent that the two images (although produced by completely different processes and means) provide a comparable visual aspect. In the model output image, the street-network equally constitutes the backbone of the city illumination.

The study by Frangiamone (2014) described the light pollution in the city of Geneva (Switzerland). Analog to the study of Berlin, the nocturnal illuminance data was captured by aerial photography. Images were taken in May 2014 from an altitude of 4200m above ground. The images from this study were used in the process of finding the correct color scale for the visualization of the model output. A visual comparison of the images from Geneva and the model output maps equally suggest a high similarity of the visual impression. Figure 60 shows a comparison of a similar scale view (1:15000) on the two urban areas. Image A is an achromatic version of the aerial image from the study of Frangiamone (2014).

Image B is an extract from the model output, showing a central area of Winterthur. Despite the rather different building and street-network characteristics, it becomes obvious that the light patterns feature a common pattern: The street network determines the main illumination. Houses are the 'dark' oases in the illuminated cities. An obvious difference in image A is several bright light points which seem to produce no light cone (especially at the edge of the large black area (which is the lake of Geneva). These spots are luminaires of the 'globe' type (see appendix J). These lamps do not have a reflector or shield towards the sky and emit light into all directions. As confirmed by the city of Winterthur, this lamp type is not in use in the public lighting. Consequently, such lamp-type was not modelled and cannot be found in the output in image B.

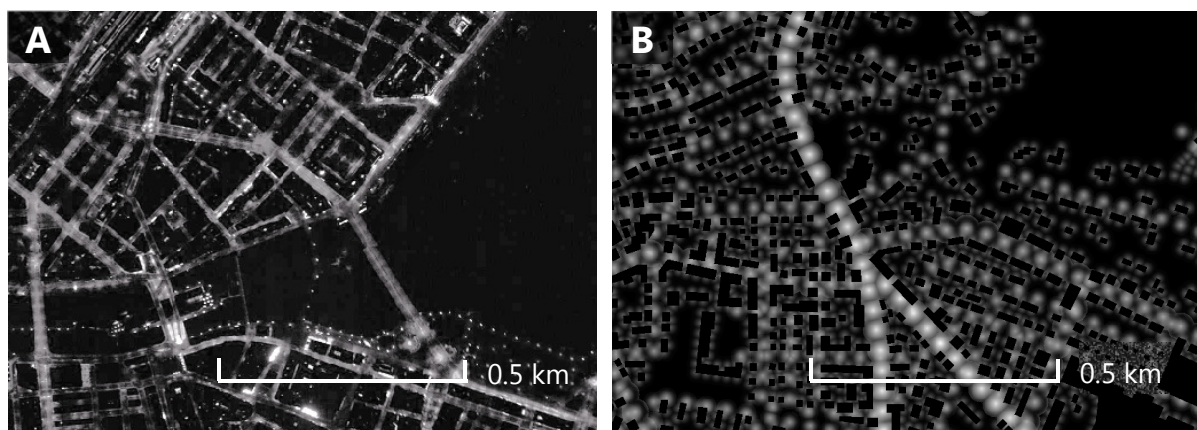


Figure 60: Comparison of an aerial photo (A) from the study by the city of Geneva (Frangiamone, 2014) and the model output (B). Both images are at similar scale (approx. 1:15000) and produced in an achromatic version. Despite the different structure of the city, the model proves to come up with a similar visual impression as the 'real life' image taken from the air (image A).

Source (image A): Frangiamone (2014)

The comparison of the model output with the ISS image yields results that prove the capability of the model. It can be noticed that with decreasing scale the results become more illustrative and seemingly closer to reality. Hence, for illustration purposes at a scale of $<1:10000$, the output brings a proven added value. This becomes particularly obvious when comparing the model output to the small scale maps published in the ‘first world atlas of the artificial night sky brightness’ from Cinzano, et al. (2001). The maps were produced by using DMSP satellite data and therefore inherently limited to the illustration of the light pollution at small scale.

Although that Cinzano et al. are mapping the ‘night sky brightness’ (as opposed to the luminance which is the measure in the model), the maps are deemed to be generally comparable. A detail of Cinzano’s map is shown in Figure 61. The model output which was calculated for the area marked by the red square shows to a large degree more detail and insight. It is assumed that the small variation in the data throughout extended areas in Cinzano’s image is due to the coarse DMSP satellite resolution (5x5km).

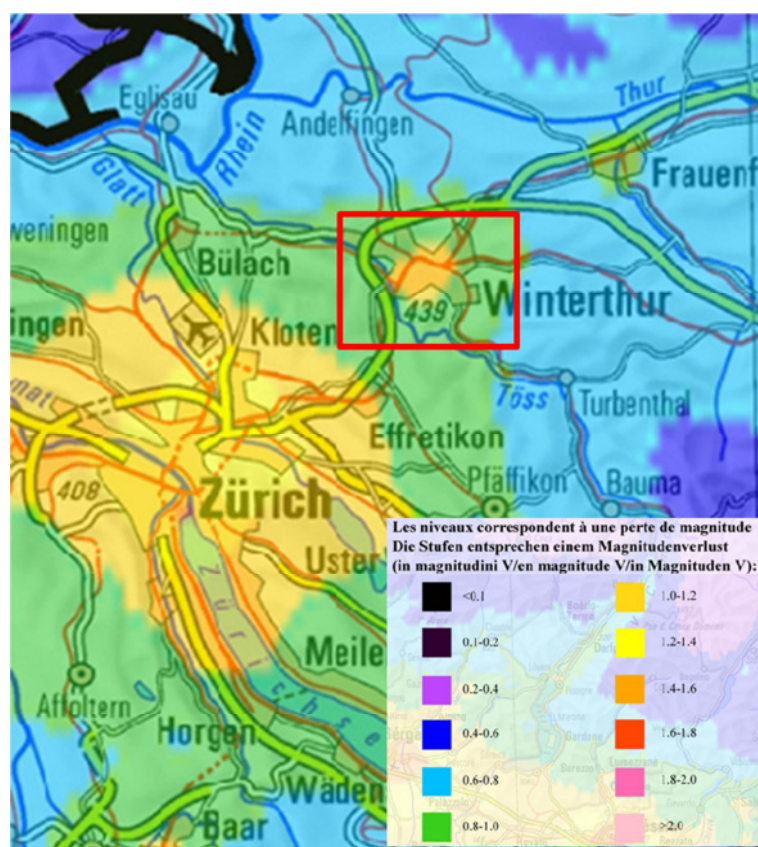
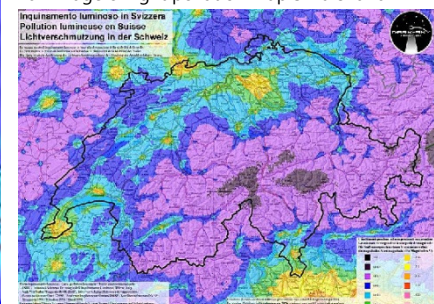


Figure 61: Extract from the light pollution map by Cinzano et al. based on DMSP satellite data. The significance for a small area as the research area is limited due to the coarse resolution of the satellite data.

Data source: Darksky Switzerland

Cartographical modification: Stefan M. Bruehlmann

Full image of light pollution map Switzerland



Taking into account the above facts, it can be understood that the model in its current set-up can produce significant results. Particularly light pollution information at large scale level (e.g. street level) could be produced at low costs and within a reasonable time. This is a novelty considering the logistical and organizational effort that an aerial survey project requires. The maps from the model provide significant

insight in the distribution of light at a detailed level. The results are comparable widely with those produced by aerial images and even more so by images sensed by satellites.

The model as explained in the previous pages, represents a basic and a non-conclusive version that includes only a limited number of light sources and applies a basic calculation of the spread of light. Additionally, the albedo assumption is based on simple assumptions. Consequently, there is scope for further improvement in both the input data quality and the data processing in the model.

Table 6 summarizes and assesses the main elements that are of relevance for the validity of the model:

Table 6: Qualitative assessment of the validity of the Light Pollution Model

Topic		Validity	Remarks
Item	Condition	Assessment	-
Illumination values	Accuracy of Lux values	Similar visual impression	
Illumination color	Accuracy of RGB	Similar visual impression compared to aerial photos	Depending on inventory of luminaires
Interval of light sources	Correct distance between light sources	High accuracy	Measured based on daylight orthophoto
Propagation of light	Realistic spread of light around a lamp	Reasonable accuracy	ArcGIS not able to model a fully realistic light cone.
Hierarchy of Street network	Allocation of the correct lamp type to the relevant street	High accuracy	Based on street network by Swisstopo
Completeness	No light emitting sources are missing	No obvious features missing	Complexity of light sources depends on the research area.
Precision/Detail	Detailed view at large scale	1m resolution allows for detailed analysis	More detailed analysis than in aerial photo possible

The items above describe some important 'quality' factors for the model output. All features are deemed to be at a high or sufficient quality for the purpose of illustrating the light pollution at a scale of <1:10'000.

Eventually, the quality and validity of the model output depends largely on the application of the model output. If the output is mainly used for illustration and awareness raising purposes (e.g. small scale maps of entire cities), several factors mentioned in Table 6 are of lesser importance. If, however, quantitative analysis at street level or the simulation of various scenarios shall be made, all of the mentioned conditions need to be fully met.

Considering a more quantitative and large scale use of the modelled data, there are nevertheless several limitations. They are discussed in the following section.

5.2 Limitations

Several limitations of the described process and model have to be mentioned. Following, the most significant limitations are discussed. All become relevant in case the model should be exploited for quantitative analysis and planning tasks which require an enhanced level of data quality and precision.

The limitations are related to three main fields: 1) the restricted availability of data and knowledge used for modelling the light points; 2) the complexity of modelling rules for the light spread; 3) the non-consideration of additional factors influencing the light pollution

1) The availability of data and knowledge used for modelling the light points is crucial for a high quality outcome. Reliable digital maps are necessary that provide an accurate and complete street network and inventory of buildings, parking lots etc. High quality data from Swisstopo guaranteed for complete inclusion of these features. A limitation in the approach of this study is however the non-availability of local knowledge about data sources and feature details. A detailed inventory of public or even private light sources or an understanding of the architecture of certain buildings would be necessary. Having for example data of the public lighting at hand (locations of luminaires, type of luminaire, light intensities, etc.) would strongly improve the model.

An important aspect of this limitation is the difficulty to receive data about the *type* of the light inventories: Increasingly cities are introducing LED lamps. This lamp type features a different light temperature (measured in Kelvin) than conventional lighting (see Appendix E). Not knowing about where such LED luminaires are already installed, the visual outcome can be compromised.

2) The modelling rules for the light spread were determined by sample measurements in the field. A variety of different lamp types are installed in a city like Winterthur. For the modelling of the light spread (light cone) simple formulae were used. Analysis done in the PHILIPS light planning software 'Dialux and Calculux' (Koninklijke Philips N.V., 2014) proved that the pattern of the light propagation (light cone) is strongly dependent on the type of the lamp and are far from being uniform.

Figure 62 shows a 3D illustration of the complex light distribution between two luminaires each at 30m from the other. With abovementioned planning tools the spatial distribution of Lux values can be calculated for any location on a defined area (street). The formula applied in the model does not produce Lux values that match the accuracy of the Calculux software.

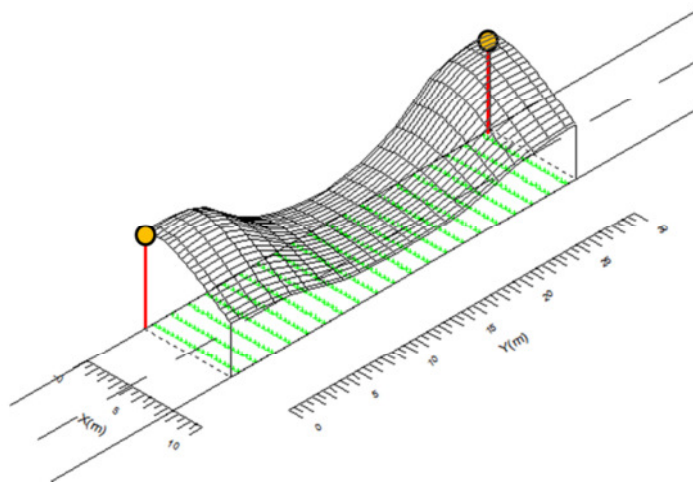


Figure 62: Illustration of the calculated light intensity along a street using the 'Calculux' software by PHILIPS N.V. The grid shows the different Lux values between two luminaires. For each of the green points on the street a Lux value is calculated. The pattern of the light distribution is largely dependent on the type of the luminaire used.

Luminaire type: SGS102 1xSON-PP250W MR / Street width: 7m, height of light source: 10m, distance between lights: 30m.

Illustration: Stefan M. Bruehlmann with PHILIPS Calculux Version 7.7.0.1

3) The non-consideration of additional factors influencing the light pollution relates to the fact that light pollution – as seen from space – is a product of a multitude of factors. The intensity of the light sources on the ground seen from space is influenced by additional factor that can be classified into these three categories: (a) Air molecules; (b) Dust in the atmosphere and (c) Water vapor in the atmosphere. Category (b) may include considerable parts of man-made aerosols such as air pollution (Narisada & Schreuder, 2004).

The model does not include a correction factor for the above phenomenon. The examination of several aerial images and DSLR images from space (ISS station) suggest that a certain correction factor could lead to more realistic images. Such a correction factor could help to slightly 'blur' the overall impression and to accommodate for the abovementioned aerosols.

5.3 Fields of application

As noted earlier, there is currently a poor availability of detailed and reliable light pollution information for the various stakeholders interested in such data. The modelled maps therefore have the potential to satisfy the pertinent information needs.

Various fields of application of the model can be imagined. These fields can be clustered into three categories of purposes: a) Raising the awareness of the light pollution issue through visualization; b) Providing information to special interest groups; c) Optimizing the planning of light sources. The three categories have certainly rather different requirement. For instance, the level of information detail would presumably be much lower for 'awareness campaigns' compared to the need for very accurate and large scale data for planning purposes. With corresponding adaptations, the model could serve all three of above fields of application.

Table 7: Fields of application of the model**a) Mapping to raise awareness**

Application	Detail
Make the light pollution issue known	Local media to use modelled maps as illustration to raise the awareness of the light pollution issue.
Inform the citizens	Municipality to provide light pollution data to the citizens. Light pollution map can be integrated as a layer into the public GIS on the municipalities' Geo-Portal.

b) Providing information to special interest user group

Application	Detail
Astronomer	Model output to be transformed into a 'night sky brightness' map (see Figure 63). Provides information about the darkest observation spots.
Conservationists / Biologists	Model output to link with other datasets and gain new insight (e.g. the city of Geneva has linked light pollution maps to animal road kill data sets in order to find out a possible co-relation; (Frangiamone, 2014)

c) Optimizing the planning of light sources

Application	Detail
Illumination intensity scenarios	Model to be used to run simulation when applying alternative light intensities to the public lighting (e.g. 10% lower illumination to residential streets)
Lighting technology scenarios	Model to be used to run simulation when applying alternative lamp technology in the public lighting (e.g. increase the number of LED lamps by 5%)
Risk mitigation in light planning	Model output as a help to anticipate undesired outcome in light planning.
Calculation of energy use	Model output to be linked to consumption data and to calculate energy costs. Link to scenarios. Optimize energy use through optimal location of public lighting.

Table 7 summarizes the main applications and uses of the model. The current state of the model can already fully respond to the data needs by the purpose categories a) and b). As for the applications described under c) the model would need to be enhanced. In particular, interfaces to public lighting inventories (exact location of luminaires, type of technology, cost and consumption of electricity by light source etc.) would have to be established.

Chapter 6.2 refers to this point and suggests some more fields where further research is needed to enhance the model.

As shown in Table 7, (amateur)-astronomers are a group of stakeholders that have a strong interest in the quality of the night sky. Figure 63 below shows an example of a 'night sky brightness' map. Darker areas represent places where the night sky is darker (the stars are better visible) than in the brighter areas. The measurements were taken with the Sky Quality Meter (SQM) in moonless and clear nights in February 2014 in Winterthur.

To create a complete and detailed map over an extended area (such as the research area) thousands of measurements with the SQM would be necessary. A large-extent map based on real measurements is almost impossible to realize; unless a lot of personnel and monetary resources are invested. In any case,

favorable metrological conditions for measurements are nevertheless a prerequisite. Experience showed that such conditions are rather rare events. Apart from completely clear skies the night must be moonless. Moonlight is influencing the measurements considerably.

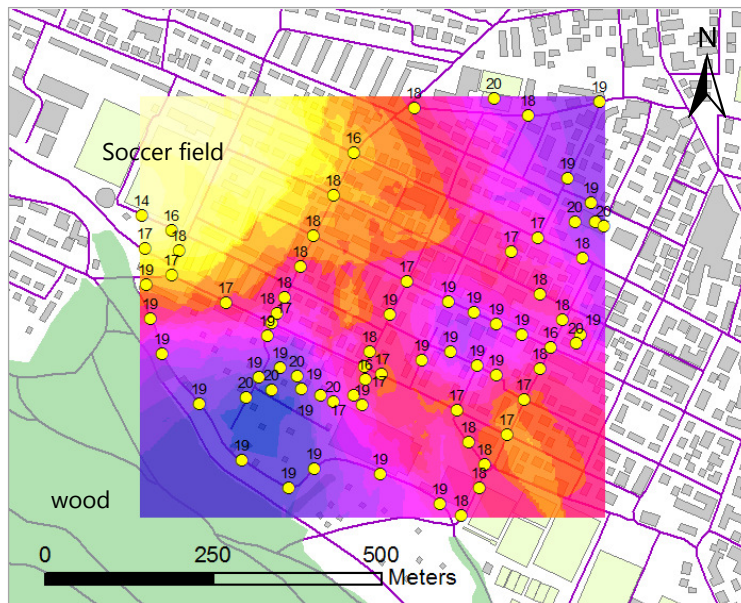


Figure 63: Night sky brightness map. (Values in mag/arcsec²) The map is the result of a point feature interpolation of 72 measured values in a square of the dimensions 690x620 meters. The measurements were taken with the Sky Quality Meter device (see chapter 3.5.5 'Data from 'Sky Quality Meter') on 13 and 17 February 2014 between 21 and 22h. A cloudless and moonless sky was a condition for the quality of the measurements. The map shows the high influence of an illuminated sports field (top left of the image), whereas the sports fields at the lower right of the image were not illuminate at the moment of measurements.

Cartography: Stefan M. Bruehlmann

The modelled results could close this gap. The model is suitable to produce a 'Night sky brightness' map at a local scale. There is a co-relation between light measurements on the ground and night sky brightness (Unihedron, 2008). The model result would need to be transformed (possibly by applying additional operations) into the 'Night sky brightness' map scale, which ranges from 14 (total light pollution) to 23 (pristine sky). The value of 21.8 is considered to represent a natural unpolluted starry sky. Star-gazers could benefit from such a map.

Night sky brightness maps exist, but only at small scales. The maps produced by Tapissier (2014), for example, show not enough detail to visualize 'dark sky islands' as visible over the wooded areas in the lower left part of the map in Figure 63.

5.4 Application to other areas/regions/countries

The research area covered a territory of 107.4 km² and came up with a detailed light pollution map of the Winterthur area. Similar maps could be produced for other urban centers of Switzerland, given the fact that the data for the modelling process is identically available for any other region in the country. The digital layers from Swisstopo include data (street network, location and shape of buildings, etc.) for the full extent of the area shown in Figure 64. The comparison of the research area (red square) with the totality of the country's surface suggests a considerable effort to extend the model to an area of the size of a small country such as Switzerland. The data processing time would likewise increase with the size of the area. If the hurdle of enormous data volumes can be taken, the result however would be a comprehensive

understanding of the light pollution in the entire country of Switzerland and the possibility for country-wide analysis.

Scaling the model to a wider area requires – apart from the mentioned digital map features – a considerable input of local knowledge and on-spot measurements. Only with repeated observations in the field, the model can become more sophisticated. Ideally municipalities and/or light planning experts contribute with specific data to feed and improve the model. Information about street categories, the type of lamps in place, the distance between the lamps, the existence of special illuminated objects (churches, historical buildings) etc. would be of particular use.

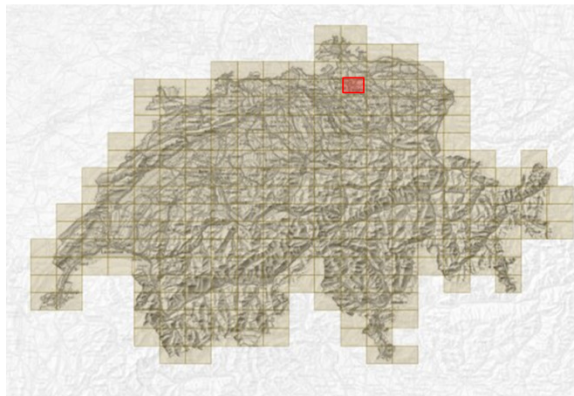


Figure 64: Digital mapped data coverage from Swisstopo (available in format 1:25'000). The research area around the city of Winterthur is marked with a red square. The country surface is approx. 380 times larger than the research area, suggesting a considerable data processing effort to produce a countrywide light pollution map.

Cartography: Stefan M. Bruehlmann

The general set-up of the model can be applied to other regions outside Switzerland. It is however assumed that, depending on the area, a thorough analysis about the existing light sources needs to precede the model set-up. Own research showed that each region or country has its own very specific light sources. This research - which is limited to a small area in Switzerland - did not deal with the whole potential variety of light sources. The research only included a limited number of light sources which were determined by the characteristics of the region.

It was assumed that various known light sources did not occur or were negligible in the research area. Examples which might have a high importance in other regions/countries are: greenhouses (Netherlands), large scale industrial areas (miscellaneous countries); motorways (i.e. Brussels capital region, Belgium; (Energuide, 2012); oil exploitation (Norway, UK), night fishing (Japan) night skiing (alpine countries, Finland), to mention just a few.

The model could be successfully applied in regions/countries with existing digital mapped data from official sources. Alternatively, a good coverage of OSM data could be used too. In either case, the data must be complete and of excellent quality. In countries with a poor or non-existing coverage of digital mapped data the model is likely to produce insufficient results. Missing data would have to be digitized or extensive measurement and observations in the field would have to be undertaken. This would entail large investments in time and money.

6 Conclusion

6.1 Knowledge gained

A lack of local light pollution data was mentioned as a motivation for this thesis. It was noted that light pollution is predominantly documented at a global or regional level. To date, satellites imagery is the main source of information to monitor and map the development of light pollution. Due to the relatively small resolution of the data provided by satellites, the analysis of light pollution cannot be done at a local scale. Alternative data – gathered from nocturnal aerial surveys are costly and not widespread. Therefore, an alternative and cheaper way to come up with light pollution data at a local scale was developed.

The research question of this study was, whether a GIS model could produce light pollution data that is reliable and useful for visualization and planning purposes at a local scale. The results presented in this study proved the capabilities of a modelled approach in GIS: The presented light pollution maps have demonstrated their validity. They visually and statistically match the chosen reference scenario (ISS imagery) to a large degree. At this point in time, no comparable maps – modelled with a desktop GIS – have been presented in a comparable quality and resolution down to street level.

Hence, the main conclusion drawn from this research is that light pollution (i.e. upward light emissions) can be modelled in GIS. A prerequisite is, however, the availability of suitable base data. Such data includes an inventory of the street network, since public street lighting is by far the most important factor for light pollution. Other necessary base data include an inventory of further highly important light emitting sources such as parking, shopping facilities and sports fields.

For this study, data from the National Topographic Agency (swisstopo) was used and proved to be complete and reliable. Where this type of ‘official’ data is not available, OSM data could fill the gap. The research included the verification of OSM data as well. Certain light emitting sources were extracted from OSM as they were not provided by the National Map agency. The extracting and handling of the OSM data proved to be more labor- and time intensive compared to the use of official topographic data. Certain quality issues could also be observed. Notably, the street classification system did not completely match the ‘official’ hierarchy.

The set-up of the model required extensive field measurements of the light intensities at street level. Much knowledge was gained with respect to the variable light intensities in function of the different light sources. It was understood that light fluxes are very local and highly dependent on the type of the street lamps used. Additionally, each lamp type appeared to have its very own light footprint, which made the modelling very difficult. The light propagation of each light source is very individual and depends on the construction of the lamp, especially on the lamp reflector. Nevertheless, more than 80’000 light sources (light points) were modelled and integrated into the calculation of the final ‘light pollution map’

A comparison of the model output with an existing ISS image confirmed the quality of the model set up: more than 75% of the pixels of the model output image exactly matched the comparison ISS image pixels. 93.1% of all pixels showed little or no difference in illumination. Several reasons could be found for the 6.9% of pixels not matching the ISS image – the most important lying in the difficult orthorectification process of the ISS image, given its limited quality (metrological conditions; motion blur, etc.). Despite repeated efforts by NASA (Higgins, 2014b) to capture a night view of Winterthur, no better image of the research area could be received within the time requirements of this thesis.

In conclusion, the research results confirmed that a modelled approach to map ‘light pollution’ is feasible. The quality of the outcome however depends on the availability of data to model the light sources and on a solid knowledge about the local peculiarities. Without local understanding of the situation, important light sources might be missed or wrongly assessed.

An important understanding gained from this research is that satellite imagery can apply for analysis at a local scale only in a very limited way. The resolution of all current satellite imagery products is not sufficient. As for aerial night photography, it could provide very useful information in a sufficient resolution – even for planning purposes. It is, however, understood that such surveys will not become common practice in future, as a result of the elevated cost and organizational effort implied. The recently observed proliferation of unmanned aerial vehicles (UAV) and intensive research in this field (<http://www.idsc.ethz.ch/>) could help to realize less expensive surveys. A bottleneck however remains the camera itself which requires an enormous lens speed in order to avoid motion blur during night time recordings. Suitable cameras are still a considerable weight factor.

An insight gained from this research is that the model can be further improved by integrating additional light sources and by adding further rules. With ten different layers the model is considered to cover the most prominent light sources. Any further layer (e.g. lights from cars in the street, or the consideration of the number of stories of a building) is considered to complicate the model without much contribution to the final outcome. The current calculations of the model are already very processing intensive (given the 1m raster resolution). If prospective users of the model integrate further layers and rules, a powerful hardware infrastructure would certainly be a prerequisite.

Finally, the research showed that the appreciation of the quality of the model output largely depends on the potential readers/users’ perspective. Generally, two categories of light pollution map stakeholders could be identified: a) stakeholders with a detailed perspective e.g. light planners, municipalities, biologists and b) stakeholders with a more global view (e.g. the wider public, light pollution campaigners, astronomers). Given the modelled approach of the solution described in this study the latter group can certainly draw more useful information. The first group will currently be confronted with data that provides limited spatial accuracy, detail and reliability: for example, at street level, the model output can

not yet be used for concrete light planning activities. To do so more master data would need to be part of the model (see chapter 6.2, below)

6.2 Future direction and further research

In future, light pollution will increasingly rank higher on the agenda of governments, municipalities, scientists and the individual citizen. The energy crisis and the need for a responsible use of natural resources are essential drivers for the case. More light pollution related data and knowledge will be required. GIS can contribute to produce knowledge in form of numerical analysis and maps.

This research is a first step into this direction. The study covers the basic concepts of modelling light pollution with the use of GIS processes and techniques. It provides first answers to a very complex field of research. The presently achieved results are promising. Nevertheless, further research is urgently needed to improve the knowledge and to enhance the results. Given the time restrictions of this study, the relevant fields of future research could only be sensed, but not approached.

The following list of proposed areas is considered to be the top priorities for future research in the realm of GIS and light pollution:

- a) Improved modelling of spatial light distribution: As demonstrated in this study, light sources are manifold. Each light source has its own characteristic and pattern of light propagation. Existing light planning tools such as Calculux (Koninklijke Philips N.V., 2014) are able to model the light spread (light cone) depending on the lamp type. Geospatial capabilities are however missing. A promising field of further investigation is the merger of expert light planning tools with GIS. The integration of the two systems would open up new applications and opportunities.
- b) Translate the Lux measurements into a 'Night Sky brightness' map: 'Light pollution' is commonly expressed in terms of the 'Night sky brightness'. Many light pollution map in fact show the quality of the night sky, e.g the number of visible stars. Future research should concentrate on the relation between ground based measurements of light (Lux) and the 'night sky brightness'. The model of the present study could be used to serve as the basis for the calculation of 'Night sky brightness' maps at a more local scale than ever before.
- c) Validate and improve the model set-up by comparing it with a high resolution ISS image: The validation of the model depends on a qualitatively excellent image to which the modelled results can be compared. In this study only a low quality image was available for this purpose. According to NASA (Higgins, 2014b), the shoot of a high resolution image from the ISS of the research area is still on schedule. Should the image become available, it ought to be compared with the modelled results again. The goal must be to improve the rules and mechanics of the model and to better match the modelled output with reality.

Generally, the deeper analysis of available night imagery (from satellite, orthophoto, ISS) is a field of research that is suggested to be approached in view of the improvement of a GIS light pollution model. The existing imagery can give important clues that determine the set up of the GIS light pollution model.

g) Acquire further knowledge on regional differences of light sources: This study has covered a very limited geographical area only. The most important light sources were identified in the research area and modelled to produce a 'light pollution map'. It is suggested that the model could be applied to other areas or countries. It is also understood that local conditions are not the same outside the research area: The inventory of light sources is different. The degree of industrialization and the construction design of the transportation network, buildings and industry are determining the light emission. Further research needs to understand the linkage between the ground based light sources and the emitted light. Regional differences need to be understood better in order to adapt the model accordingly.

6.3 Relevance of the research

The research results suggest that light pollution maps must be re-written. So far, available maps show the light pollution situation at a too coarse resolution. Darkness islands, for example, are not reflected in those maps. In their set-up and resolution, these maps are not useful to either, light planners, astronomers, or the general public. Therefore, this study suggests that modelled results can be a solution to provide valid information at a more detailed level and for the benefit of the various stakeholders.

Light planners have a need to understand the implications of their actions. Therefore, the model of this study might help to provide them with useful data regarding the light emissions of their light portfolio. An advantage of using a model is that planning scenarios can be evaluated, whereas satellite images only provide the status-quo.

The presented model does not yet include the real light source portfolio of the research area. If municipalities decided to provide all light points into a GIS model, there would be an enormous potential to model the upward light pollution and to produce very accurate light pollution maps.

Local interest groups such as the 'Dark Sky Association' of Switzerland have a valid interest to present more detailed maps than shown ever before. Until now the most detailed light pollution map was for the entire country of Switzerland. More detailed data was not available. The maps produced by the model of this research could provide the 'light pollution' situation in Switzerland at a city level. Undeniably, municipalities and the general public will find an interest in such maps – given the topicality of the issue and its impact on energy costs.

In particular, municipalities should find interest in a quantitative model of the light emission of their area. As noticed earlier, municipalities are not yet planning their light network based on a GIS model. Hence, the energy use is generally still not systematically monitored. A model such as the one presented bears the

potential to catch up on this issue. With the application of GIS processes and models, a municipality could calculate the energy use of their entire network. This could help to optimize the electrical light consumption and eventually the costs for the public lighting.

A generally increasing interest in the 'light pollution' topic was perceived by the author during this study. The loss of the natural night sky is an issue that is shared and supported by almost everyone. Therefore, any related information will be welcomed.

Consequently, individuals have the desire to know about the quality of their natural surrounding including the night sky. Light pollution maps at a local scale could provide relevant information to this stakeholder group. Their question is: "What is the light pollution in my backyard?" A modelled light pollution map could help to answer this question.

Municipalities could provide modelled light pollution maps on their 'geo portals' and promote the topic to a wide public. The author of this study is currently about to prepare a proposal to the city of Winterthur to add a 'light pollution' layer onto its geo-web portal (<http://stadtplan.winterthur.ch/>).

-Fin-

References

- Albertz, J., 2009. *Einführung in die Fernerkundung*. 4 ed. Darmstadt: WBG (Wissenschaftliche Buchgesellschaft).
- Barriou, R., Lecamus, D. & Le Henaff, F., 1985. *Albedo Réflectence*. Rennes: Centre Régional de Télédétection, Université de Rennes.
- Biggs, J. D., Fouché, T., Bilki, F. & Zadnik, M. G., 2012. Measuring and mapping the night sky brightness of Perth. *Monthly Notices of the Royal Astronomical Society*, Issue 421, pp. 1450-1464.
- Birriel, J., Wheatley, J. & McMichael, C., 2010. Documenting Local Night Sky Brightness Using Sky Quality. *The Journal of the American Association of Variable Star Observers (JAAVSO)*, Volume 38, pp. 132-137.
- Bogard, P., 2013. *The End of Night: Searching for Natural Darkness in an Age of Artificial Light*. New York: Little, Brown and Company.
- CEN, 2003. *Technical Report CEN/TR 13201, Parts 1-4, Road lighting*. Brussels: European Committee for Standardization.
- Chepesiuk, R., 2009. Missing the Dark: Health effects of Light Pollution. *Environmental Health Perspectives*, 117(1), pp. A20 - A27.
- Cinzano, P., 2005. *Night Sky Photometry with Sky Quality Meter*, Thiene, Italy: Internal Report n. 9, v.1.4.
- Cinzano, P., Falchi, F. & Elvidge, C. D., 2001. The first World Atlas of the artificial night sky brightness. *Monthly Notices of the Royal Astronomical Society*, Volume 328, pp. 689-707.
- Commission Internationale de l'Eclairage (CIE), 1997. *CIE 126-1997 Guidelines for minimizing sky glow*. Vienna: CIE.
- Cosine, 2013. *Night POD - Tracking system for manned spaceflight*. [online] Available at: <http://cosine.nl/portfolio/nightpod/> [Accessed 5 April 2014].
- Deleuil, J.-M., ed., 2009. *Eclairer la ville autrement: Innovations et expérimentations en éclairage public*. Lausanne: Presses Polytechniques et Universitaires Romandes.
- Eisenbeis, G., 2002. *Umweltbelastung durch künstliches Licht*. [Online] Available at: http://www.uni-mainz.de/FB/Biologie/Zoologie/abt1/eisenbeis/Homepage_Licht_Umwelt.htm [Accessed 10 August 2014].
- Elvidge, C. D., Baugh, K., Zhizhin, M. & Chi Hsu, F., 2013. Why VIIRS data are superior to DMSP for mapping. *Proceedings of the Asia-Pacific Advanced Network 2013*, pp. 62-69.
- Elvidge, C. D. et al., 2007. The Nightsat mission concept. *International Journal of Remote Sensing*, 28(12), pp. 2645-2670.
- Energuides, 2012. *The answer to all your questions on energy in Brussels*. [Online] Available at: <http://www.energuides.be/en/questions-answers/why-are-some-motorways-no-longer-lit/38> [Accessed 19 August 2014].

- ESRI, 2014. *ArcGIS Help 10.1 - What is ModelBuilder?*. [Online] Available at: [http://resources.arcgis.com/en/help/main/10.1/index.html#/002w00000001000000/](http://resources.arcgis.com/en/help/main/10.1/index.html#/002w00000001000000/002w00000001000000/) [Accessed 10 August 2014].
- European Commission, 2014. *Earth observation: first Copernicus satellite Sentinel 1A*. [Online] Available at: http://europa.eu/rapid/press-release_MEMO-14-251_en.htm [Accessed 4 April 2014].
- FEDRO, 2014. martin.wyss@astra.admin.ch, *Beleuchtungsstandards*. [email] Message to Stefan Bruehlmann (stefan.bruehlmann@dentaku.ch). Sent 10 June 2014: 08:47.
- Frangiamone, E., 2014. *Orthophotographie nocturne à haute résolution*. Geneva: Direction de la mensuration officielle.
- Frei, M. & Kyburz, D., 2014. *Discussion with Stadtwerk Winterthur* [Interview] (9 July 2014).
- Garstang, R. H., 1986. Model for artificial night-sky illumination. *Publications of the Astronomical Society of the Pacific*, Volume 98, pp. 364-375.
- GIS Cloud, 2014. *Mobile Data Collection*. [Online] Available at: <http://www.giscloud.com/apps/mobile-data-collection/> [Accessed 8 August 2014].
- Globe at Night, 2014. *Maps and Data*. [Online] Available at: <http://www.globeatnight.org/maps.php> [Accessed 1 September 2014].
- Google Earth, 2014. *Google Earth*. [Online] Available at: http://www.google.co.uk/intl/en_uk/earth/download/ge/agree.html [Accessed 08 August 2014].
- Hale, J. D. et al., 2013. Mapping Lightscapes: Spatial Patterning of Artificial Lighting in an Urban Landscape. *PLoS ONE*, 8(5), p. e61460.
- Hänel, A., 2014. *Fachgruppe Dark Sky der Vereinigung der Sternfreunde e.V.; Gesetze gegen Lichtverschmutzung*. [Online] Available at: <http://www.lichtverschmutzung.de/seiten/gesetze.php> [Accessed 18 August 2014].
- Heat Island Group, 1999. *Pavement Albedo*. [Online] Available at: <http://web.archive.org/web/20070829153207/http://eetd.lbl.gov/HeatIsland/Pavements/Albedo/> [Accessed 23 August 2014].
- Higgins, M., 2014a. melissa.higgins@nasa.gov, *ISS Imagery of Winterthur at night*. [email] Message to Stefan Bruehlmann (sb@dentaku.ch). Sent 5 March 2014, 16:55h: NASA Johnson Space Center, Houston, USA.
- Higgins, M., 2014b. melissa.higgins@nasa.gov, *Imagery of Winterthur from ISS*. [email] Message to Stefan Bruehlmann (sb@dentaku.ch). Sent 3 October 2014, 13:59h: NASA Johnson Space Center, Houston, USA.
- Institution of Lighting Professionals, 2012. *Guidance for the Reduction of Obtrusive Light*. [Online] Available at: <https://www.theilp.org.uk/documents/obtrusive-light/> [Accessed 18 July 2014].
- Keeney, D. L., 2012. *Lights of Mankind*. Guilford: Lyons Press.

- Klaus, G. et al., 2005. *Empfehlungen zur Vermeidung von Lichtemissionen*. Bern: Bundesamt für Umwelt, Wald und Landschaft (BUWAL).
- Koninklijke Philips N.V., 2014. *Lighting simulation software - Plug-in for DIALux, Relux and 3ds Max design*. [Online] Available at: http://www.lighting.philips.com/main/connect/tools_literature/diaLux_and_other_downloads.wpd [Accessed 1 September 2014].
- Kuechly, H. U. et al., 2012. Aerial survey and spatial analysis of sources of light pollution in Berlin, Germany. *Remote Sensing of Environment*, Issue 126, pp. 39-50.
- Longcore, T. & Rich, C., 2004. Ecological light pollution. *Frontiers in Ecology and the Environment*, 2(4), pp. 191-198.
- Longely, P. A., Goodchild, M. F., Maguire, D. J. & Rhind, D. W., 2011. *Geographic Information Systems & Science*. 3rd ed. Hoboken: John Wiley & Sons.
- Luzern, S., 2014. *Plan Lumière*. [Online] Available at: http://www.stadtluern.ch/de/aktuelles/projekte/projekteaktuell/?themenbereich_id=16&thema_id=115 [Accessed 1 June 2014].
- Markvart, T. & Castañer, L. eds., 2003. *Practical Handbook of Photovoltaics: Fundamentals and Applications*. Oxford: Elsevier Advanced Technology.
- Narisada, K. & Schreuder, D., 2004. *Light Pollution Handbook*. Dordrecht: Springer.
- NASA Earth Science and Remote Sensing Unit, 2014. *The Gateway to Astronaut Photography of Earth*. [Online] Available at: <http://eol.jsc.nasa.gov/sseop/metadata/camera.htm> [Accessed 3 July 2014].
- NASA, 2014. *Visible Earth - A catalog of NASA image and animations of our home planet*. [Online] Available at: <http://visibleearth.nasa.gov/view.php?id=55167> [Accessed 10 September 2014].
- National Geographic, 2014. *Our Vanishing Night / Photographs by Jim Richardson*. [Online] Available at: <http://ngm.nationalgeographic.com/2008/11/light-pollution/richardson-photography> [Accessed 1 August 2014].
- NOAA National Geophysical Data Center, 2014. *DMSP & VIIRS Data Download*. [Online] Available at: <http://ngdc.noaa.gov/eog/download.html> [Accessed 20 March 2014].
- Ochi, N., 2013. *hikarigai.net*. [Online] Available at: hikarigai.net/oldsite/rep/20110416AGM2011.pdf [Accessed 14 June 2014].
- Open Street Map, 2014. *OSM*. [Online] Available at: <http://www.openstreetmap.ch/> [Accessed 04 August 2014].
- Posch, T., Freyhoff, A. & Uhlmann, T., 2012. *Das Ende der Nacht - Die globale Lichtverschmutzung und ihre Folgen*. 1st ed. Weinheim: Wiley-VCH.
- Pun, C. S. J. & So, C. W., 2012. Night-sky brightness monitoring in Hong Kong. *Environmental Monitoring and Assessment*, Volume 184, pp. 2537-2557.

- Pun, C. S. J., So, C. W., Leung, W. Y. & Wong, C. F., 2014. Contributions of artificial lighting sources on light pollution in Hong Kong measured through a night sky monitoring network. *Journal of Quantitative Spectroscopy and Radiative Transfer*, Volume 139, pp. 90-108.
- Rensselaer Polytechnic Institute, 2007. *Lighting Research Center / What is light pollution*. [Online] Available at: <http://www.lrc.rpi.edu/programs/nlpip/lightinganswers/lightpollution/lightPollution.asp> [Accessed 8 July 2014].
- Rich, C. & Longcore, T., 2006. *Ecological consequences of artificial night lighting*. Washington: Island Press.
- Roesch, A. C., 2000. *Assessment of the Land Surface Scheme in Climate Models with Focus on Surface Albedo and Snow Cover*. Zurich: ETH Geographisches Institut Eidgenössische Technische Hochschule Zürich.
- Ryer, A., 2014. *International Light Technologies, Light Measurement Handbook*. [Online] Available at: <http://www.intl-lighttech.com/services/ilt-light-measurement-handbook> [Accessed 30 April 2014].
- Stadt Winterthur, 2008. *Gesamtkonzept Stadtlicht Winterthur*. Winterthur: Stadtrat Winterthur.
- Stadt Winterthur, 2014. *Einwohnerkontrolle*. [Online] Available at: <http://einwohnerkontrolle.winterthur.ch/en/> [Accessed 31 August 2014].
- Swiss Federal Statistical Office, 2014. *Regional Portraits - Cities with more than 20'000 inhabitants*. [Online] Available at: <http://www.bfs.admin.ch/bfs/portal/en/index/regionen/staedte.html> [Accessed 01 August 2014].
- Swiss Ornithological Institute, 2005. *Dérangements dus à la lumière*. [Online] Available at: <http://www.vogelwarte.ch/derangements-dus-a-la-lumiere.html> [Accessed 8 July 2014].
- Swisstopo, 2014. *SWISSIMAGE, The Digital Color Orthophotomosaic of Switzerland*. [Online] Available at: <http://www.swisstopo.admin.ch/internet/swisstopo/en/home/products/images/ortho/swissimage.html> [Accessed 08 August 2014].
- Swisstopo, 2014. *VECTOR 25*. [Online] Available at: <http://www.swisstopo.admin.ch/internet/swisstopo/en/home/products/landscape/vector25.html> [Accessed 04 August 2014].
- Tapissier, F., 2014. *Cartes de pollution lumineuse de France*. [Online] Available at: http://www.avex-asso.org/dossiers/wordpress/?page_id=38 [Accessed 1 June 2014].
- Tavoosi, H., Darvishzadeh, R., Shakiba, A. & Mirbagheri, B., 2009. *Modelling Light Pollution in Suburbs*. Yokohama, Japan, The seventh International Conference on Urban Climate, 29 June - 3 July 2009.
- UNESCO World Heritage Center, 2014. *Astronomy and World Heritage Thematic Initiative*. [Online] Available at: <http://whc.unesco.org/en/astronomy/> [Accessed 3 September 2014].
- Unihedron, 2008. *SQM Instruction sheet*. [Online] Available at: http://unihedron.com/projects/sqm-l/Instruction_sheet.pdf [Accessed 18 September 2014].

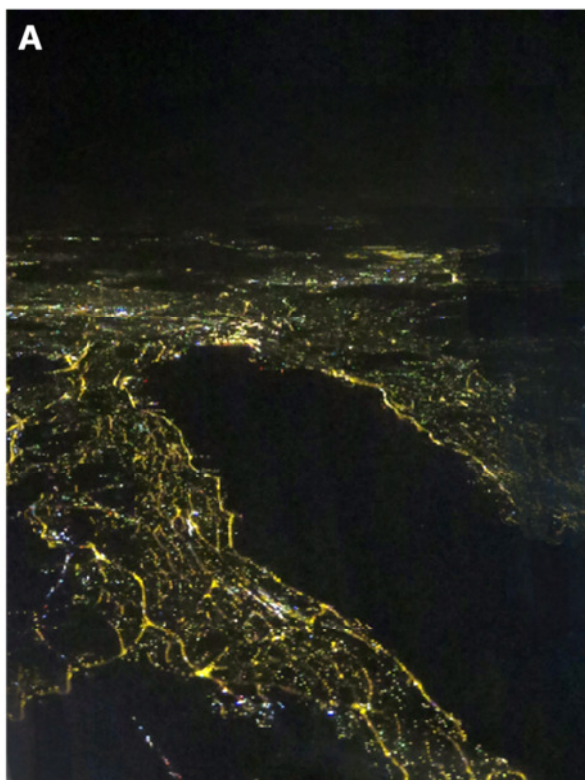
- Unihedron, 2014. *Portable Tools for Physics and Astronomy*. [Online] Available at: <http://unihedron.com/> [Accessed 10 August 2014].
- Unihedron, 2014. *Sky Quality Meter - L*. [Online] Available at: <http://www.unihedron.com/projects/sqm-l/> [Accessed 1 June 2014].
- Walker, M. F., 1977. The effects of urban lighting on the brightness of the night sky. *Publications of the Astronomical Society of the Pacific*, Volume 89, pp. 405-409.
- Web Center for Social Research Methods, 2006. *Structure of Research*. [Online] Available at: <http://www.socialresearchmethods.net/kb/strucres.php> [Accessed 2 August 2014].
- Winterthur, S., 2014. *Gesamtkonzept Stadtlicht Winterthur*. [Online] Available at: <http://stadtentwicklung.winterthur.ch/stadtentwicklung/projekte-studien/stadtlicht-winterthur/gesamtkonzept-stadtlicht-winterthur> [Accessed 1 June 2014].
- Wu, B. & Wong, H., 2012. Visualization and Analysis of light pollution: A Case Study. *ISPRS Annals of the Photogrammetry, Remote Sensing and Spatial Information Sciences*, Volume I-2, pp. 171-176.
- Zamorano, J. et al., 2011. *ISS nocturnal images as a scientific tool against Light Pollution*, Madrid: Universidad Complutense de Madrid - LICA report April 2011.

Colophon

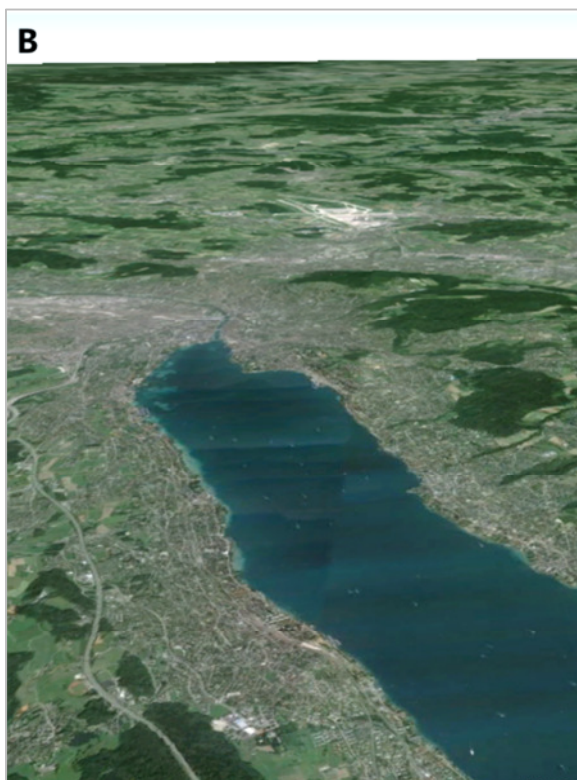
Typeface:	Minion Pro (body) Segoe UI (titles, tables, charts, legends)
Hardware:	TOSHIBA Satellite L300 Personal Computer ASUS Fonepad 7 (ME372CG) [for mobile data collection] Vellemann Type'DVM1300' Lux meter Unihedron Sky Quality Meter - L
Software:	Office 2010 ArcGIS 10.1 GisCloud, MDC version 1.5.3 CalcuLux Road, version 7.7.0.1 IrfanView, version 4.3.6 Adobe Photoshop Elements 7 Snagit 9, version 9.1.0 Mindjet, version 10.0.445
Cameras:	OLYMPUS E-3 Canon G16
Print:	Xerox 700i Digital Colour Press Copy Print Gilomen GmbH, 8400 Winterthur
Images:	2400 x 2400 dpi
Paper Quality:	100g/m ² , FSC [™] certified (https://ic.fsc.org/)
Cover photo:	Winterthur by night seen from Wolfensberg / Winterthur 47°30'39.94"N / 8°42'50.08"E Photo: Stefan M. Bruehlmann, July 2014

Appendices

Appendix A: Night images



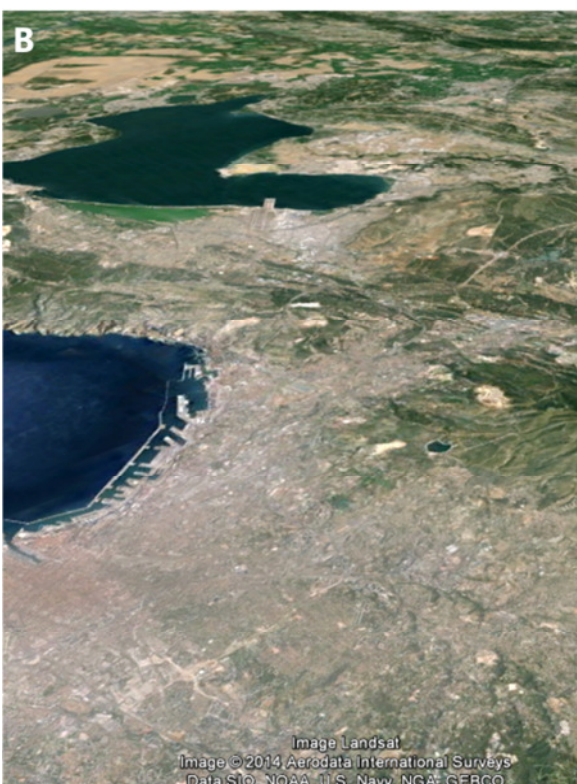
Zurich, Switzerland; alt. 4500m (Photo: Stefan M. Bruehlmann)



Diurnal view city of Zurich (Source: Landsat, 2009)



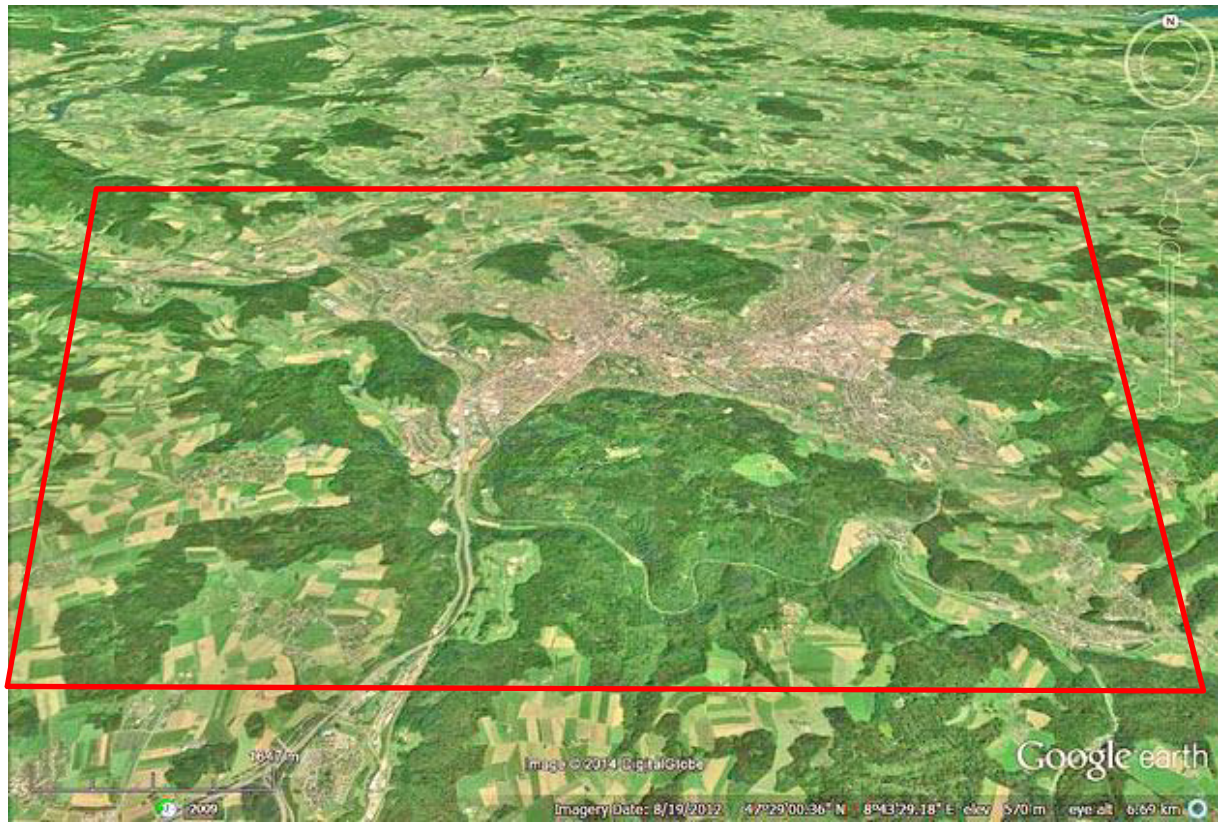
Marseille, France; alt. 10'000m (Photo: Stefan M. Bruehlmann)



Diurnal view of city of Marseille (Source: Digital Globe, 2014)

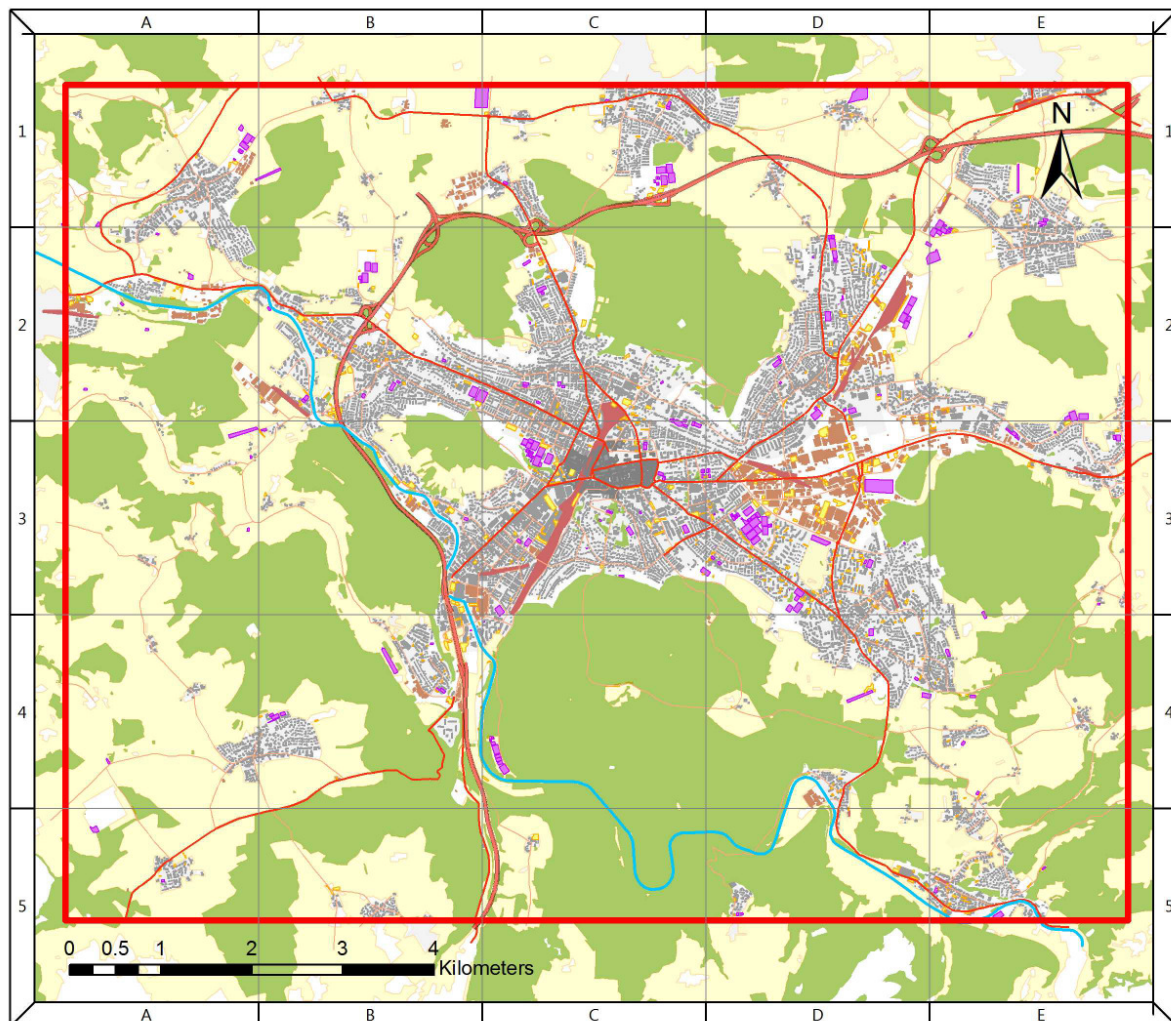
Remarks: Images A were taken from a commercial aircraft en route from Palma de Mallorca (PMI) to Zurich (ZRH); 19 October 2014; Equipment: Canon G16; ISO 4000; f4; 1/20sec

Appendix B: Study area



Remarks: The image above (Source: Google Earth, 2009) is an oblique view on the research area (red square). It gives an impression of the topography and the wider context of the area. Towards the south, there are extended forests that eventually join the pre-Alps. This area is scarcely populated. Towards the north the terrain becomes flat and the main land use is agriculture. The city is embedded within seven wooded hills. A river is crossing the city in its southern and western parts. A national motorway is visible in the lower left part of the image. This motorway is crossing the entire country, linking the cities of Geneva (most western) and St. Gallen (most eastern part of Switzerland).

Appendix C: Study area (land use)



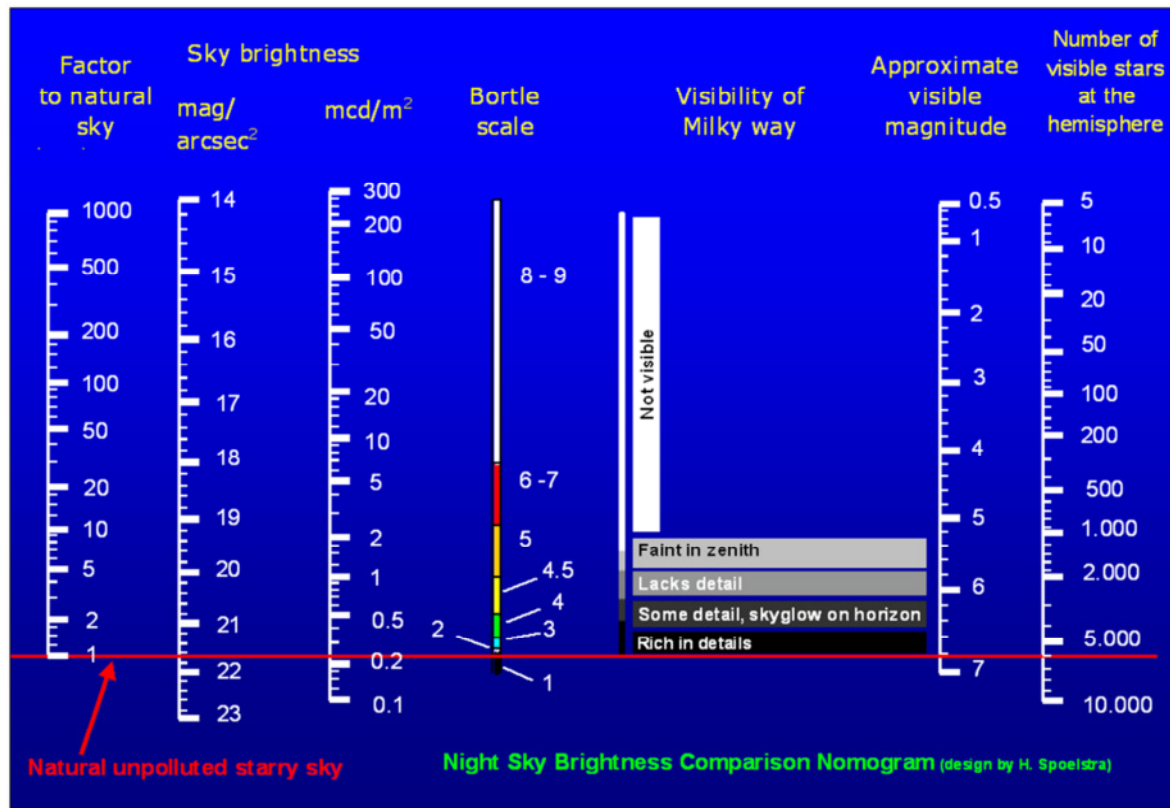
Legend

 Research Area	 Forest	 Residential Buildings
 River Toess	 Meadows/Gardens	 Industrial Buildings
 Motorway	 Car Parking	
 Class 1 Street	 Sports pitch	
 Class 2 Street	 Train Station	

Source of Data: Swisstopo / OSM
Cartography: Stefan M. Bruehlmann, 2014

Remarks: The research area encompasses the city of Winterthur (Switzerland) and its suburbs. The entire research area has a surface of 107.4 km². The center of the image (square C3) includes the historical old town – a densely built up area with houses from the 16th to the 20th century. It is this area where the highest concentration of shops can be found. Square C3 is crossed by the rail station area in north-eastern to south-western direction. Other regional train stations can be found in squares D2 and B2. Residential areas can mainly be found in squares B2 (Wülflingen), C3 (Töss); D2 (Oberwinterthur) and D3/D4 (Mattenbach/Seen). Industrial areas are mainly found in square D3 (Hegi) and in the lower part of square B3 (Töss). The city of Winterthur is surrounded by extended natural areas. The woods in the south of the city (C4) constitute the largest compact wooded area in the Canton of Zurich. There are seven distinct hills around the city. Their culmination points are at around 600 m above sea level (city level is 430m). The natural areas are veritable oasis of darkness.

Appendix D: Night sky brightness scales



Remarks: This chart serves for easy conversion between different night sky brightness scales. Measurements with the Sky Quality Meter are expressed in mag/arcsec² (second scale). The natural level is considered to be at 21.6 mag/arc sec².

Source: <http://www.darkskiesawareness.org/nomogram.php>

Appendix E: Inventory of light sources

1. Class A (Motorway); (Motorway A1)



2. Class 1 Road; (Wülflingerstrasse)



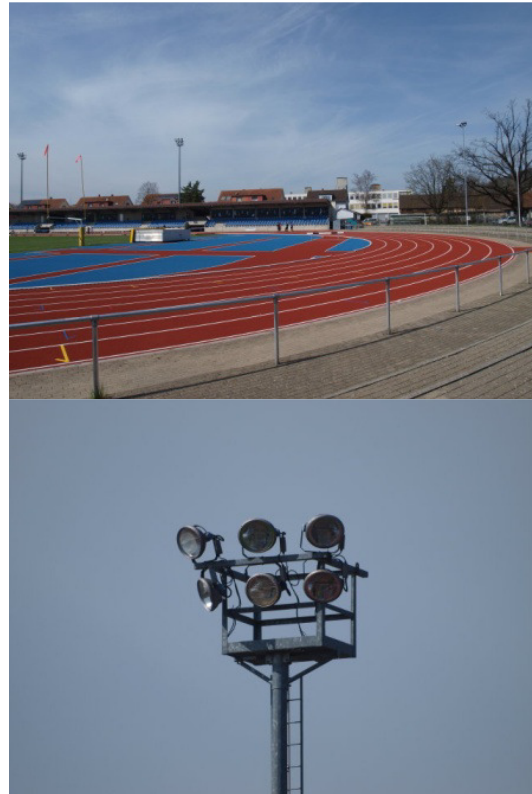
3. Class 2 Road; (Oberfeldstrasse)



4. Class Q Street (Residential); (Seidenstrasse)



5. Train Station; (Train station 'Oberwinterthur')



6. Sports Pitch; (Deutweg)



7. Parking; (Schützenwiese)



8. Old Town; (Marktgasse)



9. Residential Area; (Resedaweg / Anton Graff-Strasse)



10. Industrial Area; (Sulzer-Allee)

Remarks: Above photos illustrate the ten selected light sources that were used in the GIS model. Photo A shows the context of the situation of each light source. Photo B shows the light source (lamp) itself. There are different lamp types per category in place. Despite their common purpose they are nevertheless strongly different in their construction and features. The lamps of the public lighting are almost exclusively of the type 'Sodium Vapor' and produce the typical warm orange light. Train stations lighting which is not under the regime of the municipality (but under the 'Swiss Federal Railways') likewise uses sodium-vapor lamps.

Photos: Stefan M. Bruehlmann, March – October 2014



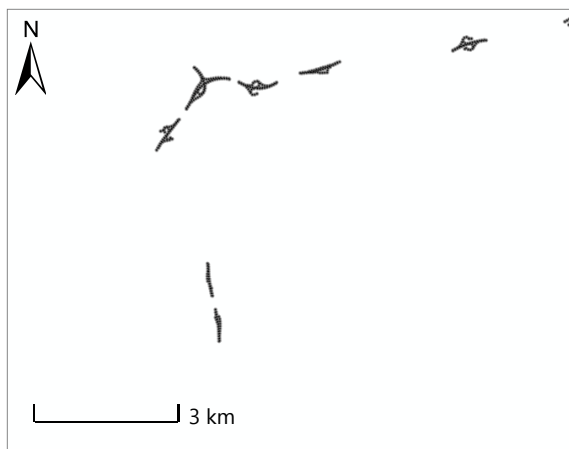
LED lamp; (Schützenwiesenweg)



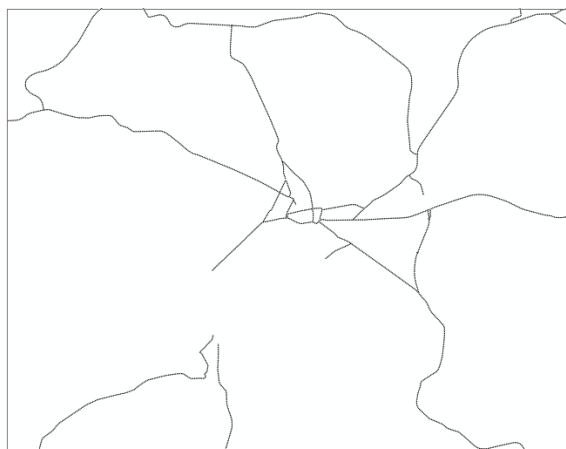
LED lamp at night; (Schützenwiesenweg)

Remarks: The municipality of Winterthur has started to experiment with LED technology. Several selected streets are illuminated by smart and energy friendly LED lamps. LED lamps provide a rather white light (2700 – 6000 Kelvin) compared to the common sodium-vapor lamps (2200 Kelvin) with their orange light.

Photos: Stefan M. Bruehlmann, November 2014

Appendix F: Light points

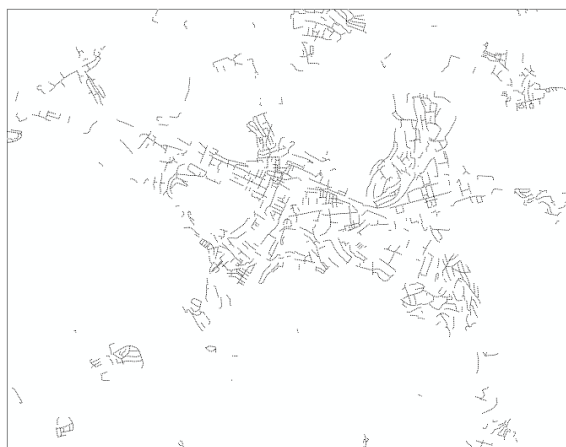
1. Class A Road (418 light points); polyline



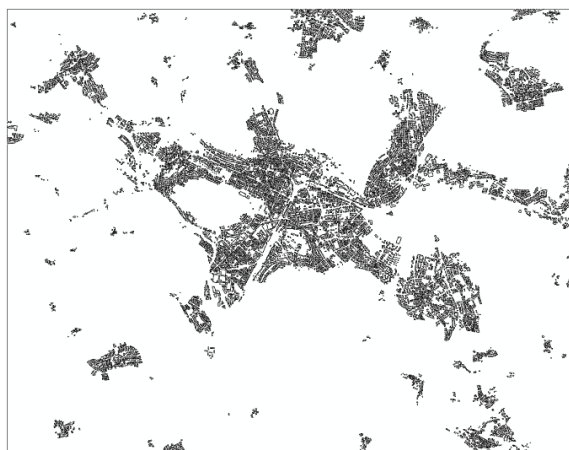
2. Class 1 Road (2097 light points); polyline



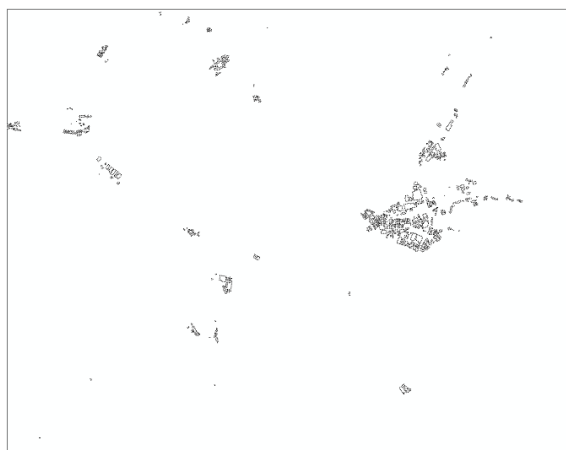
3. Class 2 Road (6051 light points); polyline



4. Class Q Road (6518 light points); polyline



5. Residential Buildings (67710 light points); polygon



6. Industrial Buildings (2714 light points); polygon



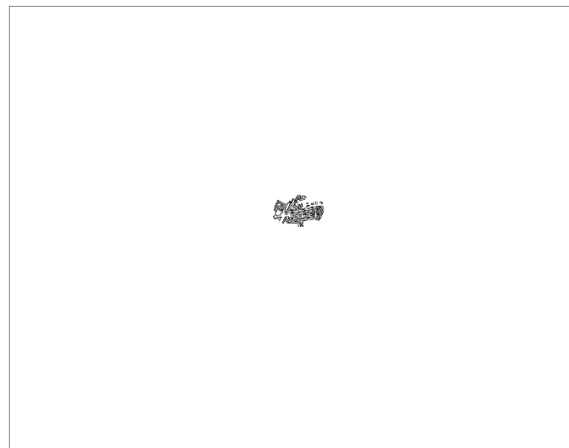
7. Train station area (583 light points); polygon (fishnet)



8. Sports pitch (738 light points); polygon (fishnet)



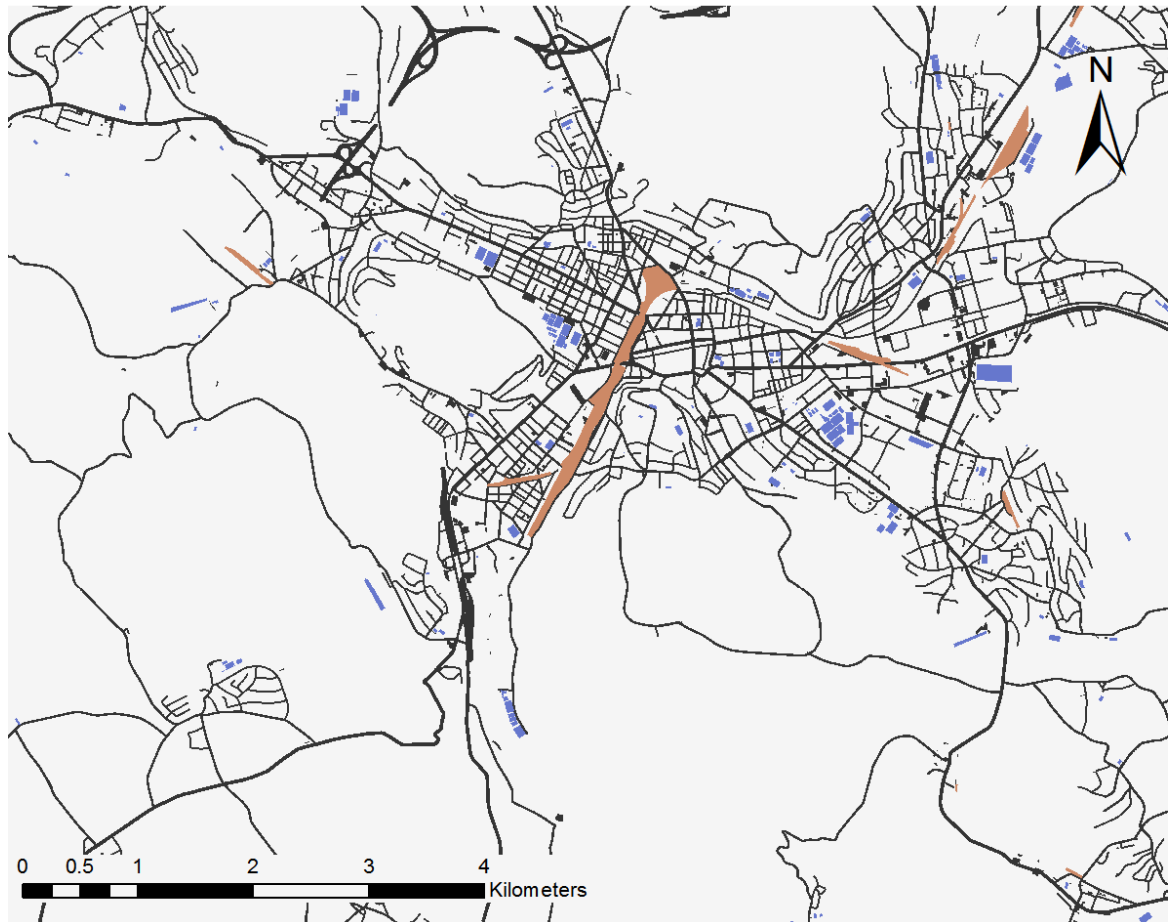
9. Parking (601 light points); polygon (fishnet)



10. Old Town (1179 light points)

Remarks: Above maps show the light points of the research area, separated by ten different light source layers. For 'polyline' features, the light points were placed along the streets. For polygon features (e.g. industrial buildings and individual houses) the light points were modelled around the polygon, as to simulate the light emissions from the windows and the lamps in the front gardens. For the 'polygon (fishnet)' features, the light points were modelled in a way to fill out the polygon with a regular grid of light points in order to illuminate the area with light (see 3.6.3).

Appendix G: Albedo map



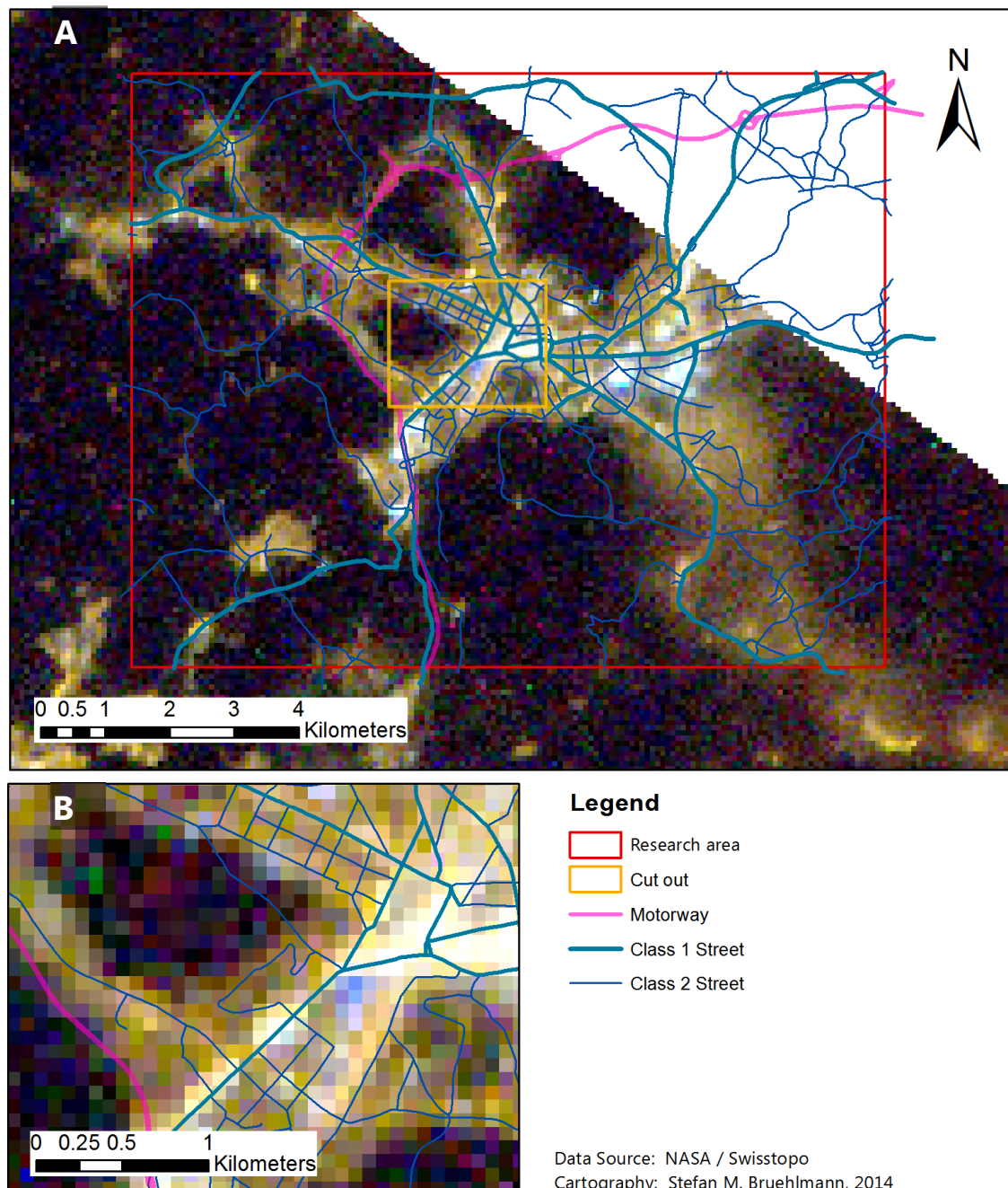
Legend

Albedo reflectance [%]

Black	15
Reddish-brown	17
Blue	20
Light gray	26

Remarks: Areas with different reflectance of the ground are represented in above map. The entire area is separated into four categories. Black colored areas represent asphalt (streets) and feature the lowest reflectance (15%). Areas in reddish color are representing stones and natural grounds and are mainly applied for the rail yards of the train stations. Areas in blue represent grass surfaces (mainly for sports pitches). The large rest of the research area is classified as 'natural area', which consists of wood and not further defined vegetation.

Appendix H: ISS Image orthorectification

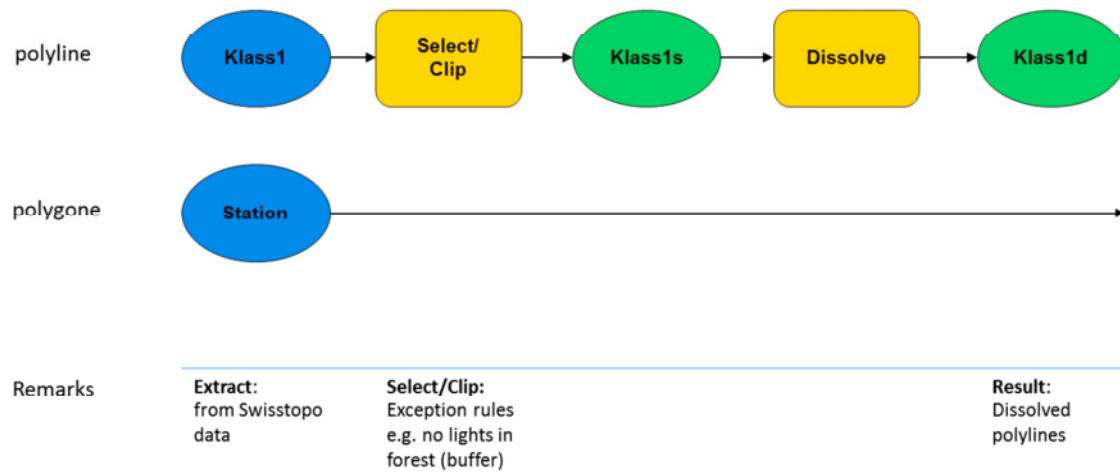


Remarks: Above maps are based on an ISS image of the city of Winterthur (see Figure 28, page 31). The main road network is overlaid for orientation. The roads gave the most significant clues for the orthorectification process. Given the coarse resolution of the ISS image, the orthorectification could only be done approximatively. Image A shows the entire research area; Image B is a cut-out of the city center and of some residential areas. The difficulty to 'rubber sheet' the light emissions according to the supposed light sources (streets) becomes obvious.

Appendix I: ArcGIS model builder

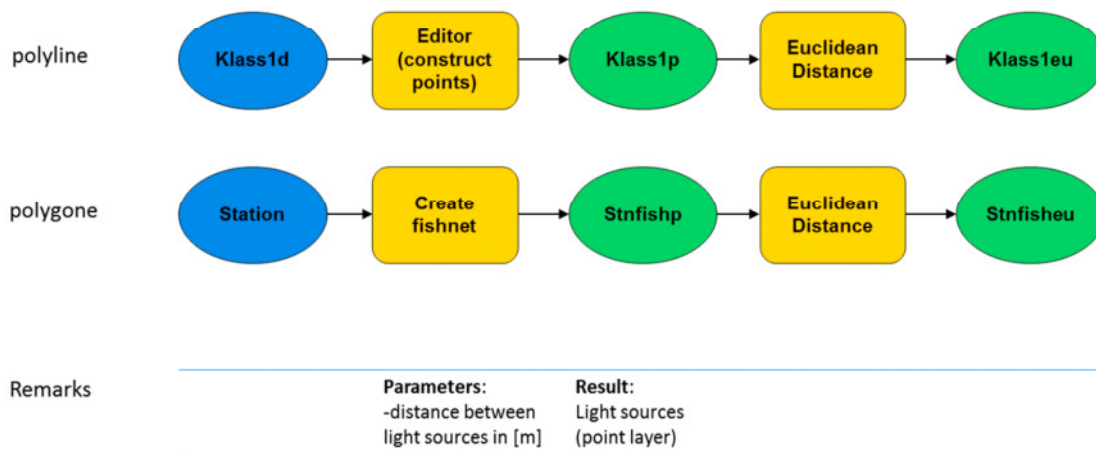
STEP1: Select /Clip and Dissolve

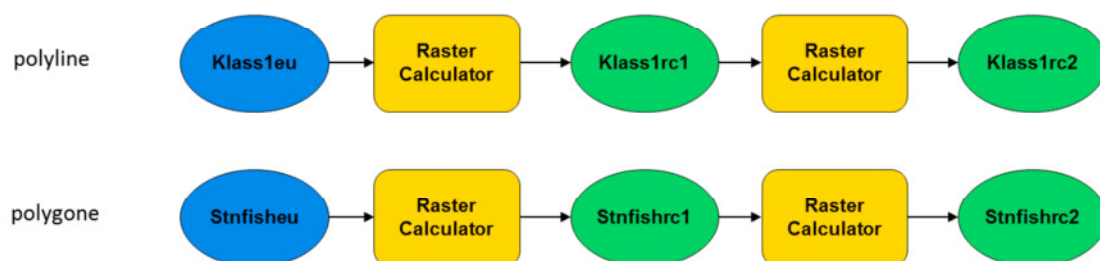
Total of 10 layers



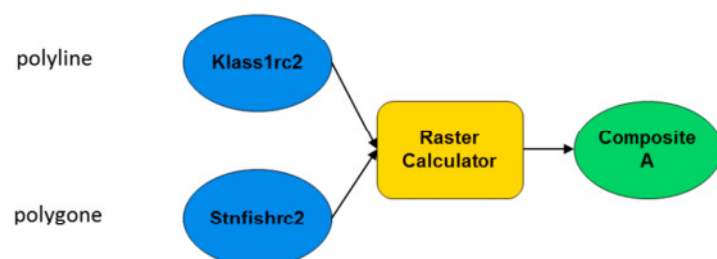
STEP2: Construct Points and Euclidean Distance

Total of 10 layers

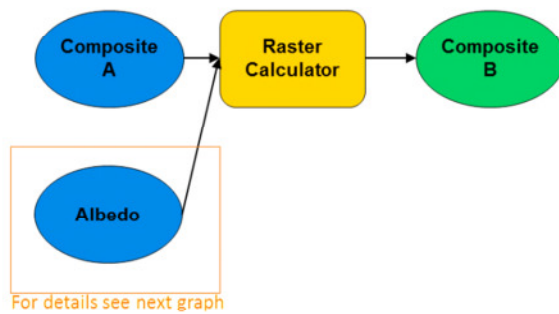


STEP3: Raster Calculation**Total of 10 layers**

Remarks	Parameters: -applying the polynomial formula	Parameters: -replace 'Null' by '0'
Expression	0.1037*("%Klass1eu%"* "%Klass1eu%") - 4.1917*"%Klass1eu%" + 44.73	Con(IsNull("%Klass1rc1%"), 0,"%Klass1rc1%")

STEP4: Summing up all layers**Total of 10 layers**

Remarks	Parameters: -applying the polynomial formula
Expression	"%Klass1rc2%" + "%Stnfishrc2%"

STEP5: Applying the ALBEDO map

Remarks

Parameters:
-Multiplying

Expression

"%CompositeA%"*
"%Albedo%"

Detail: ALBEDO (1)**Total of 10 layers**

polyline



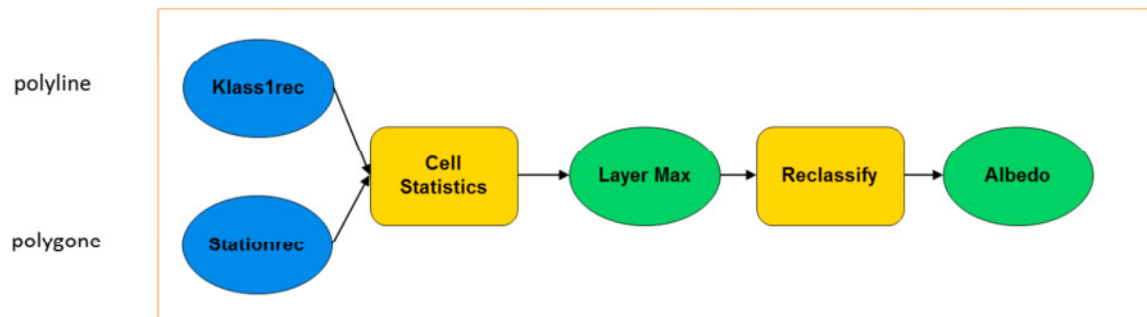
polygone



Remarks

Parameters:
Old value x
New value y

Detail: ALBEDO (2)
Total of 10 layers



Remarks

Parameters:
 Overlay statistic:
 Maximum

Parameters:
 Old value : 0
 New value: 26

Appendix J: Luminaires and lighting situations

Globe lamps



Globe lamps in a residential zone in Alcudia (Spain). In Mediterranean countries, globe lamps are still very popular, despite their high light pollution potential.

Photo: Stefan M. Bruehlmann, October 2014

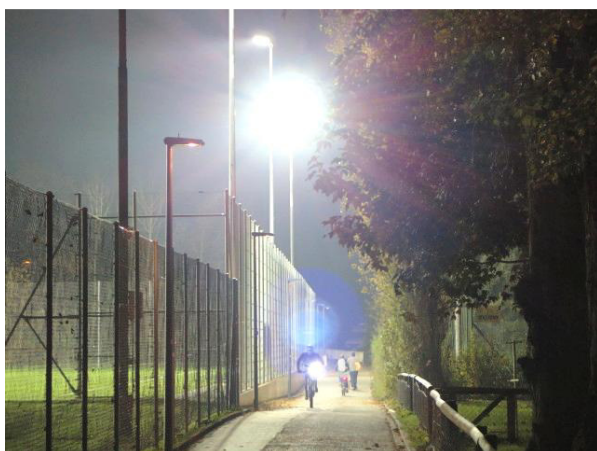
Different lighting situations



Flood light for Tennis courts and football field: The lamps are well shielded and send their light primarily downwards.



Strong light seen from ground level next to a football pitch. Despite the intensity of the artificial light, the moon can well be seen (top right of the image)



Glare from a flood light near a football pitch. A bike route leads along the pitch. Bikers are strongly blinded by the light.

Photos: Stefan M. Bruehlmann, October 2014



Small parking with two strong light sources.

Appendix K: EN 13 201 "Street Lighting"

1. Grouping of Lighting Situations

Typical speed of main user km/h	User types in the same relevant area			Sets of lighting situations
	Main user	Other allowed user	Excluded user	
> 60	Motorised traffic		Slow moving vehicles Cyclists Pedestrians	A1
		Slow moving vehicles	Cyclists Pedestrians	A2
		Slow moving vehicles Cyclists Pedestrians		A3
> 30 and ≤ 60	Motorised traffic Slow moving vehicles	Cyclists Pedestrians		B1
	Motorised traffic Slow moving vehicles Cyclists	Pedestrians		B2
	Cyclists	Pedestrians	Motorised traffic	C1
> 5 and ≤ 30			Slow moving vehicles	
	Motorised traffic Pedestrian		Slow moving vehicles Cyclists	D1
		Slow moving vehicles Cyclists		D2
	Motorised traffic Cyclists	Slow moving vehicles Pedestrians		D3
	Motorised traffic Slow moving vehicles			D4
Walking speed	Cyclists Pedestrians			
	Pedestrians		Motorised traffic Slow moving vehicles Cyclists	E1
		Motorised traffic Slow moving vehicles Cyclists		E2

Remarks: The lighting situations A1 – E2 are determined by the speed and type of the main user of the street.

Source: European Committee for Standardization, 2003

2. Recommended lighting classes

A.6 Lighting situations — set C1

Table A.11 — Recommended lighting classes

Geometric measures for traffic calming	Crime risk	Facial recognition	Traffic flow cyclists					
			Normal			High		
			←	0	→	←	0	→
No	Normal	Unnecessary	S6	S5	S4	S5	S4	S3
		Necessary	S5	S4	S3	S4	S3	S2
	Higher than normal		S4	S3	S2	S3	S2	S1
Yes			S3	S2	S1	S3	S2	S1

Alternative A classes of comparable lighting level to recommended S classes can be found in Table 4. Additional ES and EV classes to recommended S classes can be found in Table 5.

Remarks: Each lighting situation is further detailed. In the shown example for a street used by cyclists, several factors finally determine the light class, expressed in S1 – S6

Source: European Committee for Standardization, 2003

3. Recommended horizontal illuminance

Table 3 — S-series of lighting classes

Class	Horizontal illuminance	
	\overline{E} in lx ^a [minimum maintained]	E_{min} in lx [maintained]
S1	15	5
S2	10	3
S3	7,5	1,5
S4	5	1
S5	3	0,6
S6	2	0,6
S7	performance not determined	performance not determined

^a To provide for uniformity, the actual value of the maintained average illuminance may not exceed 1,5 times the minimum \overline{E} value indicated for the class.

Remarks: Depending on the light class S1 – S6, the illuminance in lux is provided, S1 defining the strictest requirements

Source: European Committee for Standardization, 2003